

# UNCLASSIFIED

AD NUMBER
ADB251342
NEW LIMITATION CHANGE
TO Approved for public release, distribution unlimited
FROM Distribution authorized to U.S. Gov't. agencies only; Proprietary Info.; Sep 99. Other requests shall be referred to U.S. Army Medical Research and Materiel Command, 504 Scott St., Fort Detrick, MD 21702-5012.
AUTHORITY
USAMRMC ltr, 18 Jun 2002

THIS PAGE IS UNCLASSIFIED

AD\_\_\_\_\_

Award Number: DAMD17-98-2-8019

TITLE: New Inhibitors of the Peripheral Site in  
Acetylcholinesterase that Specifically Block  
Organophosphorylation

PRINCIPAL INVESTIGATOR: Terrone L. Rosenberry Ph.D.

CONTRACTING ORGANIZATION: Mayo Clinic, Jacksonville  
Jacksonville, Florida 32224

REPORT DATE: September 1999

TYPE OF REPORT: Annual

PREPARED FOR: U.S. Army Medical Research and Materiel Command  
Fort Detrick, Maryland 21702-5012

DISTRIBUTION STATEMENT: Distribution authorized to U.S. Government agencies only (proprietary information, Sep 99). Other requests for this document shall be referred to U.S. Army Medical Research and Materiel Command, 504 Scott Street, Fort Detrick, Maryland 21702-5012.

The views, opinions and/or findings contained in this report are those of the author(s) and should not be construed as an official Department of the Army position, policy or decision unless so designated by other documentation.

DTIC QUALITY INSPECTED 1

20000223 009

## NOTICE

USING GOVERNMENT DRAWINGS, SPECIFICATIONS, OR OTHER DATA INCLUDED IN THIS DOCUMENT FOR ANY PURPOSE OTHER THAN GOVERNMENT PROCUREMENT DOES NOT IN ANY WAY OBLIGATE THE U.S. GOVERNMENT. THE FACT THAT THE GOVERNMENT FORMULATED OR SUPPLIED THE DRAWINGS, SPECIFICATIONS, OR OTHER DATA DOES NOT LICENSE THE HOLDER OR ANY OTHER PERSON OR CORPORATION; OR CONVEY ANY RIGHTS OR PERMISSION TO MANUFACTURE, USE, OR SELL ANY PATENTED INVENTION THAT MAY RELATE TO THEM.

### LIMITED RIGHTS LEGEND

Award Number: DAMD17-98-2-8019  
Organization: Mayo Clinic Jacksonville

Those portions of the technical data contained in this report marked as limited rights data shall not, without the written permission of the above contractor, be (a) released or disclosed outside the government, (b) used by the Government for manufacture or, in the case of computer software documentation, for preparing the same or similar computer software, or (c) used by a party other than the Government, except that the Government may release or disclose technical data to persons outside the Government, or permit the use of technical data by such persons, if (i) such release, disclosure, or use is necessary for emergency repair or overhaul or (ii) is a release or disclosure of technical data (other than detailed manufacturing or process data) to, or use of such data by, a foreign government that is in the interest of the Government and is required for evaluational or informational purposes, provided in either case that such release, disclosure or use is made subject to a prohibition that the person to whom the data is released or disclosed may not further use, release or disclose such data, and the contractor or subcontractor or subcontractor asserting the restriction is notified of such release, disclosure or use. This legend, together with the indications of the portions of this data which are subject to such limitations, shall be included on any reproduction hereof which includes any part of the portions subject to such limitations.

THIS TECHNICAL REPORT HAS BEEN REVIEWED AND IS APPROVED FOR PUBLICATION.

---

*Terrone Rosenberry, Ph.D.*

---

**REPORT DOCUMENTATION PAGE**Form Approved  
OMB No. 074-0188

Public reporting burden for this collection of information is estimated to average 1 hour per response, including the time for reviewing instructions, searching existing data sources, gathering and maintaining the data needed, and completing and reviewing this collection of information. Send comments regarding this burden estimate or any other aspect of this collection of information, including suggestions for reducing this burden to Washington Headquarters Services, Directorate for Information Operations and Reports, 1215 Jefferson Davis Highway, Suite 1204, Arlington, VA 22202-4302, and to the Office of Management and Budget, Paperwork Reduction Project (0704-0188), Washington, DC 20503

**1. AGENCY USE ONLY (Leave blank)****2. REPORT DATE**

September 1999

**3. REPORT TYPE AND DATES COVERED**

Annual (1 Sep 98 - 31 Aug 99)

**4. TITLE AND SUBTITLE**

New Inhibitors of the Peripheral Site in  
Acetylcholinesterase that Specifically Block  
Organophosphorylation

**5. FUNDING NUMBERS**

DAMD17-98-2-8019

**6. AUTHOR(S)**

Terrone L. Rosenberry Ph.D.

**7. PERFORMING ORGANIZATION NAME(S) AND ADDRESS(ES)**

Mavo Clinic, Jacksonville

Jacksonville, Florida 32224

E-MAIL: Rosenberry@mayo.edu

**8. PERFORMING ORGANIZATION  
REPORT NUMBER****9. SPONSORING / MONITORING AGENCY NAME(S) AND ADDRESS(ES)**

U.S. Army Medical Research and Materiel Command  
Fort Detrick, Maryland 21702-5012

**10. SPONSORING / MONITORING  
AGENCY REPORT NUMBER****11. SUPPLEMENTARY NOTES****12a. DISTRIBUTION / AVAILABILITY STATEMENT**

Distribution authorized to U.S. Government agencies only  
(proprietary information, Sep 99). Other requests for this  
document shall be referred to U.S. Army Medical Research and  
Materiel Command, 504 Scott Street, Fort Detrick, Maryland 21702-5012.

**12b. DISTRIBUTION CODE****13. ABSTRACT (Maximum 200 Words)**

Acetylcholinesterase (AChE) hydrolyzes its physiological substrate acetylcholine at one of the highest known catalytic rates. Little is known about how the peripheral site contributes to the catalytic mechanism of the enzyme. Our studies provide new information about enzyme mechanisms and indicate strategies for designing drugs that defend AChE against inactivation by toxic organophosphates (OPs). We have introduced and confirmed a nonequilibrium analysis and steric blockade model for AChE inhibition by small peripheral site ligands. Additionally, we have examined the effect of known AChE peripheral site inhibitors with OPs to determine what properties may be useful in finding ways to prevent organophosphorylation. Analyses with known AChE peripheral site ligands and site-specific mutants of the enzyme have revealed that the physiological role of the peripheral site is to optimize activity of AChE by loading the enzyme with acetylcholine at low substrate concentrations. In addition to our biochemical studies, we have synthesized and screened new AChE specific ligands based on the structure of known peripheral site peptide ligands. These novel compounds display specificity for the AChE peripheral site and will serve as initial structures for the development of peripheral site ligands that will specifically block OP inactivation of AChE.

**14. SUBJECT TERMS**

acetylcholinesterase, organophosphates, inhibitors, nonequilibrium  
analysis, combinatorial libraries

**15. NUMBER OF PAGES**

61

**16. PRICE CODE****17. SECURITY CLASSIFICATION  
OF REPORT**

Unclassified

**18. SECURITY CLASSIFICATION  
OF THIS PAGE**

Unclassified

**19. SECURITY CLASSIFICATION  
OF ABSTRACT**

Unclassified

**20. LIMITATION OF ABSTRACT**

Limited

NSN 7540-01-280-5500

Standard Form 298 (Rev. 2-89)  
Prescribed by ANSI Std. Z39-18  
298-102

## FOREWORD

Opinions, interpretations, conclusions and recommendations are those of the author and are not necessarily endorsed by the U.S. Army.

\_\_\_ Where copyrighted material is quoted, permission has been obtained to use such material.

\_\_\_ Where material from documents designated for limited distribution is quoted, permission has been obtained to use the material.

\_\_\_ Citations of commercial organizations and trade names in this report do not constitute an official Department of Army endorsement or approval of the products or services of these organizations.

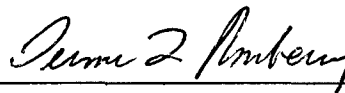
N/A In conducting research using animals, the investigator(s) adhered to the "Guide for the Care and Use of Laboratory Animals," prepared by the Committee on Care and use of Laboratory Animals of the Institute of Laboratory Resources, national Research Council (NIH Publication No. 86-23, Revised 1985).

N/A For the protection of human subjects, the investigator(s) adhered to policies of applicable Federal Law 45 CFR 46.

N/A In conducting research utilizing recombinant DNA technology, the investigator(s) adhered to current guidelines promulgated by the National Institutes of Health.

N/A In the conduct of research utilizing recombinant DNA, the investigator(s) adhered to the NIH Guidelines for Research Involving Recombinant DNA Molecules.

N/A In the conduct of research involving hazardous organisms, the investigator(s) adhered to the CDC-NIH Guide for Biosafety in Microbiological and Biomedical Laboratories.



PI - Signature

Date

**Annual Report for Award Number DAMD17-98-2-8019**  
**Covering Period 9/1/98 - 8/31/99**

---

**PROGRESS REPORT TABLE OF CONTENTS**

—— A. Progress Report Front Cover	
—— B. Standard Form (SF) 298, Report Documentation Page	2
—— C. Foreword	3
—— D. Table of Contents	4
—— E. Introduction	5
—— F. Body	6
—— G. Key Research Accomplishments	12
—— H. Reportable Outcomes	13
—— I. Conclusions	14
—— J. References	15
—— K. Appendices	17
1. Schemes	17
2. Figure Legends	18
3. Figures	20
4. Published Abstracts	27
5. Appended Manuscripts	29

**Annual Report for Award Number DAMD17-98-2-8019**  
**Covering Period 9/1/98 - 8/31/99**

## INTRODUCTION

Acetylcholinesterase (AChE) hydrolyzes its physiological substrate acetylcholine at one of the highest known catalytic rates. X-ray crystallography and mutagenesis studies have revealed that the enzyme active site consists of an acylation site near the bottom of a deep gorge and a peripheral site at its mouth. Despite this information on the enzyme structure, little is known about how the peripheral site contributes to the catalytic mechanism of the enzyme and how to exploit this site for the design of new ligands that modify enzyme activity. The purpose of our research project is to understand the way peripheral site ligands inhibit AChE activity and the functional role that this site plays in the hydrolysis of acetylcholine. Specifically, we intend to resolve the residues in AChE through which the peripheral site inhibitors fasciculin and propidium exert their inhibitory effect on the enzyme acylation site. Our studies will both provide new information about enzyme mechanisms and indicate new strategies for the design of drugs that can defend AChE against inactivation by organophosphates. Organophosphates (OPs) are rapidly hydrolyzed by AChE but dephosphorylate from the acylation site at an extremely slow rate. This slow removal of the phosphate group traps the enzyme in a phospho-intermediate state, irreversibly inactivating AChE. A goal of our project is to use the information gained in the above efforts to design new peripheral site ligands that selectively inhibit AChE phosphorylation while allowing sufficient activity with acetylcholine to maintain physiologic function. Our efforts have focused on cyclic ligands that are specific for the peripheral site and selectively hinder the access of organophosphates to the acylation site. Identification of such ligands from large combinatorial libraries could lead to the design of drugs that would protect individuals from organophosphate poisoning. The search for AChE protective compounds remains necessary due to the continued use of organophosphates as chemical warfare agents and pesticides. This report summarizes the progress of our research as outlined in the Statement of Work section of our approved research proposal.

## BODY

### *Steric blockade at the peripheral site*

The first aim from our project proposal involved the examination of our nonequilibrium hypothesis of AChE substrate hydrolysis. As outlined previously in our proposal, several of the properties of AChE catalysis and inhibition suggested that AChE does not obey simple equilibrium kinetics. First, AChE hydrolyzes its physiological substrate acetylcholine at rates approaching a diffusion-controlled reaction (1), despite the enclosure of the enzyme catalytic site within a deep gorge (2). Second, the binding and subsequent inhibition of AChE by the small peripheral site ligand propidium could not be easily explained by a mechanism involving an induced conformational change in AChE (3; 4). In Szegeletes et al. (1998) (see Appendix, 5), we examined whether substrate or inhibitor equilibrium with the enzyme influenced the process of inhibition. Our assumption was that AChE binds and turns over substrate so quickly that substrate cannot equilibrate within the enzyme active site prior to catalysis. In relation to the classical catalytic pathway for AChE (see Appendix, 5), this nonequilibrium condition is required because the enzyme acylation step  $k_2$  exceeds the substrate dissociation step  $k_{-s}$ . This assumption was both experimentally and computationally confirmed for the first time in the AChE field by our laboratory. The analysis led us further to propose an initial steric blockade model of peripheral site inhibition. This model states that the only effect of bound peripheral site ligand is to retard substrate entry into or exit from the acylation site without altering the substrate binding affinity. According to the model, the binding of small peripheral site ligands, such as the aromatic compound propidium, inhibits AChE without inducing any conformational change in the enzyme structure. Using a combination of experimental and simulated data, we were able to accurately account for the inhibitory activity of small peripheral site ligands (propidium and gallamine) for both a charged (acetylthiocholine) and neutral (phenyl acetate) AChE substrate (see Appendix, 5). We provided support for the steric blockade model and nonequilibrium assumption by showing that propidium bound to the peripheral site slowed the entry and exit of equilibrating acylation site ligands huperzine A and TMTFA (by factors up to 300 fold) but had only a small thermodynamic effect on the ligand equilibrium dissociation constant (Figure 1, see Appendix, 5).

### *Substrate binding at the peripheral site*

Our combined kinetic studies and computational simulations allowed us to extend the steric blockade model to explain several other well known but poorly understood catalytic properties of AChE in Szegeletes et al., 1999 (see Appendix, 6). At high acetylthiocholine substrate concentrations, our initial simulated data involving propidium inhibition deviated somewhat from the experimental data. This deviation was abolished by the inclusion of steps in the catalytic pathway describing the formation and dissociation of product and by the proposal that propidium bound to the peripheral site blocked product dissociation (Scheme 1, see Appendix, 6). Experimental evidence for acetylthiocholine binding to the peripheral site was obtained in competition binding studies where this substrate was found to be completely competitive with propidium and partially competitive with fasciculin for enzyme binding (Figure 2, see Appendix, 6). These observations indicated that substrate binding to the peripheral site was an initial step in the catalytic pathway and could lead to the well-known phenomenon of substrate inhibition (7). Substrate inhibition was previously hypothesized to occur when substrate concentration was high enough for a second substrate molecule to occupy the acylation



or peripheral site and prevent catalysis. Our extended model showed that substrate binding to the peripheral site can promote catalysis at low substrate concentration but inhibit it at high substrate concentration because of steric blockade of product dissociation (6). These observations led us to the hypothesis that the AChE peripheral site has evolved to serve as an initial substrate-docking site on the enzyme that precedes transfer of the substrate to the acylation site for catalysis. A consequence of this hypothesis is that this initial docking of substrate to the peripheral site accelerates hydrolysis by improving the apparent affinity of substrate for the enzyme ( $K_{app}$ ). This acceleration, resulting from an increase in the number of productive enzyme-substrate encounter complexes and a decrease in amount of substrate dissociation prior to catalysis, represents a novel form of molecular optimization for an enzyme catalyzed reaction. More importantly for our long term project goals, this strongly supports the targeting of the AChE peripheral site for the design of ligands to modify enzyme specificity or activity.

#### *Organophosphorylation and peripheral site inhibition*

The results from the research described above (see Appendix, 5; 6), in conjunction with previous work from this laboratory (8; 9), provided the most detailed information to date on the process of peripheral site inhibition of AChE. It is crucial to our proposed research project, however, to elucidate the effect of peripheral site inhibitors on the hydrolysis and subsequent inactivation of AChE by toxic OPs. In Mallender et al., 1999 (see Appendix, 10), we initiated studies of peripheral site inhibition of AChE organophosphorylation using two, fluorogenic OPs. Positively charged DEPQ (7-diethoxyphosphoryloxy-N-methylquinolinium) and neutral EMPC (7-methylethoxyphosphonyloxy-4-methylcoumarin) were used because their phosphorylation of AChE can be measured by both classical enzyme-inactivation assays (11) and by direct observation of the release of their fluorescent leaving group (10). Also, OPs obey classical equilibrium kinetics with AChE because they equilibrate in the active site before phosphorylating the active site S200 residue. Our steric blockade model predicted that propidium would be relatively ineffective as an inhibitor of equilibrating ligands and substrates at the acylation site of AChE. Thus, examination of peripheral site inhibition of OP hydrolysis served as further evaluation of our steric blockade hypothesis. Consistent with our steric blockade model, propidium had relatively modest effects on the second-order rate of phosphorylation (see Appendix, 10).

In contrast to these results, the larger polypeptide inhibitor fasciculin dramatically decreased the phosphorylation rate constants upon binding to the AChE peripheral site ( $10^3$  to  $10^5$  fold). This pronounced inhibition of both the first- and second-order phosphorylation rates was further evidence of a conformational change in the AChE acylation site uniquely resulting from fasciculin binding at the peripheral site (8). Comparison of phosphorylation data obtained by fluorometry with data obtained by enzyme inactivation measurements revealed a striking discrepancy for measurements obtained in the presence of saturating amounts of fasciculin. Bound fasciculin decreased the second-order phosphorylation rate constants only 2 - 5 fold when measured by enzyme inactivation methods (see Appendix, 10). This raised the concern that the AChE activity observed during inactivation by OPs did not arise from the fasciculin bound AChE. Indeed, varying the ratio of OP/AChE in the presence of saturating fasciculin indicated that a small portion of the AChE in the sample was reacting with DEPQ as if fasciculin was not inhibiting the enzyme (see Appendix, 10). We were able to quantify this population of "fasciculin inhibition-resistant" enzyme by careful titration of AChE with DEPQ in the presence and absence of saturating concentrations of fasciculin (see Appendix, 10). Examination of

stopped-flow measurements of the release of fluorescent OP product in the presence of saturating fasciculin also confirmed the presence of more than one OP hydrolysis rate (see Appendix, 10). This population of fasciculin inhibition-resistant AChE could be neutralized by pretreatment of the AChE-fasciculin sample with a small quantity of DEPQ, yielding EMPC phosphorylation rates with fasciculin-bound AChE that were in good agreement with data obtained from fluorometric assays (see Appendix, 10). The discovery of this fasciculin inhibition-resistant AChE population is significant because it obscures kinetic properties of the AChE-fasciculin complex measured by enzyme inactivation methods used frequently in the AChE literature (10; 11).

\* UNPUBLISHED DATA; [REDACTED]

#### *Role of D72 in substrate and ligand binding*

To this point in the research project we have focused on clarifying the role of the peripheral site in the catalytic pathway of AChE (5; 6; 10). Specifically, we now have the ability to monitor individual catalytic steps during the hydrolysis of equilibrating and nonequilibrating AChE substrates in the presence and absence of peripheral site ligands. We decided to further examine the location of substrate binding in the AChE peripheral site. As discussed earlier, in 6 we deduced that acetylthiocholine binds to the peripheral site during catalysis because of its ability to partially compete with fasciculin for binding to the enzyme. Propidium on the other hand is completely competitive with both fasciculin and acetylcholine (6; 12). Crystal structures of the fasciculin-AChE complexes show that fasciculin makes extensive contacts with the peripheral site, occluding most of the peripheral site surface from any interaction with substrate (13; 14). However, the crystal structures did reveal that residue D72 in the peripheral site was slightly too deep in the gorge to make direct contact with fasciculin and that free volume remained near D72 where acetylthiocholine could bind and still allow fasciculin association. Molecular modeling studies have indicated that the area around D72 is occupied by propidium upon AChE binding (see Appendix, 5; 15). Previous studies have also demonstrated that D72 is an important residue in determining the hydrolysis rates of acetylcholine and cationic organophosphates (15-17).

To determine whether substrate could bind in the peripheral site at D72, we constructed the human D72G mutant and measured its ability to bind substrate at the peripheral site. These studies were also conducted with wild type and the D72G mutant of *Torpedo californica* AChE to assess the importance of D72 in substrate binding at the peripheral site in AChE from another species. We also examined the effects of bound fasciculin on the rate of OP hydrolysis by human D72G to determine whether D72 plays a role in the mechanism of AChE inhibition by fasciculin. Substrate inhibition and fasciculin competition assays showed that D72 was indeed required for the binding of acetylthiocholine to the peripheral site of human AChE (Figure 3, see Appendix, 18). The D72G mutation caused significant increases in both the  $K_s$  (substrate affinity in the peripheral site as measured by fasciculin competition) and the  $K_{ss}$  (substrate inhibition constant). The effect was not as pronounced in the *Torpedo* D72G mutant indicating that AChE from different species may possess slightly different molecular surfaces for binding substrate in the peripheral site. When examining OP hydrolysis by D72G AChE, we confirmed previous studies by showing that D72 was responsible for the enhanced reactivity of cationic OPs with AChE (10; 17; 18). Examination of peripheral site inhibition with D72G and organophosphorylation did reveal unexpected results. As seen with wild type AChE, propidium was relatively ineffective as an inhibitor of organophosphorylation (as predicted by our steric blockade model) while fasciculin was still able to dramatically reduce the rate of OP hydrolysis

(see above and 10; 18). Surprisingly, the inhibitory effect of fasciculin on the maximal catalytic turnover rate ( $k_{OP}$ ) for the neutral EMPC was dramatically reduced in the D72G mutant (18). Collectively, our analyses of the D72G mutation have determined that this residue plays a significant role in the function of this enzyme. First, we have shown that D72 serves as an initial docking site for substrate at the peripheral site, serving to optimize the catalytic activity of the enzyme at low substrate concentration by lowering  $K_{app}$  (18). Second, we have determined that D72 is critical for the transmission of conformational signals from the peripheral site to the acylation site upon fasciculin binding. Even though D72 does not contact with fasciculin, it may regulate a structural feature of AChE that influences fasciculin binding and inhibitory activity.

#### *Cyclic ligand design and screening*

In addition to our biochemical studies of the enzyme mechanism, we have been equally engaged in efforts to identify novel peripheral site specific ligands that may serve as protective compounds against organophosphorylation. The ideal AChE protective peripheral site ligand must exclude OPs from the acylation site while not significantly interfering with acetylcholine passage. Our search for such ligands has focused on cyclic peptide and pseudopeptide compounds. Cyclic peptide or pseudopeptide molecules have a variety of advantages that we intend to exploit during the course of our studies. First, a cyclic molecule is shaped like a ring in which the pore can be designed, in theory, with appropriate molecular properties (i.e. exclude passage of bulky OPs while allowing smaller acetylcholine to pass). Relatively small cyclic compounds consisting of 6 to 8 amino acids possess the necessary space to permit passage of acetylcholine. The incorporation of both natural and unnatural amino acids permits the use of combinatorial methods to synthesize an enormous number of cyclic compounds in libraries of various size. Finally, cyclic peptides are conformationally constrained and amenable to available molecular modeling software.

Most of our cyclic libraries have been prepared using side chain resin attachment. This involves a benzyl ester linkage to traditional Merrifield polystyrene resin or to *para*-methylbenzhydrylamine (MBHA) resin depending on whether an Asp, Asn or Gln residue is the point of attachment. These attachment methods can be combined with various methods of  $\alpha$ -carboxyl protection, as well as with standard Boc or Fmoc-based methods of solid phase peptide chain elongation. Peptide products were purified to homogeneity by passing them through a reversed phase HPLC column via solid phase extraction followed by elution with various polarity solvents (i.e. water with increasing acetonitrile). Product purity and identity in the initial elution fraction was confirmed with electrospray ionization mass spectrometry. The lyophilized peptides were then submitted for analysis of AChE binding activity and specificity with two assays formatted for high throughput screening in a microtiter plate reader. First, each peptide is assayed for inhibition of steady-state acetylthiocholine hydrolysis in a standard AChE activity assay (19). Second, each product is tested for the ability to compete with fasciculin and decrease fasciculin association rates in a continuous AChE activity assay where fasciculin association rates are examined (8).

Our initial efforts consisted of screening large libraries of cyclic peptides synthesized with random amino acid sequences. These libraries were designed to examine the effect of ring size (5- to 9- member cyclic peptides), peptide backbone (D- amino acids, L- amino acids, unnatural peptide linkages (thioether, aminosubstituted)), and amino acid side chain composition (charge, hydrophobicity, aromaticity). Screening over 400 hundred libraries consisting of several million individual compounds detected a large variety of compounds that could inhibit

AChE activity from 0 to 75% and fasciculin association from 0 to 45% (data not shown). Despite the vast number of compounds that were indicated as positive in these screening assays, several common features began to emerge from the libraries screened. First, most of the libraries that gave positive results possessed amino acid sequences with positively charged residues. Second, there was a clear preference in binding and inhibitory activity for libraries with 7- and 8-residue cyclic peptides. The diversity of libraries identified in this screening procedure is very encouraging, as it demonstrates that numerous amino acid sequences have potential as AChE peripheral site specific inhibitors.

With the information gained from our initial screening of random peptide libraries, we initiated the directed design of the next series of cyclic compound libraries using the peptide inhibitor fasciculin as the prototype. Fasciculin serves as an excellent example of the kind of AChE inhibitor that would be necessary for the protection of the enzyme from OPs. Fasciculin is specific for the AChE peripheral site and displays an impressive affinity for the enzyme ( $K_D \sim 10 - 20 \text{ pM}$ ) (8; 20). Furthermore, the structure of fasciculin consists of three finger-like loops protruding from a central disulfide linked core (21). This makes the sequence of fasciculin amenable for the design of small cyclic peptide structures. Previous studies have shown that disulfide linked cyclic peptides based on the loops of fasciculin could bind to AChE and inhibit enzyme activity, but with affinities that were  $10^5$  times lower than the natural toxin (22). We have employed molecular modeling using the crystal structure of the AChE-fasciculin complex (13; 14) to design individual cyclic peptides and peptide libraries based on the primary amino acid sequence of loop II of fasciculin. This loop of fasciculin displays the greatest area of contact when in complex with the AChE peripheral site. Our initial efforts focused on cyclic peptides based on the fasciculin primary sequence of cyclo[Arg-Arg-His-Pro-Pro-Lys-Met-Xxx], where Xxx serves as the resin bound attachment point (Asp, Asn, Glu, or Gln) (Figure 4). Screening of eight individual cyclic peptides based on this structure, with amino acid variations at position 1 (L/D Ala, Phe, Pro and Tyr) showed that all of these compounds could significantly inhibit AChE activity (>80%) and fasciculin association (>80%). More encouraging was the finding that several of these compounds continued to display AChE binding at concentrations as low as  $1 \text{ }\mu\text{M}$ , indicating that these compounds have significant specificity and affinity for the AChE peripheral site (Figure 5).

Upon closer examination of the AChE-fasciculin crystal structure, computational evaluation of the buried surface area between loop II and the AChE peripheral site indicated several fasciculin amino acids in our cyclic peptide structure that do not make direct contact with the enzyme. Since these amino acids do not make direct contact with AChE, the amino acids at these positions can be varied using combinatorial methods to evaluate the effect of different side chains or peptide linkages on cyclic peptide activity. Such methods include the use of positional scanning and library deconvolution to assess the effect of amino acid composition. These methods have been used previously to rediscover a naturally occurring peptide ligand from large combinatorial libraries (23). We constructed three peptide libraries where one of the three amino acids was fixed and the other two positions consisted of equal amounts of the total amino acid pool tested. For this screen, the pool of amino acids tested at the three variable positions were L/D - Pro, Arg, Tyr, Leu, and Ser, resulting in a total of 30 libraries with a total of 100 individual peptides per library. Two individual peptide compounds were also synthesized for comparison (WMA-I-77-31/32, cyclo[Arg-Ala/Arg-His-Pro-Pro-Lys-Met-Asn]). These libraries displayed maximum AChE inhibition values of >85% and maximum fasciculin association inhibition values of >70%, similar to the original fasciculin-mimetic compounds (data not shown).

Furthermore, several of these libraries displayed AChE binding activity when diluted to total library concentrations below 1  $\mu$ M, corresponding to an individual peptide concentration of less than 10 nM. The inhibitory activity of these libraries may result from the collective binding of all the peptide compounds or from the binding of only a small number of peptides, and thus the affinity of the inhibitory libraries could span a wide range.

The next set of cyclic peptide compounds was designed to test the effect of different attachment residues on the function of the cyclic peptides. Our most recent libraries have used Asn as the attachment residue instead of Asp to remove the negative charge Asp would have after cleavage from the synthesis resin. For this set of peptides, we tested the difference between L, D - Asn and L, D - Gln on a fasciculin loop mimetic peptide (cyclo[Arg-Ala-His-Pro-Pro-Lys-Met-Asn/D-Asn/Gln/D-Gln]). In our AChE inhibition and fasciculin association competition assays, these four compounds showed similar effectiveness as the previous set of cyclic libraries (Figure 6). Similarly, these compounds showed AChE binding activity at concentrations as low as 100 nM, suggesting affinities in the low  $\mu$ M range. Furthermore, our screening results indicated that the peptides using L - Gln (PJR-V-95-1) showed slightly higher activity against AChE in both sets of assays (Figure 6). Our most recent characterization of compound PJR-V-95-1 includes a complete series of steady state inhibition measurements for  $K_i$  determination (Figure 7). This peptide displays a  $K_i$  of 27  $\mu$ M and behaves as a noncompetitive inhibitor of AChE hydrolysis, consistent with the results from our initial screening for enzyme inhibition and fasciculin competition at the peripheral site. Future cyclic peptide libraries will be constructed to further probe the possible modifications of fasciculin based structures on AChE binding activity. We also intend to incorporate novel backbone modifications (bicyclic crosslinking or  $\alpha$ ,  $\alpha$ -substituted amino acids (see Appendix)) to further restrain the conformation of our cyclic compounds and presumably increase their potential affinity for the AChE peripheral site.

## KEY RESEARCH ACCOMPLISHMENTS

- Introduction of nonequilibrium analysis of AChE substrate and inhibitor interaction by experimentation and computational analyses.
- Proposal and validation of steric blockade model of AChE inhibition by small peripheral site ligands. Refinement of nonequilibrium analysis to include steps involving product formation, product dissociation and peripheral site binding of substrate. Application of models to explain the phenomenon of substrate inhibition
- Analysis of the effect of peripheral site inhibition on organophosphorylation. Further validation of steric blockade model of AChE peripheral site inhibition with equilibrating organophosphate substrates. Identification of a small percentage of AChE that is resistant to fasciculin inhibition and demonstration that this population obscures organophosphate inactivation measurements of the fasciculin-AChE complex.
- Identification of D72 as a key residue in substrate binding at the AChE peripheral site. Confirmation that D72 is responsible for the preferential hydrolysis of cationic organophosphate substrates by AChE. Determination that D72 plays a role in the transmission of a conformational change induced upon fasciculin binding that results in AChE inhibition.
- Construction and screening of a large number of cyclic peptide libraries to determine the general properties that foster AChE peripheral site binding and inhibition. Implementation of molecular modeling to use the naturally occurring loops of the high affinity, peripheral site inhibitor fasciculin for the design of cyclic peptide compounds. Screening and identification of fasciculin loop mimetics that possess specificity and affinity for the AChE peripheral site.

## REPORTABLE OUTCOMES

### PAPERS

Szegletes, T., Mallender, W. D. and Rosenberry, T. L. (1998). Nonequilibrium analysis alters the mechanistic interpretation of inhibition of acetylcholinesterase by peripheral site ligands. *Biochemistry* **37**: 4206-4216

Romanovskis, P. and Spatola, A.F. (1998). Preparation of head-to-tail cyclic peptides via side-chain attachment: Implications for library synthesis. *J. Peptide Res.* **52**, 356-374.

Szegletes, T., Mallender, W. D., Thomas, P. J. and Rosenberry, T. L. (1999). Substrate binding to the peripheral site of acetylcholinesterase initiates enzymatic catalysis. Substrate inhibition arises as a secondary effect. *Biochemistry* **38**: 122-133

Mallender, W. D., Szegletes, T. and Rosenberry, T. L. (1999). Organophosphorylation of acetylcholinesterase in the presence of peripheral site ligands: Distinct effects of propidium and fasciculin. *J. Biol. Chem.* **274**: 8491-8499

Szegletes, T., Mallender, W. D., Morel, N., Bon, S., Massoulie, J. and Rosenberry, T. L. (1999). Acetylthiocholine binds to Asp 74 at the peripheral site of human acetylcholinesterase prior to entry to the acylation site. *Manuscript to be submitted.*

### ABSTRACTS

Mallender, W.D., Ma, W., Spatola, A.F., and Rosenberry, T.L. (1999) Directed design of novel high affinity, peripheral site acetylcholinesterase ligands to defend the enzyme against inactivation by organophosphates. *Biochemistry and Molecular Biology 99, American Society for Biochemistry and Molecular Biology*, May 1999.

Romanovskis, P. and Spatola, A.F. (1999) Cyclic peptides with  $\alpha$ ,  $\alpha$ -disubstituted glycine derivatives. *16th American Peptide Symposium*, July 1999.

### FUNDING APPLIED FOR BASED ON THIS RESEARCH

Muscular Dystrophy Association, Application for Neuromuscular Disease Research Development Grant, 1999. "The Acetylcholinesterase Peripheral Site as a Target for Drug Design", P.I. Dr. William D. Mallender. Submitted July 1999.

## CONCLUSIONS

We have introduced and confirmed both by experimentation and computer simulation, an alternative nonequilibrium analysis of the steady-state inhibition patterns of AChE. This analysis includes a steric blockade model which assumes that the primary effect of a small ligand bound to the peripheral site is to decrease the association and dissociation rate constants for an acylation site ligand with little effect on the equilibrium constant for ligand binding to the acylation site. Using this form of kinetic analysis and our new model for peripheral site inhibition, we concluded that the inhibition of AChE by small peripheral site ligands such as propidium occurs without invoking any conformational interaction between the peripheral site and the acylation site. Furthermore, we have determined that the physiological role of the AChE peripheral site is to accelerate hydrolysis at low substrate concentration by serving as the initial binding site for substrate. This binding event at the peripheral site optimizes catalytic efficiency by increasing the number of productive associations between enzyme and substrate while decreasing the amount of substrate dissociation prior to catalysis. By including substrate binding to the peripheral site as the initial step in the AChE catalytic pathway, we have been able to explain the well-known phenomenon of substrate inhibition as a blockade of product dissociation when substrate saturates the peripheral site. In addition to our studies with acetylthiocholine, we have also examined the hydrolysis of equilibrating substrates such as OPs. As predicted by our steric blockade model, small peripheral site ligands such as propidium were relatively ineffective as inhibitors of organophosphorylation. In contrast, the polypeptide neurotoxin fasciculin dramatically reduced phosphorylation rate constants when bound to AChE. This pronounced inhibition served as further evidence of a conformational change in AChE upon fasciculin binding. During these studies, we also identified small sub-populations of enzyme that were resistant to fasciculin inhibition even at saturating fasciculin concentrations. We have further examined substrate binding at the peripheral site of AChE by analysis of the D72G mutant enzyme. We have shown using substrate inhibition and fasciculin competition assays that D72 is the residue to which acetylthiocholine binds in the peripheral site of human AChE. Along with our biochemical analysis of AChE and AChE inhibition, we have continued our efforts to design cyclic peptide and pseudopeptide structures with specificity for the peripheral site. Our current studies with peptides based on the primary sequence of fasciculin we have identified lead peptides with significant affinity and specificity for the AChE peripheral site. Collectively, the results of our efforts thus far represent one of the most complete analyses of the AChE mechanism of catalysis and inhibition reported to date. We are now applying the information gained from these studies into the design and screening of new AChE specific ligands for the defense of the enzyme from OP poisoning.

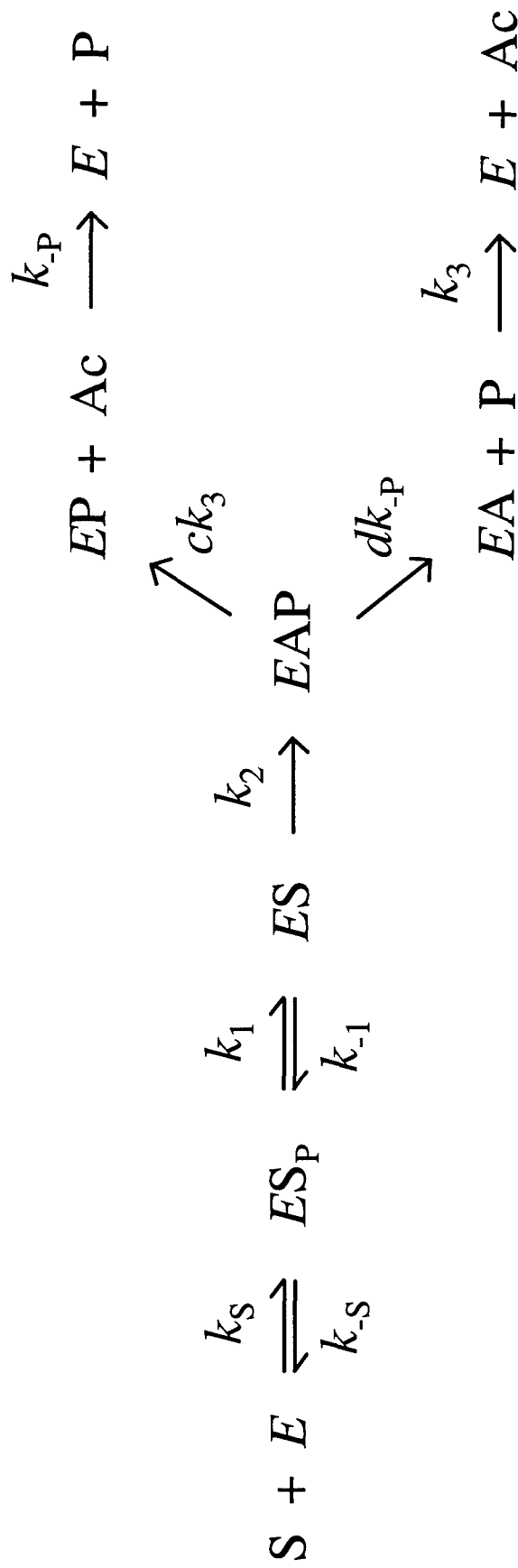


## REFERENCES

1. Rosenberry, T. L. (1975). *Proc. Nat. Acad. Sci. USA* **72**: 3834-3838
2. Sussman, J. L., Harel, M., Frolow, F., Oefner, C., Goldman, A., Toker, L. and Silman, I. (1991). *Science* **253**: 872-879
3. Barak, D., Ordentlich, A., Bromberg, A., Kronman, C., Marcus, D., Lazar, A., Ariel, N., Velan, B. and Shafferman, A. (1995). *Biochemistry* **34**: 15444-15452
4. Ordentlich, A., Barak, D., Kronman, C., Flashner, Y., Leitner, M., Segall, Y., Ariel, N., Cohen, S., Velan, B. and Shafferman, A. (1993). *J. Biol. Chem.* **268**: 17083-17095
5. Szegletes, T., Mallender, W. D. and Rosenberry, T. L. (1998). *Biochemistry* **37**: 4206-4216
6. Szegletes, T., Mallender, W. D., Thomas, P. J. and Rosenberry, T. L. (1999). *Biochemistry* **38**: 122-133
7. Radic, Z., Reiner, E. and Taylor, P. (1991). *Mol. Pharmacol.* **39**: 98-104
8. Eastman, J., Wilson, E. J., Cervenansky, C. and Rosenberry, T. L. (1995). *J. Biol. Chem.* **270**: 19694-19701
9. Rosenberry, T. L., Rabl, C. R. and Neumann, E. (1996). *Biochemistry* **35**: 685-690
10. Mallender, W. D., Szegletes, T. and Rosenberry, T. L. (1999). *J. Biol. Chem.* **274**: 8491-8499
11. Radic, Z. and Taylor, P. (1999). *Chem.-Biol. Interact.* **119-120**: 111-117
12. Eastman, J., Wilson, E. J., Cervenansky, C. and Rosenberry, T. L. (1995). In: **Enzymes of the Cholinesterase Family, Proceedings of the 5th International Meeting on Cholinesterases**, (Quinn, D. M., Balasubramanian, A. S., Doctor, B. P. and Taylor, P., ed.), Plenum Press, New York, pp. 209-217
13. Harel, M., Kleywegt, G. J., Ravelli, R. B. G., Silman, I. and Sussman, J. L. (1995). *Structure* **3**: 1355-1366
14. Bourne, Y., Taylor, P. and Marchot, P. (1995). *Cell* **83**: 503-512
15. Barak, D., Kronman, C., Ordentlich, A., Ariel, N., Bromberg, A., Marcus, D., Lazar, A., Velan, B. and Shafferman, A. (1994). *J. Biol. Chem.* **269**: 6296-6305
16. Radic, Z., Pickering, N. A., Vellom, D. C., Camp, S. and Taylor, P. (1993). *Biochemistry* **32**: 12074-12084
17. Hosea, N. A., Radic, Z., Tsigelny, I., Berman, H. A., Quinn, D. M. and Taylor, P. (1996). *Biochemistry* **35**: 10995-11004
18. Szegletes, T., Mallender, W. D., Morel, N., Bon, S., Massoulie, J. and Rosenberry, T. L. (1999). *Manuscript in preparation*.
19. Ellman, G. L., Courtney, K. D., Andres, J., V. and Featherstone, R. M. (1961). *Biochem. Pharmacol.* **7**: 88-95
20. Karlsson, E., Mbugua, P. M. and Rodriguez-Ithurralde, D. (1984). *J. Physiol. (Paris)* **79**: 232-240

21. le Du, J. H., Marchot, P., Bourgis, P. E. and Fontecilla-Camps, J. C. (1992). *J. Biol. Chem.* **267**: 22122-22130
22. Falkenstein, R. J. and Pena, C. (1997). *Biochemica et Biophysica Acta* **1340**: 143-151
23. Spatola, A. F., Crozet, Y., deWit, D. and Yanagisawa, M. (1996). *J. Med. Chem.* **39**: 3842-3846

Scheme 1



Modified catalytic pathway of AChE. The catalytic pathway has been altered to contain steps for the initial binding of substrate to the peripheral site ( $ES_P$ ) and the formation and dissociation of products (**Ac and P**) (see 6).

## Figure Legends

Figure 1. Determination of association and dissociation rate constants for TMTFA with both AChE and the AChE-propidium complex. AChE (50 - 800 pM) was incubated with TMTFA (0.03 - 320 nM) and propidium (0 - 100  $\mu$ M) and aliquots were assayed for AChE activity at various times. Assay points ( $v$ ) were normalized to parallel control assays ( $v_{\text{TMTFA}=0}$ ) containing identical [AChE] and [propidium] but without TMTFA. First, reaction time courses for 6 association and 5 dissociation reactions in the absence of propidium were simultaneously fit using the SCOP simulation program. Then reaction time courses for 5 association reactions containing 100  $\mu$ M propidium and 8 dissociation reactions containing 20 - 100  $\mu$ M propidium were simultaneously fit. *Panel A.* Assay points and calculated fits to 4 association reactions containing 100  $\mu$ M propidium, 800 pM AChE, and TMTFA (total concentration: -O- 320 nM; - $\square$ - 64 nM; - $\Delta$ - 33 nM; - $\diamond$ - 6.4 nM). *Panel B.* Assay points and calculated lines to 4 dissociation reactions containing propidium (-O- 0  $\mu$ M; - $\square$ - 20  $\mu$ M; - $\Delta$ - 40  $\mu$ M; - $\diamond$ - 100  $\mu$ M), AChE (total concentration: -O- 62 pM; - $\square$ - 250 pM; - $\Delta$ - 620 pM; - $\diamond$ - 620 pM), and TMTFA (total concentration: -O- 77 pM; - $\square$ - 310 pM; - $\Delta$ - 770 pM; - $\diamond$ - 770 pM) (see 5).

Figure 2. Acetylthiocholine binding to the AChE peripheral site. *Panel A.* The hydrolysis rate  $v$  ( $\Delta A_{412 \text{ nm}}/\text{min}$ ) for the approach to equilibrium fasciculin (F) binding was measured with 10 mM acetylthiocholine, 50 pM AChE, F (a, 5 nM; b, 3 nM; c, 2 nM; d, 1 nM), and buffered 50 mM NaCl by continuous spectrophotometric assay. Rate constants ( $k$ ) obtained were then plotted against the fasciculin concentration to obtain  $k_{\text{on}}$  (plot not shown). *Panel B.* The dependence of  $k_{\text{on}}$  on the acetylthiocholine concentration was examined. Indicated points representing the average of three or four  $k_{\text{on}}$  measurements (except at 15 mM) were fitted to give apparent  $K_S$  estimates of  $3.6 \pm 1.0$  mM in the absence of propidium (O) and  $0.6 \pm 0.1$  mM with 20  $\mu$ M propidium ( $\Delta$ ). A mean  $K_S$  of 1.5 mM was used to assign  $k_S$  and to generate *both* lines representing the simulated dependence of  $k_{\text{on}}$  on [S] (see 6).

**\* UNPUBLISHED DATA:**

Figure 3. Acetylthiocholine binding to the peripheral site of human AChE. Reaction mixtures with varying amounts of acetylthiocholine were supplemented with NaCl such that [S] + [NaCl] = 60 mM to maintain constant ionic strength. *Panel A.* Substrate inhibition with acetylthiocholine. Points represent initial velocities ( $\mu\text{M}/\text{min}$ ) measured at the indicated substrate concentrations with wild type (-O-) or D72G (- $\square$ -) AChE (90 pM). Lines fitted with the Haldane equation were virtually superimposable with those shown and gave  $K_{\text{app}} = 88 \pm 4$   $\mu$ M and  $K_{\text{SS}} = 20 \pm 1$  mM for wild type AChE and  $K_{\text{app}} = 1610 \pm 80$   $\mu$ M and  $K_{\text{SS}} = 330 \pm 70$  mM for the D72G mutant. *Panel B:* Inhibition of fasciculin 3 binding by acetylthiocholine. Association rate constants  $k_{\text{on}}$  for fasciculin 3 measured at the indicated substrate concentrations with wild type (-O-) or D72G (- $\square$ -) AChE were determined (data not shown). Points represent one series of  $k_{\text{on}}$  measurements, and lines were obtained by fitting  $k_{\text{FP}}/k_{\text{F}}$  to  $0.52 \pm 0.06$  (wild type) or  $0.6 \pm 0.5$  (D72G). A line for the wild type AChE closely to that shown and gave  $K_S = 1.3 \pm 1.0$  mM and  $k_{\text{FP}}/k_{\text{F}} = 0.52 \pm 0.06$  (18).

Figure 4. Structure of cyclic octapeptide lead analog. Primary sequence of cyclic peptide is cyclo[Arg-Ala-His-Pro-Pro-Lys-Met-Xxx] where Xxx varies between L,D-Asn ( $n = 1$ ) and L,D-Gln ( $n = 2$ ).

## ~~UNPUBLISHED DATA:~~

Figure 5. Screening of cyclic peptide series WMA-I-76 for AChE binding activity. Cyclic peptides, based on the loop II primary sequence of fasciculin, were assayed for the ability to bind to AChE at the peripheral site. The peptide sequence tested was cyclo[Arg-Arg-His-Pro-Pro-Lys-Met-Xxx], where Xxx was Asn and position 1 was varied with amino acids L,D-Ala, Phe, Pro and Tyr. *Panel A.* Cyclic inhibitors were incubated with AChE (33 pM) and tested for inhibition of enzyme activity under standard assay conditions (19). Results are plotted as percentage inhibition of reaction velocities ( $\Delta A_{412 \text{ nm}}/\text{min}$ ) based on controls without cyclic peptide inhibitors. *Panel B.* Cyclic inhibitors were incubated with AChE (400 pM) and tested for the ability to retard the association rate of fasciculin (2 nM) under standard assay conditions (19). Rates of approach to equilibrium,  $k$ , were calculated for each reaction and results are plotted as percentage competition based on controls without cyclic peptide inhibitors.

Figure 6. Screening of cyclic peptide series PJR-V for AChE binding activity. The effect of different attachment residues was tested on the AChE binding activity of cyclic peptides based on loop II of fasciculin. The peptide sequence tested was cyclo[Arg-Ala-His-Pro-Pro-Lys-Met-Xxx], where Xxx was varied with amino acids L,D-Asn and L,D-Gln. *Panel A.* Cyclic inhibitors were incubated with AChE (33 pM) and tested for inhibition of enzyme activity under standard assay conditions (19). Results are plotted as percentage inhibition of reaction velocities ( $\Delta A_{412 \text{ nm}}/\text{min}$ ) based on controls without cyclic peptide inhibitors. *Panel B.* Cyclic inhibitors were incubated with AChE (400 pM) and tested for the ability to retard the association rate of fasciculin (2 nM) under standard assay conditions (19). Rates of approach to equilibrium,  $k$ , were calculated for each reaction and results are plotted as percentage competition based on controls without cyclic peptide inhibitors.

Figure 7. Steady state inhibition of AChE hydrolysis of acetylthiocholine by cyclic peptide inhibitor. *Panel A.* Reciprocal plots of initial velocities ( $\Delta A_{412 \text{ nm}}/\text{min}$ ) and substrate concentrations were determined. Cyclic peptide PJR-V-95-1 concentrations in A were 0 (O), 10  $\mu\text{M}$  ( $\square$ ), and 30  $\mu\text{M}$  ( $\Delta$ ). *Panel B.* The slopes of plots in A were normalized by dividing by the slope in the absence of inhibitor and plotted against the inhibitor concentration to derive  $K_i$  values for PJR-V-95-1 of  $26.5 \pm 5.4 \mu\text{M}$ .

Figure 1

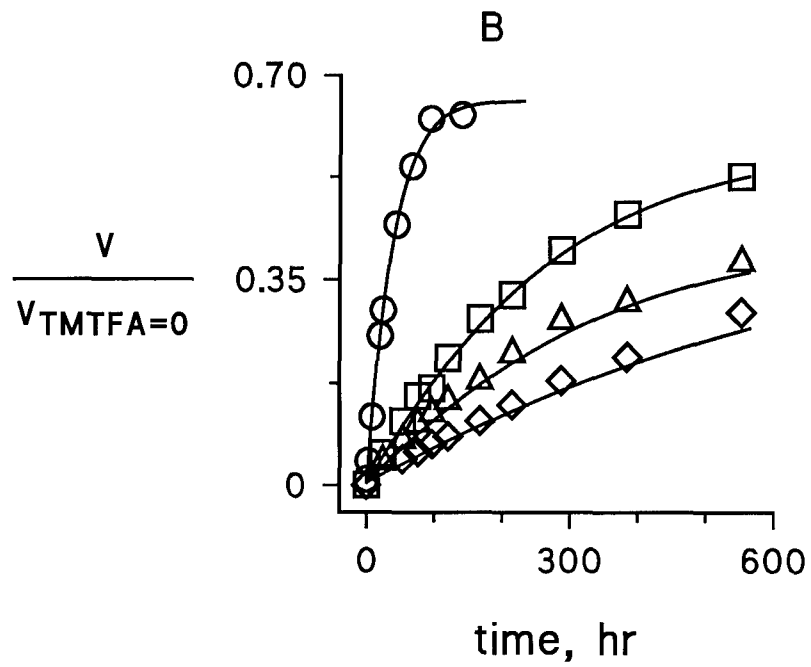
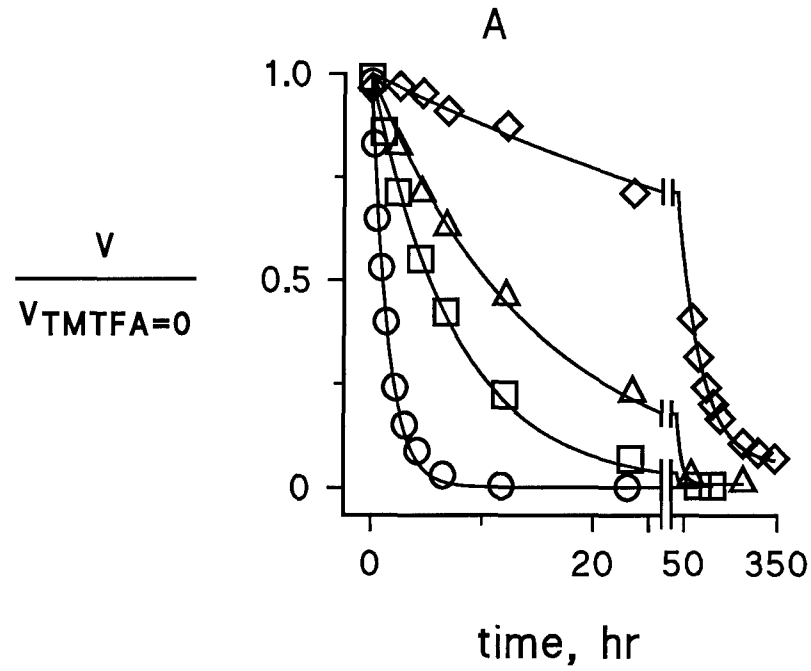


Figure 2

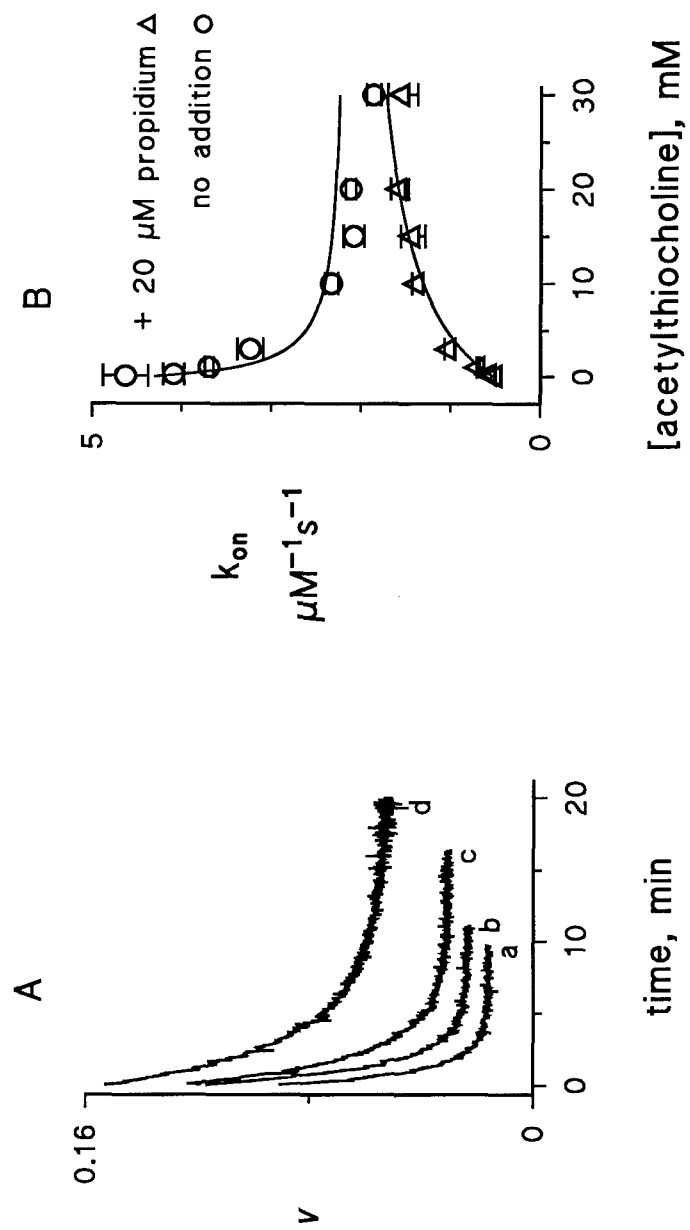


Figure 3

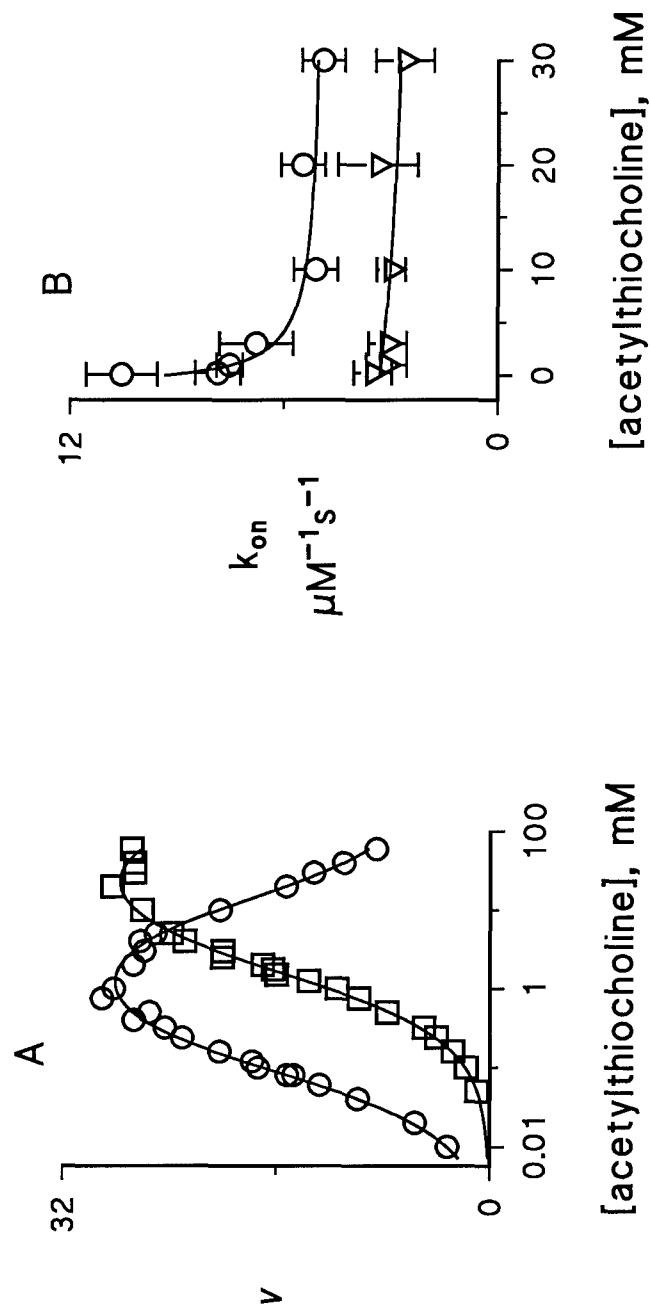
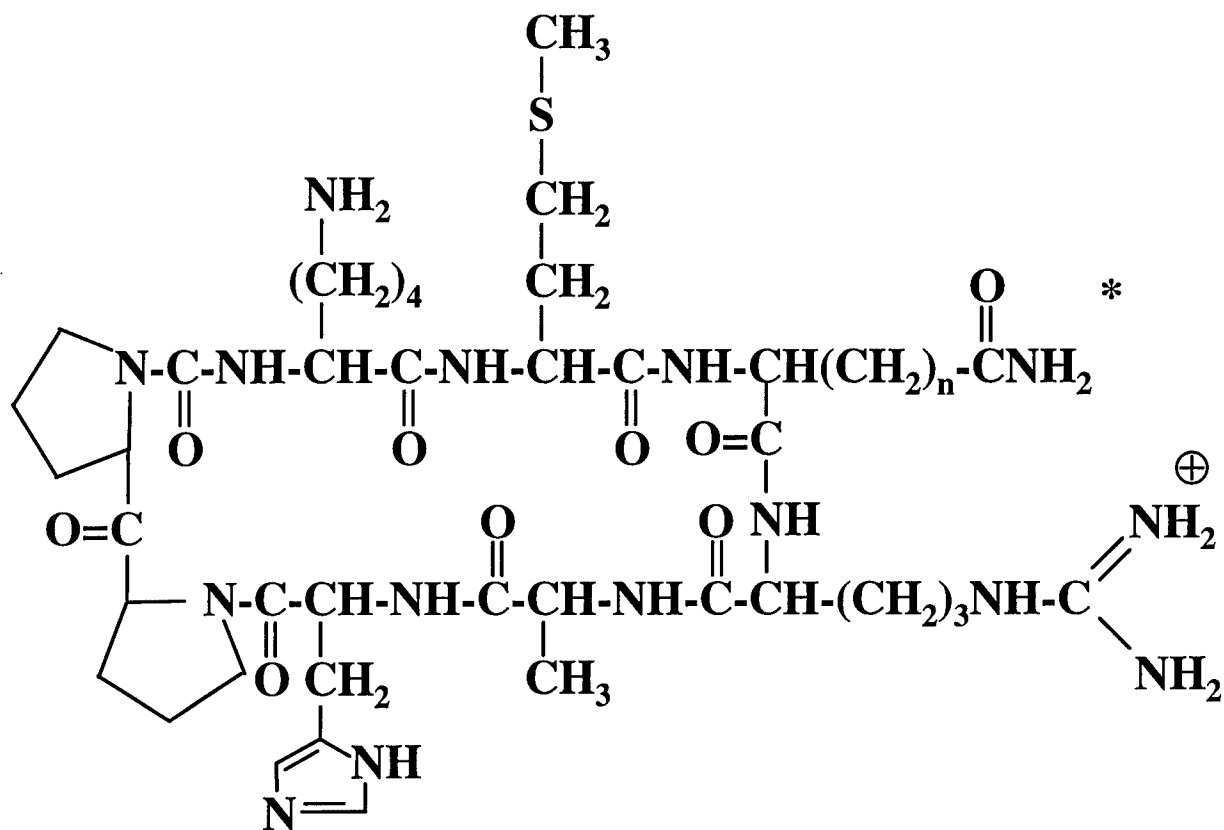




Figure 4



\*n = 1, Asn and D-Asn; n = 2, Gln and D-Gln

Figure 5

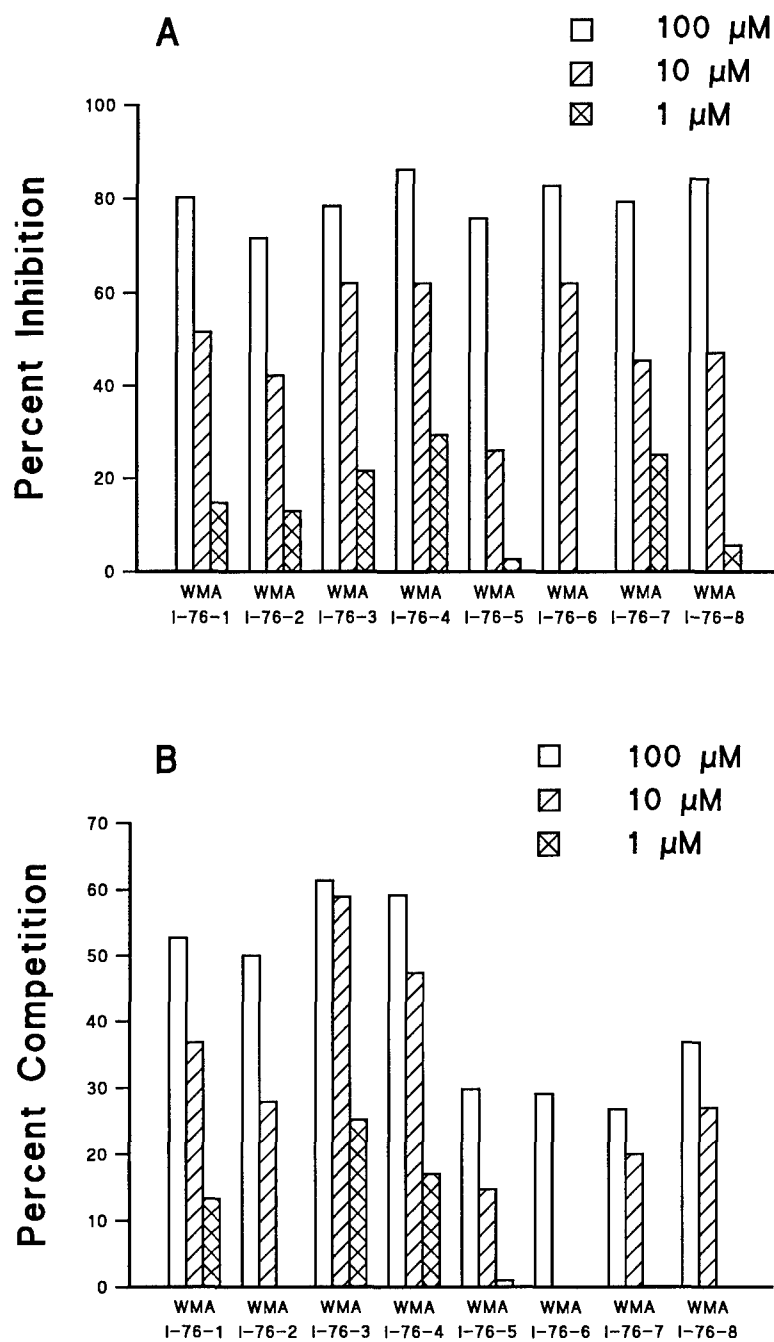


Figure 6

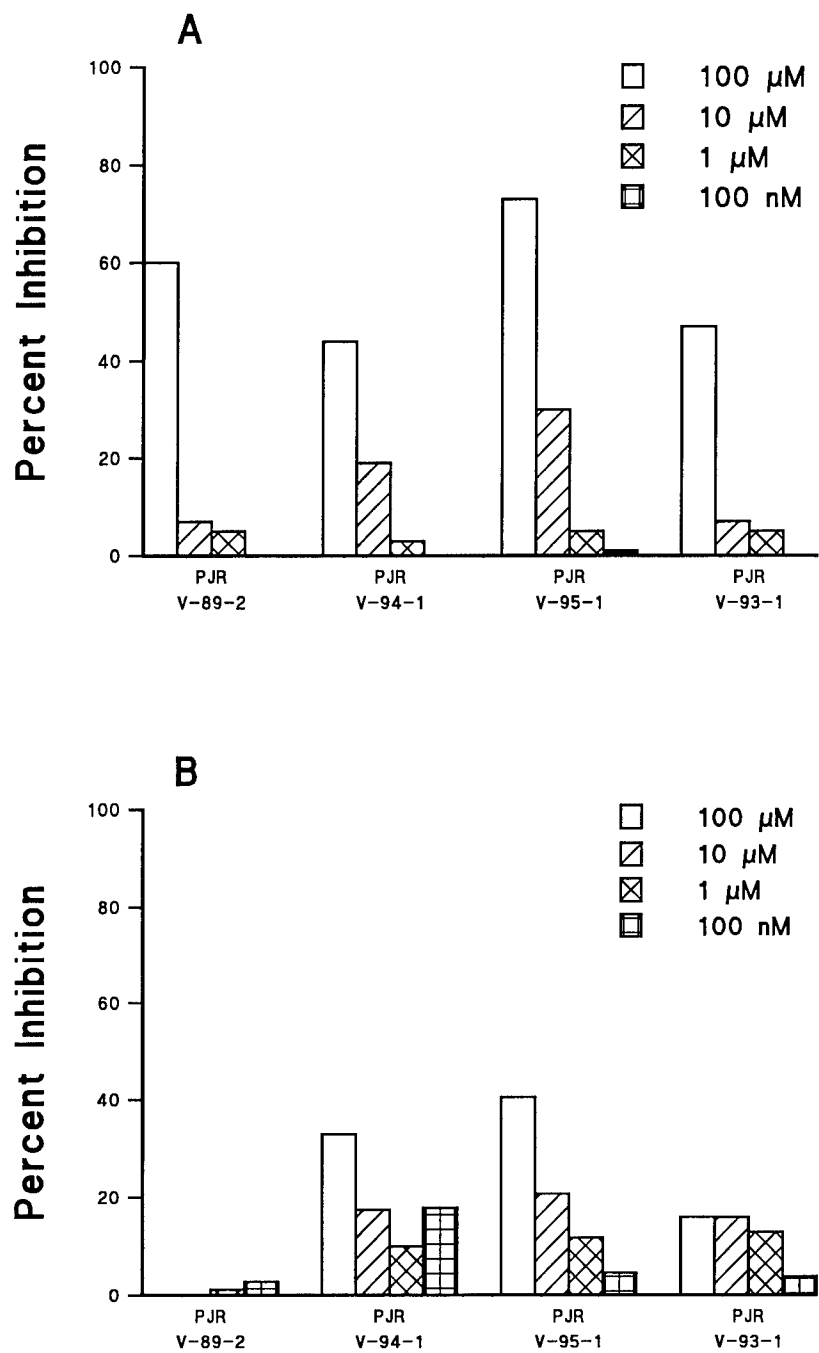
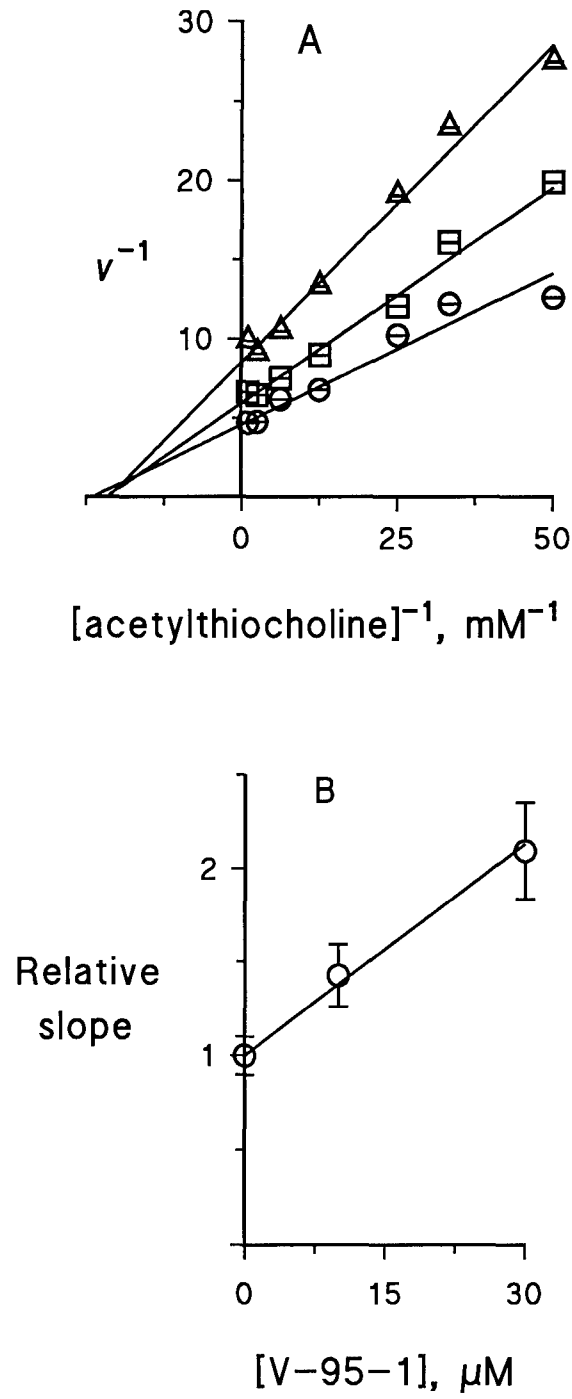


Figure 7



## Published Abstracts

*Presented at the American Society for Biochemistry and Molecular Biology 1999 Meeting*

### **DIRECTED DESIGN OF NOVEL HIGH AFFINITY, PERIPHERAL SITE ACETYLCHOLINESTERASE LIGANDS TO DEFEND THE ENZYME AGAINST INACTIVATION BY ORGANOPHOSPHATES**

William D. Mallender<sup>#</sup>, Wanli Ma<sup>\*</sup>, Arno F. Spatola<sup>\*</sup> and Terrone L. Rosenberry<sup>#</sup>.

<sup>#</sup> Department of Research, Mayo Clinic Jacksonville, Jacksonville, FL 32224.

<sup>\*</sup> Department of Chemistry, University of Louisville, Louisville, KY 40292.

Acetylcholinesterase (AChE) hydrolyzes its physiological substrate, acetylcholine, at one of the highest known catalytic rates. Various studies of AChE have demonstrated two sites of ligand interaction: an acylation site near the catalytic triad at the base of the active site gorge which is transiently acetylated at S200 during substrate turnover, and a peripheral site at the entrance to the gorge. Organophosphates (compounds found in pesticides and chemical warfare agents) inactivate AChE by phosphorylating S200 in a nearly irreversible fashion. Currently, there are compounds available to reactivate AChE by accelerating dephosphorylation, but no compounds exist for pre-treatment to protect AChE during exposure to organophosphate agents. In our studies, molecular modeling has been used to examine the interactions between AChE and the peripheral site-specific ligand fasciculin II, a small snake venom neurotoxic peptide. With such information, novel cyclic peptide and pseudopeptide compounds are being prepared by combinatorial techniques and assayed for selective binding to the peripheral site of AChE. In conjunction with these efforts, studies with site-directed AChE mutants and fluorogenic organophosphates are underway to better define how the peripheral site participates in the binding and catalysis of these toxic substrates. Our goal is to identify new peripheral site ligands that enhance substrate selectivity of the enzyme, preventing phosphorylation while permitting near physiological rates of acetylcholine hydrolysis.

*Presented at the American Peptide Symposium 1999 Meeting*

### **CYCLIC PEPTIDES WITH $\alpha,\alpha$ -DISUBSTITUTED GLYCINE DERIVATIVES.**

**Peteris Romanovskis** and Arno F. Spatola from Department of Chemistry, University of Louisville, Louisville, KY 40292, U.S.A.

Cyclic analogs of linear peptides represent promising candidates for the generation of structural diversity in search of new biologically active compounds [Romanovskis, P.; Spatola, A. F. *J. Peptide Res.*, **52**, 356-(1998)]. They can also serve as scaffolding for creation of peptidomimetics, thus expanding the diversity. This report deals with the synthesis of conformationally constrained head-to-tail cyclic peptides. It is known that bulky substituents on amide nitrogens can facilitate cyclization [Ehrlich, A. et al., *J. Org. Chem.*, **61**, 88331 (1996)]; however, less is known about the impact of C $^{\alpha,\alpha}$ -disubstituted amino acid residues on cyclization. We have explored the use of "di-UPS" (unnatural peptide synthesis with  $\alpha,\alpha$ -disubstituted glycine) chemistry [Scott, W. L. et al., *Tetrahedron Lett.*, **38**, 3695 (1997)], in conjunction with Boc(Fmoc)/ONB and Fmoc/OtBu strategies for the solid phase synthesis of BQ-123 (endothelin antagonist) and its retroinverso analogs. Our approach involves attachment of the first amino

acid to the solid support through its side chain, chain elongation and/or introduction of the C<sup>α,α</sup>-disubstituted residue (either as a building block or through di-UPS), completion of the peptide chain, and on-resin cyclization. During the di-UPS procedure, we faced the following: di-UPS reaction control; stability of trifunctional amino acid side chains during the course of di-UPS; overalkylation and transesterification; difficulties with acylation of bulky C<sup>α,α</sup>-disubstituted residues; and lability of the "twisted amides" during HF cleavage. Attempts to obtain cyclic model peptides with C<sup>α,α</sup>-disubstituted amino acids next to proline so far have failed (presumably because of the lability of the Xxx-Pro bond under strong acidic conditions). Nevertheless, with appropriate precautions, insertion of an α,α-disubstituted amino acid in cyclic peptides is possible both by direct substitution as well as by the di-UPS procedure. [Supported by NIH GM33376 and U.S. Army/Mayo Clinic Jacksonville.]

# Nonequilibrium Analysis Alters the Mechanistic Interpretation of Inhibition of Acetylcholinesterase by Peripheral Site Ligands<sup>†</sup>

Tivadar Szegletes, William D. Mallender, and Terrone L. Rosenberry\*

Department of Pharmacology, Mayo Foundation for Medical Education and Research, and Department of Research, Mayo Clinic Jacksonville, Jacksonville, Florida 32224

Received August 29, 1997; Revised Manuscript Received November 13, 1997

**ABSTRACT:** The active site gorge of acetylcholinesterase (AChE) contains two sites of ligand binding, an acylation site near the base of the gorge with a catalytic triad characteristic of serine hydrolases, and a peripheral site at the mouth of the gorge some 10–20 Å from the acylation site. Many ligands that bind exclusively to the peripheral site inhibit substrate hydrolysis at the acylation site, but the mechanistic interpretation of this inhibition has been unclear. Previous interpretations have been based on analyses of inhibition patterns obtained from steady-state kinetic models that assume equilibrium ligand binding. These analyses indicate that inhibitors bound to the peripheral site decrease acylation and deacylation rate constants and/or decrease substrate affinity at the acylation site by factors of up to 100. Conformational interactions have been proposed to account for such large inhibitory effects transmitted over the distance between the two sites, but site-specific mutagenesis has failed to reveal residues that mediate the proposed conformational linkage. Since examination of individual rate constants in the AChE catalytic pathway reveals that assumptions of equilibrium ligand binding cannot be justified, we introduce here an alternative nonequilibrium analysis of the steady-state inhibition patterns. This analysis incorporates a steric blockade hypothesis which assumes that the only effect of a bound peripheral site ligand is to decrease the association and dissociation rate constants for an acylation site ligand without altering the equilibrium constant for ligand binding to the acylation site. Simulations based on this nonequilibrium steric blockade model were in good agreement with experimental data for inhibition by the peripheral site ligands propidium and gallamine at low concentrations of either acetylthiocholine or phenyl acetate if binding of these ligands slows substrate association and dissociation rate constants by factors of 5–70. Direct measurements with the acylation site ligands huperzine A and *m*-(*N,N,N*-trimethylammonio)trifluoroacetophenone showed that bound propidium decreased the association rate constants 49- and 380-fold and the dissociation rate constants 10- and 60-fold, respectively, relative to the rate constants for these acylation site ligands with free AChE, in reasonable agreement with the nonequilibrium steric blockade model. We conclude that this model can account for the inhibition of AChE by small peripheral site ligands such as propidium without invoking any conformational interaction between the peripheral and acylation sites.

Acetylcholinesterase (AChE)<sup>1</sup> hydrolyzes its physiological substrate acetylcholine at one of the highest known catalytic rates (1), and the unique features of AChE structure that determine its catalytic power have been pursued for many years. A major advance occurred with the X-ray crystallographic determination of the three-dimensional structure of *Torpedo californica* AChE (TcAChE) (2). This structure revealed an active site gorge lined with aromatic residues that is about 20 Å deep. Two sites of ligand interaction in AChE were first demonstrated in ligand binding studies (3) and later confirmed by crystallography, site-specific mutagenesis, and molecular modeling: an *acylation site* at the base of the gorge and a *peripheral site* at its mouth. In the

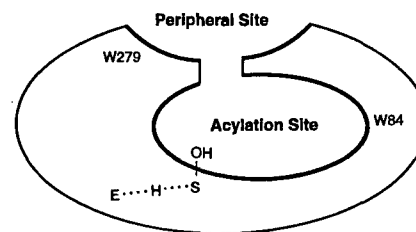


FIGURE 1: Schematic diagram of the sites for ligand binding in AChE.

acylation site (Figure 1) residue S200 (TcAChE sequence numbering) is acylated and deacylated during substrate turnover, H440 and E327 participate with S200 in a catalytic triad (E–H–S), and W84 binds to the trimethylammonium group of acetylcholine as acyl transfer to S200 is initiated. The peripheral site involves other residues including W279 (4–9). Ligands can bind selectively to either the acylation or the peripheral sites, and ternary complexes with distinct ligands bound to each site can form (3). Peripheral site ligands that form these ternary complexes include the

<sup>†</sup> This work was supported by Grant NS-16577 from the National Institutes of Health and by grants from the Muscular Dystrophy Association of America. W.D.M. was supported by a Kendall-Mayo Postdoctoral Fellowship.

\* To whom correspondence should be addressed.

<sup>1</sup> Abbreviations: AChE, acetylcholinesterase; TcAChE, acetylcholinesterase from *Torpedo californica*; DTNB, 5,5'-dithiobis(2-nitrobenzoic acid); TMTFA, *m*-(*N,N,N*-trimethylammonio)trifluoroacetophenone.

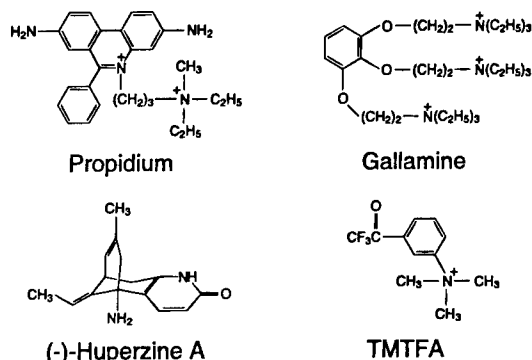
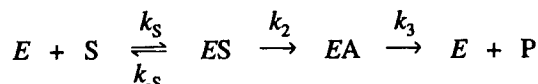


FIGURE 2: Structures of peripheral site and acylation site ligands.

phenanthridinium derivative propidium (Figure 2) and the fasciculins, a family of very similar snake venom neurotoxins composed of 61-amino acid polypeptides (10, 11).

In this paper we address the question of how ligand binding to the peripheral site alters AChE catalytic activity. While it is well documented that ligand binding to this site can inhibit substrate hydrolysis, the mechanism of this inhibition is less clear. Specifically, an understanding of the inhibition mechanism may depend on whether the substrate and inhibitor are equilibrated with AChE. This point can be examined in the conventional pathway for the hydrolysis of acetylcholine (S) by AChE (E) in Scheme 1.<sup>2</sup> The initial

Scheme 1



enzyme-substrate complex *ES* proceeds to an acylated enzyme intermediate *EA* which is then hydrolyzed to product *P* and *E* (see ref 12). Under classical steady-state conditions (13), hydrolysis rates *v* vary with [*S*] according to the Michaelis-Menten equation (eq 1a) to give the maximum hydrolysis rate *V*<sub>max</sub>, the apparent first-order rate constant *k*<sub>cat</sub>, and the second-order rate constant *k*<sub>cat</sub>/*K*<sub>app</sub> (eqs 1b and 1c).

$$v = \frac{d[P]}{dt} = \frac{V_{\max}[S]}{[S] + K_{\text{app}}} \quad (1a)$$

$$\frac{V_{\max}}{[E]_{\text{tot}}} = k_{\text{cat}} = \frac{k_2 k_3}{k_2 + k_3} \quad \frac{k_{\text{cat}}}{K_{\text{app}}} = \frac{k_S k_2}{k_S + k_2} \quad (1b, 1c)$$

One way in which AChE has optimized these rate constants is by accelerating the acylation step *k*<sub>2</sub> so that it exceeds *k*<sub>cat</sub> (eq 1b), which for AChE is about 10<sup>4</sup> s<sup>-1</sup> (1). Of more importance to the arguments here, *k*<sub>2</sub> also exceeds *k*<sub>-S</sub> (1, 14). As a result, *ES* is not in equilibrium with *E* and *S*. The failure of *ES* to equilibrate with *E* and *S* is readily accommodated by eq 1c: *k*<sub>cat</sub>/*K*<sub>app</sub> approaches *k*<sub>S</sub>, the substrate association rate constant. However, when an inhibitor binds to the nonequilibrated *ES* intermediate, the steady-state inhibition patterns present a greater challenge. The conventional interpretation of the classic noncompetitive inhibition pattern, for example, assumes that *ES* is equilibrated (see

ref 15). We avoid this equilibrium assumption here for the first time in the AChE literature by solving the appropriate differential rate equations with the simulation program SCoP. In particular, we examine the simple hypothesis that the only effect of peripheral site inhibitors such as propidium is to impose a steric blockade that decreases association and dissociation rate constants for substrates without altering their ratio, the equilibrium association constant. We test this hypothesis also by examining the effect of peripheral site ligands on the rate constants for the binding of acylation site inhibitors. Our results indicate that failure to achieve equilibrium can have a profound impact on the classical interpretation of AChE inhibition and indeed alter mechanistic conclusions.

## EXPERIMENTAL PROCEDURES

**Materials.** Human erythrocyte AChE was purified as outlined previously and active site concentrations were determined by assuming 410 units/nmol (16, 17). (-)-Huperzine A and propidium iodide were purchased from Calbiochem and gallamine triethiodide from Aldrich Chemical Co. Huperzine A concentrations were adjusted with an extinction coefficient<sup>3</sup>  $\epsilon_{308 \text{ nm}} = 10400 \text{ M}^{-1} \text{ cm}^{-1}$ . TMTFA was kindly provided by Dr. Daniel Quinn (University of Iowa), and stock TMTFA concentrations were calibrated by titration with AChE.

**Steady-State Measurements of AChE-Catalyzed Substrate Hydrolysis.** Hydrolysis rates *v* were measured at various substrate (*S*) concentrations in buffer composed of 20 mM sodium phosphate and 0.02% Triton X-100 at pH 7.0 and 25 °C unless otherwise indicated. Acetylthiocholine assay solutions (1 mL) included 0.33 mM DTNB, and hydrolysis was monitored by formation of the thiolate dianion of DTNB at 412 nm ( $\Delta\epsilon_{412 \text{ nm}} = 14.15 \text{ mM}^{-1} \text{ cm}^{-1}$  (18)) for 1–5 min on a Varian Cary 3A spectrophotometer (19). Acetylthiocholine concentrations were low enough (<0.5 mM) in the absence of inhibitors (20) that compensation for substrate inhibition was unnecessary. Hydrolysis rates for phenyl acetate (0.2–5 mM, ≤1% methanol final) were measured in 1-ml assay solutions at 270 nm ( $\Delta\epsilon_{270 \text{ nm}} = 1.40 \text{ mM}^{-1} \text{ cm}^{-1}$ ) for 1–5 min (21). Reciprocal plots of *v*<sup>-1</sup> vs [*S*]<sup>-1</sup> at all inhibitor (*I*) concentrations here were linear, and slopes and intercepts of these plots were calculated by weighted linear regression analyses which assumed that *v* has a constant percent error. Nonlinear regression analyses of these slopes and intercepts vs [*I*] were conducted with Fig.P (BioSoft, version 6.0) as described, with slope and intercept values weighted by the reciprocal of their variance (also see ref 22).

**Simulations of Kinetic Equations.** When the reversible reactions in Scheme 2 below are not at equilibrium, the corresponding differential equations were solved with the program denoted SCoP (version 3.51) developed at the NIH National Center for Research Resources and available from Simulation Resources, Inc. (Berien Springs, MI). A model file was constructed with differential equations for each enzyme intermediate except *E* and with values of all rate constants. Mass conservation was introduced by substitution of  $[E] = [E]_{\text{tot}} - \sum [M]$ , where  $[E]_{\text{tot}}$  is the total concentration

<sup>2</sup> Scheme 1 assumes substrate concentrations low enough that *ESS* or *EAS* species leading to substrate inhibition are negligible (see ref 1).

<sup>3</sup> Personal communication from B. P. Doctor, Walter Reed Army Institute of Research, Washington, DC.



Table 1: Inhibition of AChE-Catalyzed Hydrolysis of Acetylthiocholine by Propidium<sup>a</sup>

case	$k_S$ ( $\mu\text{M}^{-1} \text{s}^{-1}$ )	$k_{-S}$ ( $\text{s}^{-1}$ )	$k_2, k_3$ ( $\text{s}^{-1}$ )	$k_1$ ( $\mu\text{M}^{-1} \text{s}^{-1}$ )	$k_{-1}$ ( $\text{s}^{-1}$ )	$k_{S2}$ ( $\mu\text{M}^{-1} \text{s}^{-1}$ )	$k_{-S2}$ ( $\text{s}^{-1}$ )	$K_{\text{app}}^b$ (mM)	$K_I^b$ ( $\mu\text{M}$ )	slope $\alpha^b$	intercept $\beta^b$
1	<b>200</b>	<b><math>3 \times 10^3</math></b>	<b><math>1.4 \times 10^4</math></b>	<b>200</b>	<b>200</b>	<b>3</b>	<b>45</b>	0.043	1.00	0.0197	$0.09 \pm 0.01$
2	200	$3 \times 10^3$	$1.4 \times 10^4$	200	200	<b>0.3</b>	<b>4.5</b>	0.043	1.01	$0.0033 \pm 0.0001$	$0.030 \pm 0.001$
3	200	$3 \times 10^3$	$1.4 \times 10^4$	200	200	<b>200</b>	<b><math>3 \times 10^3</math></b>	0.043	1.00	1.00	1.00
4	200	<b><math>3 \times 10^5</math></b>	$1.4 \times 10^4$	200	200	<b>3</b>	<b><math>4.5 \times 10^3</math></b>	0.79	1.00	0.26	$0.78 \pm 0.05$
5	200	<b><math>3 \times 10^7</math></b>	$1.4 \times 10^4$	200	200	3	<b><math>4.5 \times 10^5</math></b>	75	1.00	0.97	1.00

<sup>a</sup> Simulations for cases 1–5 were generated as outlined in the text with indicated rate constant values. Bold entries indicate a change from the previous case. Values of  $K_{\text{app}}$ ,  $K_I$  and  $\alpha$  and  $\beta$  were calculated by weighted least-squares analysis of replots as in Figure 4. <sup>b</sup> Standard errors were less than 2% of the mean unless otherwise indicated.

of enzyme and  $\Sigma [\text{M}]$  is the sum of the concentrations of all enzyme intermediates. An analogous mass conservation was introduced for  $[\text{S}]$ . Simulation and curve-fitting files were generated by SCoP from the model file by employing the numerical solver cloda. This solver for stiff and nonstiff sets of differential equations uses an improved Gear method (23, 24).

Rate constants used in these simulations (see Tables 1 and 2) were justified as follows. For acetylthiocholine, direct estimates of  $k_2$  and  $k_3$  (available only for eel AChE) gave  $k_2/k_3 = 1.3$  (25). Noting a 2-fold smaller  $k_{\text{cat}}$  of 7000  $\text{s}^{-1}$  for human AChE (26) and assuming  $k_2 = k_3$  for this enzyme, substitution into eq 1b gave  $k_2 = k_3 = 1.4 \times 10^4 \text{s}^{-1}$ . Solvent deuterium oxide ( $\text{D}_2\text{O}$ ) isotope effects provided an estimate of  $k_{-S}$ :  $k_{\text{cat}}$  for acetylthiocholine was slowed by a factor of  $2.03 \pm 0.05$  when  $\text{H}_2\text{O}$  was replaced by  $\text{D}_2\text{O}$ , a value close to a typical factor of 2.5 for enzyme-catalyzed steps that are rate limited by proton transfer (14), but  $k_{\text{cat}}/K_{\text{app}}$  decreased by a factor of only  $1.21 \pm 0.02$  in  $\text{D}_2\text{O}$  (22). Inserting this value in eq 1c and assuming that  $k_2$  decreased by a factor of 2.5 in  $\text{D}_2\text{O}$  while  $k_S$  and  $k_{-S}$  were unaffected, then  $k_2/k_{-S} = 6$  and, from  $k_2$  above,  $k_{-S} = 3 \times 10^3 \text{s}^{-1}$ . An estimate of  $k_S = 2 \times 10^8 \text{M}^{-1} \text{s}^{-1}$  was obtained by substitution of these values of  $k_2$  and  $k_{-S}$  and the observed value of  $K_{\text{app}} = 45 \mu\text{M}$  (see Table 2) into eq 1c. For phenyl acetate,  $k_{\text{cat}}$  was assumed equal to that of acetylthiocholine (1) and the same value of  $1.4 \times 10^4 \text{s}^{-1}$  was assigned for  $k_2$  and  $k_3$ . From observed  $\text{D}_2\text{O}$  isotope effects of  $2.45 \pm 0.08$  for  $k_{\text{cat}}$  and  $1.48 \pm 0.05$  for  $k_{\text{cat}}/K_{\text{app}}$  (22),  $k_2$  was assumed to decrease by a factor of 2.5 in  $\text{D}_2\text{O}$  while  $k_S$  and  $k_{-S}$  were unaffected, yielding  $k_2/k_{-S} = 2.1$  and  $k_{-S} = 7 \times 10^3 \text{s}^{-1}$ . These values together with the observed value of  $K_{\text{app}} = 1.31 \text{mM}$  (see Table 2) gave  $k_S = 8 \times 10^6 \text{M}^{-1} \text{s}^{-1}$  for phenyl acetate from eq 1c. For propidium and gallamine, an estimate of  $k_1 = 2 \times 10^8 \text{M}^{-1} \text{s}^{-1}$  was based on association rate constants of  $5 \times 10^7 \text{M}^{-1} \text{s}^{-1}$  for the bisquaternary ligand ambenonium (20) and  $4 \times 10^8 \text{M}^{-1} \text{s}^{-1}$  for *N*-methylacridinium (27) with human AChE. Values for  $k_{-1}$  were then calculated from  $k_{-1} = (k_1)(K_I)$ , where  $K_I$  was the observed equilibrium inhibition constant for propidium or gallamine (see Table 2).

**Slow Equilibration of an Acylation Site Ligand in the Presence of a Peripheral Site Inhibitor.** The slow interaction of an acylation site ligand (L) with AChE in the presence of a peripheral site inhibitor I as shown in Scheme 3 in the Results was analyzed by procedures used previously (22) to describe the interaction of fasciculin 2 with AChE. Bovine serum albumin (1 mg/mL) was incubated overnight in buffer (20 mM sodium phosphate, 0.02% Triton X-100, pH 7.0) containing 0.33 mM 5,5'-dithiobis(2-nitrobenzoic acid)

(DTNB), and association reactions were initiated by adding AChE, the inhibitor propidium, and the acylation site ligand (huperzine A or TMTFA) at 23 °C. Except where indicated, binding was measured under pseudo-first-order conditions in which the concentration of ligand was adjusted to at least 10 times the concentration of AChE. At various times a 1.0-mL aliquot was removed to a cuvette, 40  $\mu\text{L}$  of acetylthiocholine and DTNB were added to final concentrations of 0.5 mM and 0.33 mM, respectively, and a continuous assay trace was immediately recorded at 412 nm. Background rates in the absence of AChE were subtracted. Dissociation reactions were measured by incubating ligand with AChE for 1–24 h, diluting  $\geq 200$ -fold to the indicated final concentrations, and assaying 1.0-mL aliquots as above.

Assay rates  $v$  from association and dissociation reactions of huperzine A and TMTFA were divided by control assay rates in the absence of these ligands ( $v_{\text{H}=0}$  or  $v_{\text{TMTFA}=0}$ ) to give a normalized value  $v_{(\text{N})}$ . For huperzine A these values were fitted by nonlinear regression analysis (Fig.P) to eq 2, where  $v_{(\text{N})\text{initial}}$  and  $v_{(\text{N})\text{final}}$  are the calculated values of  $v_{(\text{N})}$  at time zero and at equilibrium, respectively, and the observed

$$v_{(\text{N})} = v_{(\text{N})\text{final}} + (v_{(\text{N})\text{initial}} - v_{(\text{N})\text{final}})e^{-kt} \quad (2)$$

pseudo first-order rate constant  $k$  for the approach to equilibrium is given by eq 3.

$$k = k_{\text{on}}[\text{L}] + k_{\text{off}} \quad (3)$$

In eq 3,

$$k_{\text{on}} = \frac{k_L + k_{L2} \frac{[\text{I}]}{K_I}}{1 + \frac{[\text{I}]}{K_I}} \quad k_{\text{off}} = \frac{k_{-L} + k_{-L2} \frac{[\text{I}]}{K_{LI}}}{1 + \frac{[\text{I}]}{K_{LI}}} \quad (4a, 4b)$$

**Structure Analysis and Molecular Graphics.** Construction and analysis of three-dimensional models were performed on a Silicon Graphics workstation Indigo2 IMPACT using QUANTA96 modeling software (Molecular Simulations, Inc.). Modeling of the ternary TcAChE enzyme–inhibitor complexes began with the crystal structure coordinates for the TcAChE–huperzine A complex [Protein Data Bank (PDB) file: 1VOT] (28) and the TcAChE–TMTFA complex (PDB file: 1AMN) (29). Propidium was manually docked into the peripheral site as previously described (7). Briefly, the aromatic and alkyl portions of propidium were positioned in the peripheral site and active site gorge by avoiding unfavorable contacts with the TcAChE structure. The resulting structures were optimized by energy minimization

Table 2: Observed and Simulated Inhibition of AChE-Catalyzed Hydrolysis of Acetylthiocholine and Phenyl Acetate by Peripheral Site Ligands<sup>a</sup>

substrate inhibitor	observed parameters				simulated parameters <sup>b</sup>			
	$K_{app}$ (mM)	$K_I$ ( $\mu$ M)	$\alpha$	$\beta$	$k_{S2}/k_S$	$K_I^c$ ( $\mu$ M)	$\alpha^c$	$\beta$
acetylthiocholine	0.045 $\pm$ 0.003							
propidium		1.1 $\pm$ 0.1	0.019 $\pm$ 0.004	0.10 $\pm$ 0.01	0.015	1.00	0.0197	0.09 $\pm$ 0.01
gallamine		37 $\pm$ 2	0.019 $\pm$ 0.002	0.44 $\pm$ 0.03	0.015	35	0.0189	0.5 $\pm$ 0.1
phenyl acetate	1.31 $\pm$ 0.15							
propidium		0.8 $\pm$ 0.1	0.071 $\pm$ 0.008	0.46 $\pm$ 0.02	0.05	1.01	0.076	0.4 $\pm$ 0.1
gallamine		31 $\pm$ 5	0.25 $\pm$ 0.01	1.0 $\pm$ 0.1	0.2	39	0.27	0.95 $\pm$ 0.03

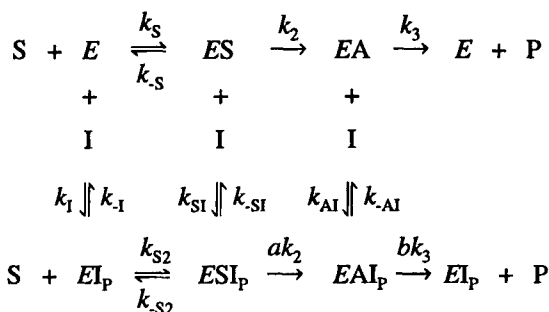
<sup>a</sup> Values of  $K_{app}$ ,  $K_I$ ,  $\alpha$ , and  $\beta$  were calculated by analysis of replots as in Figures 3 and 4. The ratio of  $k_{S2}/k_S$  in each simulation was assigned to give optimal agreement between the observed and simulated parameters. <sup>b</sup> Simulations were conducted with the rate constants from case 1 in Table 1 except as follows: When gallamine replaced propidium,  $k_{-1} = 6 \times 10^3 \text{ s}^{-1}$ ; when phenyl acetate replaced acetylthiocholine,  $k_S = 8 \mu\text{M}^{-1} \text{ s}^{-1}$  and  $k_{-S} = 7 \times 10^3 \text{ s}^{-1}$ ; with phenyl acetate and propidium,  $k_{S2} = 0.4 \mu\text{M}^{-1} \text{ s}^{-1}$  and  $k_{-S2} = 350 \text{ s}^{-1}$ ; and with phenyl acetate and gallamine,  $k_{S2} = 1.6 \mu\text{M}^{-1} \text{ s}^{-1}$  and  $k_{-S2} = 1.4 \times 10^3 \text{ s}^{-1}$ . Simulated  $K_{app}$  values were identical to the experimental  $K_{app}$ , as expected from the assignment of rate constants in Table 1. <sup>c</sup> Standard errors were less than 2% of the mean.

using the CHARMM module of QUANTA96 (conjugate gradient). Initial structural refinement included only the propidium and gorge solvent molecules while final optimization added all amino acid side chains vicinal to propidium and the acylation site ligand.

## RESULTS

**Equilibrium Model of AChE Inhibition.** When ligands bind to the peripheral site, AChE activity is often inhibited. The inhibitor (I) can bind to each of the three enzyme species from Scheme 1, as modeled in Scheme 2. For example,  $ESI_P$

Scheme 2



represents a ternary complex with S at the acylation site and I at the peripheral site (denoted by the subscript P). The acylation rate constant  $k_2$  is altered by a factor  $a$  in this ternary complex, and the deacylation rate constant  $k_3$  is altered by a factor  $b$  in the  $EAI_P$  complex. To characterize how a peripheral site ligand inhibits AChE, it is useful to know whether substrate affinities are altered and whether the relative rate constants  $a$  and  $b$  are less than 1 when the inhibitor is bound. Unfortunately, for acetylcholine and other carboxylester substrates, the acylation and deacylation rate constants are too fast to permit direct measurement by any rapid kinetic technique. Consequently, investigations of Scheme 2 have employed steady-state kinetic analyses based on extensions of the Michaelis–Menten expression. However, this approach is problematic. In contrast to the simple steady-state solution in the absence of inhibitor, the general steady-state solution for  $v$  in Scheme 2 is too complex for useful comparison to experimental data (30, 31). To obtain a more tractable simplified solution, it has invariably been assumed with AChE that the reversible reactions in Scheme 2 are at equilibrium (i.e.,  $k_{-S} \gg k_2$ ;  $k_{-S2} \gg ak_2$ ;  $k_{-SI} \gg k_2$ ;

$k_{-SI} \gg ak_2$ ;  $k_{-AI} \gg k_3$ ;  $k_{-AI} \gg bk_3$ ; 32; 33; see ref 22). This solution is given in eq 5, where  $K_X = k_{-X}/k_X$ .

$$v^{-1} = \frac{1}{V_{\max}} \left[ \frac{k_{\text{cat}} \left( 1 + \frac{[I]}{K_{SI}} \right)}{k_2 \left( 1 + \frac{a[I]}{K_{SI}} \right)} + \frac{k_{\text{cat}} \left( 1 + \frac{[I]}{K_{AI}} \right)}{k_3 \left( 1 + \frac{b[I]}{K_{AI}} \right)} + \frac{K_{\text{app}} \left( 1 + \frac{[I]}{K_I} \right)}{[S] \left( 1 + \frac{a[I]}{K_{SI}} \right)} \right] \quad (5)$$

Many inhibition patterns observed with AChE are consistent with eq 5. For example, propidium inhibition of phenyl acetate and acetylthiocholine hydrolysis gave the steady-state kinetic data in Figure 3a,b and Figure 4a,b. The slopes of the reciprocal plots in Figure 3a increased with propidium concentration (Figure 3b), and analyses of these slopes by eq 6 allowed estimation of  $K_I$ , the equilibrium dissociation

$$\frac{\text{slope } (v^{-1} \text{ vs } [S]^{-1})}{K_{\text{app}}/V_{\max}} = \frac{\left( 1 + \frac{[I]}{K_I} \right)}{\left( 1 + \frac{a[I]}{K_{SI}} \right)} \quad (6)$$

constant for I with E, and the experimental parameter  $\alpha$ . At saturating concentrations of I ( $[I] \gg K_I/\alpha$ ), the slope in eq 6 =  $K_{\text{app}}/\alpha V_{\max}$ . Therefore,  $\alpha$  is simply the ratio of the second-order rate constant with saturating I, which we denote  $k_{\text{cat}}'/K_{\text{app}}'$ , to that in the absence of I. When equilibrium is assumed as in eq 5,  $\alpha = aK_I/K_{SI} = aK_S/K_{S2}$ . Within an equilibrium framework, the low values of  $\alpha = 0.071$  for propidium and phenyl acetate in Figure 3b and 0.019 for propidium and acetylthiocholine in Figure 4b require either that  $ESI_P$  does not form ( $K_S/K_{S2} \approx 0$ ) or that  $a \approx 0$ . While these two possibilities can in principle be distinguished by analysis of the intercepts of the reciprocal plots in Figures 3a and 4a, contributions from inhibition of both acylation and deacylation complicate the interpretation (eq 5). For example, the intercepts in Figure 4b also increased with propidium concentration but in a less linear fashion than the slopes. If we denote  $\beta k_{\text{cat}}$  as the first-order hydrolysis rate constant for the pathway through the ternary complexes  $ESI_P$  and  $EAI_P$ , the intercept data in Figure 4b gave  $\beta = 0.10$ . Uncertainties in the ratio of  $k_2$  to  $k_3$  and in  $b$  make it difficult

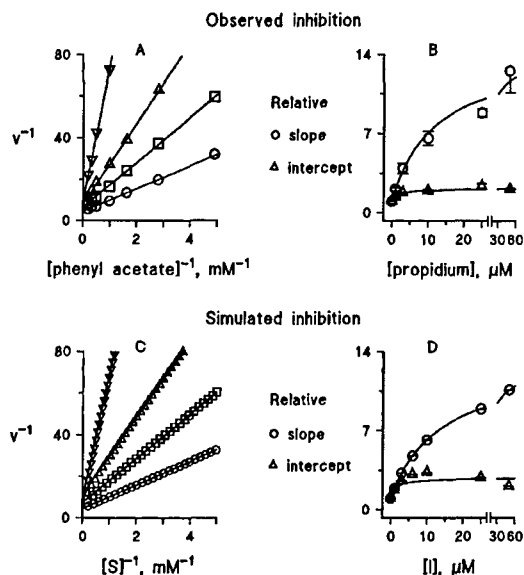


FIGURE 3: Observed and simulated inhibition of AChE-catalyzed phenyl acetate hydrolysis by propidium. Part A: Reciprocal plots of measured initial velocities (mM/min) and substrate concentrations were fitted by weighted linear regression analysis according to eq 5 at various fixed propidium concentrations ((O) 0  $\mu$ M, ( $\square$ ) 1  $\mu$ M, ( $\Delta$ ) 3  $\mu$ M, ( $\nabla$ ) 50  $\mu$ M) and 0.5 nM E. Four additional points are offscale and not shown. Part B: Slopes of reciprocal plots including those in part A were normalized by dividing by  $K_{app}/V_{max}$  (the slope in the absence of propidium) and fitted by weighted nonlinear regression analysis to eq 6 to give  $K_I = 0.8 \pm 0.1$  and  $\alpha = 0.071 \pm 0.008$  (see Table 2). Normalized intercepts of the reciprocal plots were fitted to an equation of the same form as eq 6 to give  $\beta = 0.46 \pm 0.02$  (see footnote 4 and Table 2). Part C: Plots of  $v^{-1}$  vs  $[S]^{-1}$  at various  $[I]$  ((O) 0  $\mu$ M; ( $\square$ ) 1  $\mu$ M; ( $\Delta$ ) 3  $\mu$ M; ( $\nabla$ ) 50  $\mu$ M) were generated by the SCoP simulation program with rate constant parameters listed for phenyl acetate and propidium in Table 2. Lines were extrapolated from linear regions of these plots encompassing  $[S] = 0.02K_{app}$  to  $0.2K_{app}$ . Part D: Slopes and intercepts of lines calculated as in part C were analyzed by replot analysis as in part B to obtain the simulated estimates of  $K_I$ ,  $\alpha$ , and  $\beta$  in Table 2.

to estimate a value of  $a$  from this value of  $\beta$ , and about all that can be concluded within this equilibrium model for propidium inhibition of acetylthiocholine hydrolysis is that  $a$  and/or  $b$  is at most 0.1. Values of  $\beta$  are useful, however, because they provide a basis for comparison of the experimental data with the simulated data below.

**Nonequilibrium Analysis of AChE Inhibition.** We noted in the Introduction that the equilibrium model assumes  $k_{-5} \gg k_2$  and that this assumption does not hold for acetylthiocholine hydrolysis by AChE. Nevertheless, the rate equation in eq 5 which assumes equilibrium can still fit the observed inhibition in Figure 4. Are the mechanistic conclusions that  $K_I/K_{SI} \approx 0$  or  $a \approx 0$  with propidium bound to the peripheral site invalid? To address this question it is necessary to solve the rate equations for Scheme 2 without equilibrium assumptions. This solution has not been examined previously because the corresponding differential equations cannot be solved analytically. These equations can be solved numerically with the SCoP simulation program if reasonable estimates of all rate constants in Scheme 2 are available. Rate constant assignments for acetylthiocholine or phenyl

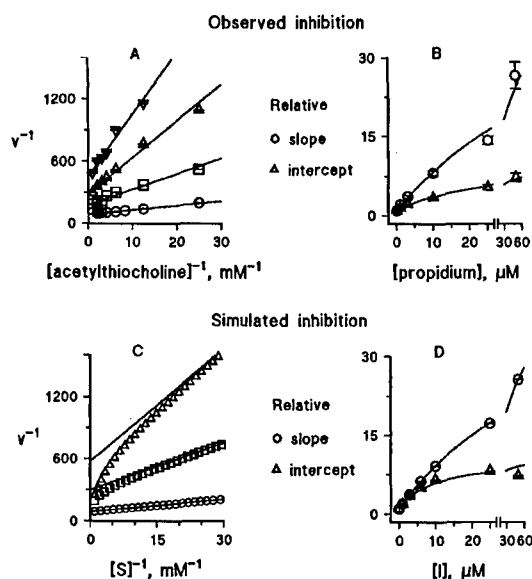


FIGURE 4: Observed and simulated inhibition of AChE-catalyzed acetylthiocholine hydrolysis by propidium. Analyses were conducted as in Figure 3. Part A: Reciprocal plots were obtained at fixed propidium concentrations ((O) 0  $\mu$ M, ( $\square$ ) 3  $\mu$ M, ( $\Delta$ ) 10  $\mu$ M, ( $\nabla$ ) 25  $\mu$ M) and 25 pM E. Two additional points are offscale and not shown. Part B: Normalized slopes and intercepts of reciprocal plots including those in part A were analyzed to give  $K_I = 1.1 \pm 0.1$ ,  $\alpha = 0.019 \pm 0.004$ , and  $\beta = 0.10 \pm 0.01$  (see Table 1, Case 1). Part C: Plots of  $v^{-1}$  vs  $[S]^{-1}$  at various  $[I]$  ((O) 0  $\mu$ M; ( $\square$ ) 3  $\mu$ M; ( $\Delta$ ) 10  $\mu$ M) were generated by the SCoP simulation program with rate constant parameters listed for acetylthiocholine and propidium in Table 2. Lines were extrapolated from linear regions of these plots encompassing  $[S] = 0.02K_{app}$  to  $0.2K_{app}$ . Part D: Slopes and intercepts of lines calculated as in part C were analyzed by replot analysis as in part B to obtain the simulated estimates of  $K_I$ ,  $\alpha$ , and  $\beta$  in Table 2.

acetate interaction alone with AChE were deduced as described in the Experimental Procedures and are shown in Table 1 (case 1, columns 2–4) or in Table 2. They are likely to be accurate within a factor of 2. Phenyl acetate hydrolysis by AChE also does not involve equilibrium substrate binding, and the primary difference between the assigned rate constants for acetylthiocholine and phenyl acetate was a lower value of  $k_5$  for phenyl acetate (see Experimental Procedures and footnote a in Table 2). Rate constants for propidium interaction with free AChE and the ES and EA intermediates in Scheme 2 are less certain, so we propose a simplifying hypothesis based on the location of the peripheral site at the mouth of the active site gorge. We hypothesize that the effect of propidium binding to this site is simply a steric blockade that decreases equally the association and dissociation rate constants for substrates without altering any other rate constants in Scheme 2. Thus, this steric blockade hypothesis postulates that bound propidium does not alter the thermodynamics of substrate interaction with AChE ( $K_{S2} = K_S$ ). It also stipulates that bound propidium has no effect on acylation and deacylation rate constants ( $a = b = 1$ ), and that bound substrate does not alter propidium interactions ( $k_1 = k_{SI} = k_{AI}$  and  $k_{-1} = k_{-SI} = k_{-AI}$ ). In this case values for only the two rate constants  $k_1$  and  $k_{-1}$  for propidium interaction are required. The key feature of the hypothesis is that bound propidium slows substrate entry into and exit from the acylation site ( $k_{S2} < k_5$  and  $k_{-S2} < k_{-5}$ ). The only experimental indication to date of the extent of this slowdown involves the effect of fasciculin 2 binding to the peripheral

<sup>4</sup>  $\beta^{-1}$  is defined as the maximal factor by which the intercepts in Figure 3b increased at high concentrations of propidium. Within the equilibrium framework in eq 5,  $\beta = ab(k_2 + k_3)/(ak_2 + bk_3)$  and  $\beta k_{cat} = abk_2k_3/(ak_2 + bk_3)$ .

site on *N*-methylacridinium binding to the acylation site: association and dissociation rate constants for *N*-methylacridinium decreased 8000- and 2000-fold, respectively, in the AChE–fasciculin 2 complex relative to those in free AChE (27). Steric blockade by the smaller propidium is likely to be less than that by fasciculin 2. In our simulations (Table 2 and Figures 3c and 4c) we assigned decreases in  $k_{S2}$  and  $k_{-S2}$  that gave optimal agreement with experimental data, but we also surveyed a range of decreases in these constants as described below.

The SCoP simulation procedure involved solving the set of differential equations corresponding to Scheme 2 to obtain  $v = d[P]/dt$ . By adjusting the total substrate and AChE amounts and the time, a series of calculated  $v$  and  $[S]$  pairs were generated as substrate was progressively converted to product at various fixed  $[I]$ . Transformation of these pairs to  $v^{-1}$  and  $[S]^{-1}$  produced reciprocal plots analogous to the experimental data in Figures 3 and 4. Simulated propidium inhibition of phenyl acetate hydrolysis with  $k_{S2}$  and  $k_{-S2}$  assigned at 5% of  $k_S$  and  $k_{-S}$ , respectively, is illustrated in Figure 3c. The simulated reciprocal plots were nearly linear over a substrate concentration range corresponding to that accessible experimentally in Figure 3a. Simulated case 1 in Table 1 for propidium and acetylthiocholine, in which  $k_{S2}$  and  $k_{-S2}$  were 1.5% of  $k_S$  and  $k_{-S}$ , respectively, is illustrated in Figure 4c. The reciprocal plots were linear at low substrate concentrations, but they deviated downward at concentrations corresponding to the higher substrate concentrations examined experimentally in Figure 4a. These deviations can be eliminated if our steric blockade hypothesis is extended to include a decrease in product dissociation rate constant by bound peripheral site ligand<sup>5</sup> (see Discussion). However, simulations from our initial hypothesis can account for inhibition observed over the lower substrate concentrations typically employed in inhibition analyses of AChE, as the following comparisons indicate. The slopes and intercepts of the linear regions of the simulated reciprocal plots ( $[S] < 0.2K_{app}$ ) increased as  $[I]$  became larger. The dependence of these slopes and intercepts on  $[I]$  was analyzed by nonlinear regression analyses (Figures 3d and 4d) exactly as done for the experimental data in Figures 3b and 4b. The corresponding curves (Figure 3b vs 3d and Figure 4b vs 4d) showed remarkable similarity, indicating that qualitatively our nonequilibrium hypothesis can account for inhibition of substrate hydrolysis by propidium. For a more quantitative comparison of the simulations with the experimental data, three parameters ( $K_I$ ,  $\alpha$ , and  $\beta$ ) were examined for propidium inhibition of acetylthiocholine and phenyl acetate hydrolysis (Table 2). The  $K_I$  estimates agreed well, indicating that the  $K_I$  estimate from the simulated data still corresponds to the equilibrium constant despite the imposed nonequilibrium conditions. Furthermore, simulated  $\alpha$  and  $\beta$  estimates were within about 10% of the corresponding experimental estimates for both substrates. Therefore, quantitatively as well as qualitatively, our nonequilibrium hypothesis can account for the inhibition of phenyl acetate and acetylthiocholine hydrolysis by propidium observed in Figures 3 and 4.

To demonstrate the sensitivity of the simulations to the input values, key simulation rate constants were varied and

the effects on calculated values of  $\alpha$  and  $\beta$  were assessed. When  $k_{S2}$  and  $k_{-S2}$  were reduced 10-fold to 0.15% of  $k_S$  and  $k_{-S}$ , estimates of  $\alpha$  and  $\beta$  decreased by factors of three to six (Table 1, case 2). With  $k_{S2}$  and  $k_{-S2}$  set at 15% of  $k_S$  and  $k_{-S}$ , estimates of  $\alpha$  and  $\beta$  increased to 0.18 and 0.7, respectively (data not shown), and when  $k_{S2} = k_S$  and  $k_{-S2} = k_{-S}$ ,  $\alpha$  and  $\beta$  became 1.00 (Table 1, case 3). Case 3 demonstrates that, when propidium binding has no effect on any of the rate constants involving substrate hydrolysis, no inhibition is detected even though ligand binding is not at equilibrium.

Under equilibrium conditions our steric blockade hypothesis should result in no inhibition by peripheral site inhibitors. This is clear from eq 5, because the hypothesis stipulates no effect of inhibitor on either substrate binding ( $K_{S1} = K_I$ ) or  $k_{cat}$  ( $a = b = 1$ ). Equilibrium in Scheme 2 is approached when  $k_2/k_{-S}$  and  $ak_2/k_{-S2}$  become small. For example, if the rate constants in case 1 of Table 1 are assumed except for a 100-fold increase in  $k_{-S}$  and  $k_{-S2}$  ( $k_2/k_{-S} = 0.047$  and  $ak_2/k_{-S2} = 3.1$ ),  $\alpha$  and  $\beta$  increase (Table 1, case 4) but still reflect some propidium inhibition. A further 100-fold increase in  $k_{-S}$  and  $k_{-S2}$  (to  $k_2/k_{-S} = 0.00047$  and  $ak_2/k_{-S2} = 0.031$ ) increases  $\alpha$  to 0.97 and  $\beta$  to 1.00 (Table 1, case 5) and essentially abolishes the inhibition.

It is reassuring that the nonequilibrium model can account quantitatively for propidium inhibition of acetylthiocholine and phenyl acetate hydrolysis, but does this simulation model have any predictive value for the inhibition observed with other peripheral site inhibitors? Gallamine appears to bind exclusively to the peripheral site (3). The  $K_I$  for gallamine is 30- to 40-fold larger than the  $K_I$  for propidium (Table 2), and this lower affinity permits comparison of experimental and simulated values of  $\alpha$  and  $\beta$  for a lower affinity inhibitor. The data with acetylthiocholine as substrate are shown in row 2 of Table 2, where the  $k_I$  for gallamine was assumed to be the same as that for propidium and  $k_{-1} = (k_I)(K_I)$  was 30 times greater than the  $k_{-1}$  for propidium. When  $k_{S2}$  and  $k_{-S2}$  were maintained at the same values found to be optimal for propidium inhibition of acetylthiocholine hydrolysis (1.5% of  $k_S$  and  $k_{-S}$ , respectively), the simulated estimates of  $\alpha$  and  $\beta$  were again within about 10% of the respective observed values. Gallamine was a less effective inhibitor of phenyl acetate hydrolysis, and the experimental and simulated values were in best accord when the simulated values of  $k_{S2}$  and  $k_{-S2}$  were 15–20% of  $k_S$  and  $k_{-S}$ , respectively (Table 2, row 4). Thus the simulations indicate that propidium or gallamine binding to the peripheral site does not reduce the rate constants of substrate association and dissociation for the neutral substrate phenyl acetate as much as for the cationic substrate acetylthiocholine.

*Slow Equilibration of Acylation Site Ligands when Propidium Is Bound to the Peripheral Site.* The correlation of the simulation results with experimental data in Table 2 is impressive for steady-state inhibition of both acetylthiocholine and phenyl acetate hydrolysis by propidium or gallamine. However, it is important to design additional tests of the steric blockade hypothesis that do not incorporate unknown variables such as the relative magnitudes of  $k_{S2}$  and  $k_S$ . Reversible inhibitors that equilibrate slowly with the acylation site without interfering with the peripheral site offer such a test. The interaction of an acylation site ligand (L) with AChE (E) in the presence of propidium (I) is shown in

<sup>5</sup> T. Szegletes, P. Thomas, W. D. Mallender, and T. L. Rosenberry, manuscript in preparation.

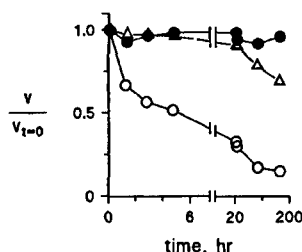
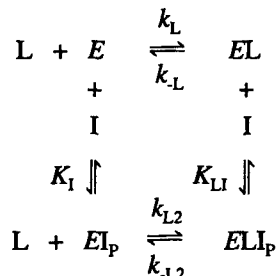


FIGURE 5: Stabilization of AChE-propidium complexes by bovine serum albumin. Incubations were conducted at 23 °C in 20 mM sodium phosphate, 0.02% Triton X-100, (pH 7.0) with (○) 1 nM AChE and 100  $\mu$ M propidium; (●) 1 nM AChE, 100  $\mu$ M propidium, and 1.0 mg/mL bovine serum albumin; or (Δ) 50 pM AChE. At the indicated times aliquots were assayed with acetylthiocholine as outlined in the Experimental Procedures. Assay points  $v$  were normalized to a control activity measured at time 0 ( $v_{t=0}$ ). Since the inactivation was not strictly first order, lines simply connect the points. In curve (○), about 50% of the activity was lost after 6 h.

Scheme 3, where I binding to  $E$  and  $EL$  is assumed to reach equilibrium instantaneously with dissociation constants  $K_I$

Scheme 3



and  $K_{LI}$ , respectively. Binding of  $L$  to  $E$  and  $EI_P$  is much slower and occurs with association rate constants  $k_L$  and  $k_{L2}$  and dissociation rate constants  $k_{-L}$  and  $k_{-L2}$ , respectively. Two acylation site ligands for which the rate constants in Scheme 3 can be measured without resorting to rapid kinetics instrumentation are huperzine A (34) and the transition state analogue TMTFA (35) (see structures in Figure 2). These ligands are also attractive because crystal structures of their complexes with AChE have been determined (see Discussion).

Before assessing the effects of propidium on the association and dissociation rate constants for these acylation site ligands, it was important to confirm AChE stability during incubation with propidium over periods of several days. Propidium in fact was observed to inactivate AChE slowly in 0.02% Triton X-100 and 20 mM sodium phosphate (pH 7.0) alone (Figure 5), but this inactivation was prevented by addition of bovine serum albumin at 1 mg/mL. It has long been known that added protein can stabilize AChE activity (e.g., gelatin; see ref 36). However, to our knowledge this is the first report that a peripheral site ligand like propidium can promote the inactivation of AChE and that added protein can prevent this enhancement of inactivation. Bovine serum albumin was included in all subsequent experiments with acylation site ligands.

Association and dissociation rate constants for huperzine A were obtained by first determining the rate constant  $k$  for the approach to equilibrium binding at various concentrations of  $L$  and propidium according to eq 2, next resolving  $k_{on}$

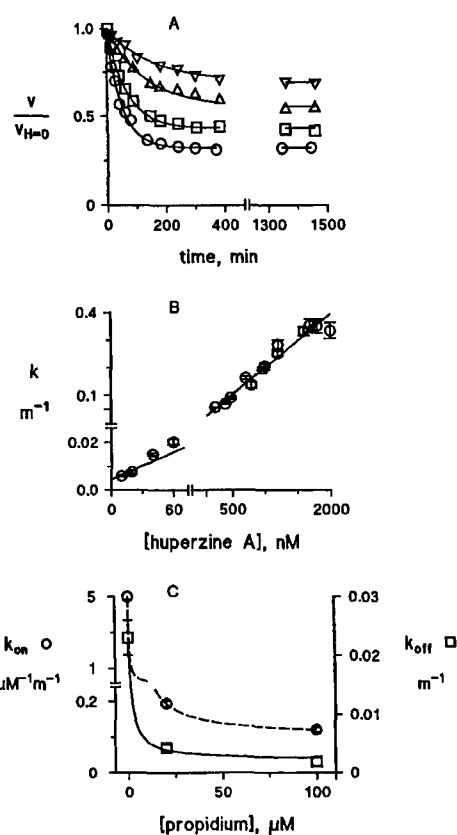


FIGURE 6: Determination of association and dissociation rate constants for huperzine A with both AChE and the AChE-propidium complex. Ligand binding was assumed to occur according to Scheme 3. Part A: Association reactions were initiated by mixing AChE (150 pM) with huperzine A ((○) 60 nM, (□) 40 nM, (Δ) 20 nM, (▽) 10 nM) and 20  $\mu$ M propidium, and aliquots were assayed at the indicated times as outlined in the Experimental Procedures. Assay points  $v$  were normalized to a control 150 pM AChE activity with 20  $\mu$ M propidium but without huperzine A ( $v_{H=0}$ ) and fitted to eq 2 to obtain a value of  $k$  for each curve. Part B: Values of  $k$  obtained from both part A and additional measurements at 20  $\mu$ M propidium were plotted against the huperzine A concentration according to eq 3 to obtain  $k_{on} = 0.195 \pm 0.007 \mu\text{M}^{-1}\text{min}^{-1}$  and  $k_{off} = 0.0043 \pm 0.0006 \text{ min}^{-1}$ . In the absence of propidium,  $k_{on} = k_L$  and  $k_{off} = k_{-L}$  and a similar analysis was used to obtain the estimates of  $k_L$  and  $k_{-L}$  in Table 3. Part C: Values of  $k_{on}$  and  $k_{off}$  were plotted against the propidium concentration according to eqs 4a,b. The above  $k_L$  value was fixed in eq 4a, and the  $k_{on}$  estimates at 20  $\mu$ M and 100  $\mu$ M propidium were then fitted to this equation to obtain the estimates of  $k_{L2}$  and  $K_I$  in Table 3. Equation 4b was rearranged to the form  $k_{off} = (k_{-L} + W[I]/K_I)/(1 + W[I]/K_I)$ . The previously obtained  $k_{-L}$ ,  $K_I$ , and  $W = k_{L2}/k_L$  were then fixed, and this equation was used to fit the  $k_{-L2}$  value in Table 3.

and  $k_{off}$  from the dependence of  $k$  on  $[L]$  (eq 3), and then fitting  $k_{on}$  and  $k_{off}$  to eqs 4a and b. These steps are illustrated in Figure 6a–c. A family of curves showing the approach to equilibrium at several concentrations of huperzine A is shown in Figure 6a, and the  $k$  values obtained as in Figure 6a are graphed against the huperzine A concentration in Figure 6b. Estimates of  $k_{on}$  and  $k_{off}$  from plots such as that in Figure 6b at two fixed concentrations of propidium and in its absence were fitted to eqs 4a,b in Figure 6c. Rate constants obtained from this fitting procedure are given in Table 3. The decrease in the huperzine A association rate constant when propidium is bound at the peripheral site was indicated by the ratio of  $k_L$  to  $k_{L2}$ , a 49-fold decrease.

Table 3: Propidium Inhibition of Association and Dissociation Rate Constants for Acylation Site Ligands<sup>a</sup>

kinetic constant	units	acylation site ligand	
		huperzine A	TMTFA
$k_L$	$\mu\text{M}^{-1} \text{m}^{-1}$	$5.0 \pm 0.2$	$4.9 \pm 0.1$
$k_{L2}$	$\mu\text{M}^{-1} \text{m}^{-1}$	$0.102 \pm 0.009$	$0.013 \pm 0.003$
$k_{-L}$	$\text{m}^{-1}$	$0.023 \pm 0.003$	$(2.4 \pm 0.1) \times 10^{-4}$
$k_{-L2}$	$\text{m}^{-1}$	$0.0022 \pm 0.0005$	$(4.2 \pm 0.9) \times 10^{-6}$
$K_L$	nM	$4.6 \pm 0.7$	$0.049 \pm 0.003$
$K_{L2}$	nM	$22 \pm 5$	$0.32 \pm 0.02$
$K_I$	$\mu\text{M}$	$0.39 \pm 0.06$	$0.43 \pm 0.05$

<sup>a</sup> Values of kinetic constants were calculated as described in Figures 6 and 7.

Similarly, the decrease in the huperzine A dissociation rate constant when propidium is bound at the peripheral site, indicated by the ratio of  $k_{-L}$  to  $k_{-L2}$ , was about 10-fold. The steric blockade hypothesis is largely supported by these data, as both rate constants were reduced an order of magnitude or more when propidium was bound. A small thermodynamic effect of propidium binding on  $K_L$  for huperzine A, however, was also revealed by the fact that the two rate constants were not reduced equally.

The transition state analogue TMTFA has a much higher affinity for the acylation site than huperzine A. The apparent  $K_L$  of 49 pM in Table 3 is in reasonable agreement with previous estimates (35, 37). This high affinity prevented application of eq 2, particularly for association reactions at low concentrations of TMTFA that were not in sufficient excess of AChE and for dissociation reactions where the free TMTFA concentration increased significantly over the course of the reaction. Therefore, several individual reaction profiles were fitted simultaneously with the SCoP program to obtain the rate and equilibrium constants in Table 3. Several of these simultaneous fits are shown in Figure 7. The reduction in TMTFA association and dissociation rate constants with propidium bound to the peripheral site was even more pronounced than for huperzine A. The association rate constant  $k_{L2}$  was 380-fold smaller than  $k_L$  with free AChE, and the dissociation rate constant  $k_{-L2}$  was 60-fold smaller than  $k_{-L}$  with free AChE. These data provide further support for the steric blockade hypothesis, again with a small thermodynamic effect of bound propidium on the TMTFA affinity.

## DISCUSSION

We illustrate here a nonequilibrium alternative to the equilibrium analysis of AChE inhibition by peripheral site ligands. We have examined a very simple hypothesis that bound peripheral site inhibitors only decrease association and dissociation rate constants for acylation site ligands *without* effects on the thermodynamics of the binding of these ligands or the rate constants for substrate acylation and deacylation. In other words, the peripheral site inhibitor is proposed to act as a "permeable cork" at the mouth of the active site "bottle" and thus to slow ligand entry to and exit from the acylation site. This steric blockade hypothesis can account for most if not all of the observed steady-state inhibition. Within an equilibrium framework, AChE inhibition by propidium previously has been attributed entirely to a conformational change at the acylation site induced by the binding of propidium to the peripheral site (38). This would

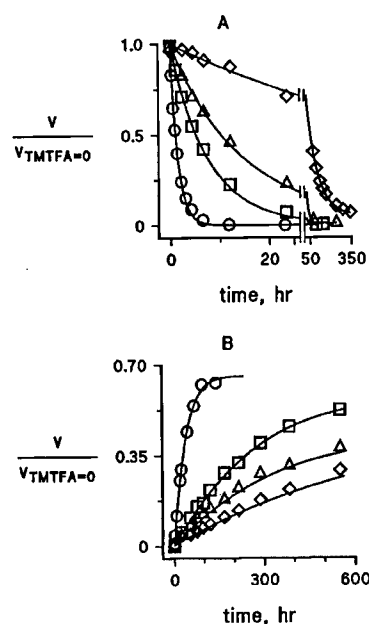


FIGURE 7: Determination of association and dissociation rate constants for TMTFA with both AChE and the AChE-propidium complex. AChE (50–800 pM) was incubated with TMTFA (0.03–320 nM) and propidium (0–100  $\mu\text{M}$ ) and aliquots were assayed for AChE activity at various times as outlined in the Experimental Procedures. Assay points ( $v$ ) were normalized to parallel control assays ( $v_{\text{TMTFA}=0}$ ) containing identical [AChE] and [propidium] but without TMTFA. Ligand binding was assumed to occur according to Scheme 3, and the SCoP fitting program was applied directly to the differential equations corresponding to Scheme 3. First, reaction time courses for six association and five dissociation reactions in the absence of propidium were simultaneously fit to give the values of  $k_L$  and  $k_{-L}$  in Table 3. These values were then fixed in the SCoP program and reaction time courses for five association reactions containing 100  $\mu\text{M}$  propidium and eight dissociation reactions containing 20–100  $\mu\text{M}$  propidium were simultaneously fit to give the values of  $k_{L2}$ ,  $K_{L2}$ , and  $K_I$  values in Table 3. Part A: Assay points and calculated fits to 4 association reactions containing 100  $\mu\text{M}$  propidium, 800 pM AChE, and TMTFA (total concentration: (○) 320 nM, (□) 64 nM, (Δ) 33 nM, (◇) 6.4 nM). Part B: Assay points and calculated lines to four dissociation reactions containing propidium ((○) 0  $\mu\text{M}$ ; (□) 20  $\mu\text{M}$ ; (Δ) 40  $\mu\text{M}$ ; (◇) 100  $\mu\text{M}$ ), AChE (total concentration: (○) 62 pM, (□) 250 pM, (Δ) 620 pM, (◇) 620 pM), and TMTFA (total concentration: (○) 77 pM, (□) 310 pM, (Δ) 770 pM, (◇) 770 pM).

appear reasonable in view of the spatial separation between propidium in the peripheral site and acetylthiocholine in the acylation site. According to the equilibrium model in eq 5, the low values of  $\alpha$  and  $\beta$  in Figures 3b and 4b can occur only if  $a$  (or  $b$  and  $K_I/K_{SI}$ ) are much less than one, and these inhibitory effects would indeed appear to require a conformational interaction between the two sites. However, the conformational interaction hypothesis fails to provide a satisfactory explanation for several observations. First, propidium only partially inhibits the hydrolysis of *p*-nitrophenyl acetate, showing an  $\alpha$  value of about 0.3 (39). It is unclear why a proposed conformational interaction would result in  $\alpha$  values ranging from less than 0.02 for a good substrate like acetylthiocholine to 0.3 for *p*-nitrophenyl acetate, but this observation is readily accommodated by the steric blockade hypothesis: For *p*-nitrophenyl acetate, the estimated  $K_{\text{app}}$  is 35-fold higher and  $k_{\text{cat}}$  is 3-fold lower than the corresponding estimates for acetylthiocholine (39). These values indicate that the ratios  $k_2/k_{-2}$  and  $ak_2/k_{-2}$  are smaller for *p*-nitrophenyl acetate than for either acetylthiocholine or

phenyl acetate, placing the AChE interactions of this substrate near equilibrium where the steric blockade hypothesis predicts little inhibition. Second, in some mutants (W84A and Y130A) the  $K_I$  for propidium inhibition of acetylthiocholine hydrolysis increases up to 100-fold, while the  $K_{eq}$  for propidium binding as determined by fluorescence titration remains unchanged (38). In these mutants the  $k_{cat}$  for acetylthiocholine decreased 10- to 50-fold and/or  $K_{app}$  increased by more than 2 orders of magnitude (37, 38), again indicating decreases in  $k_2/k_{-S}$  and  $ak_2/k_{-S2}$  that should result in less inhibition according to the steric blockade hypothesis. In fact, case 5 in Table 1 predicts no inhibition when increases in  $k_{-S}$  and  $k_{-S2}$  result in a 2000-fold increase in  $K_{app}$ , an increase comparable to the 700-fold reported for acetylthiocholine with the W84A mutant (38).

The simulations of steady-state substrate hydrolysis in Tables 1 and 2 provide insight into the mechanism by which peripheral site inhibition can arise within the steric blockade hypothesis. First, the ratios  $k_2/k_{-S}$  and  $ak_2/k_{-S2}$  must be large enough that the  $ES$  and  $ESI_P$  complexes in Scheme 2 fail to achieve equilibrium. The  $k_2/k_{-S}$  ratio has been denoted  $C$ , the commitment to catalysis (14), and eq 1c shows that as  $C$  approaches and then exceeds unity the second-order substrate hydrolysis rate constant  $k_{cat}/K_{app}$  approaches  $k_S$ . According to Scheme 1, this reflects a change in the rate-limiting step from  $k_2$  to  $k_S$ . At saturating levels of peripheral site inhibitor, the second-order substrate hydrolysis rate constant  $k_{cat}'/K_{app}'$  is given by eq 7 under equilibrium conditions and approximated by eq 7 under nonequilibrium conditions (22).

$$\frac{k_{cat}'}{K_{app}'} = \frac{k_{S2}ak_2}{k_{S2} + ak_2} \quad (7)$$

As  $ak_2$  exceeds  $k_{-S2}$  in the  $ESI_P$  complex, the rate-limiting step similarly becomes  $k_{S2}$ . Second,  $k_{S2}$  must be smaller than  $k_S$ . In this case, increasing saturation of the peripheral site slows the second-order hydrolysis rate constant from  $k_S$  to  $k_{S2}$ , and this slowdown is reflected in a value of  $\alpha < 1$ . No further restrictions on rate constants are necessary to obtain inhibition, but it is noteworthy that the relative magnitude of  $k_{-1}$  does influence the value of the inhibition parameter  $\beta$ , the relative value of  $k_{cat}$  in the ternary complex. The simulated  $\beta$  of 0.5 for gallamine inhibition of acetylthiocholine hydrolysis was significantly larger than the simulated  $\beta$  of 0.09 for propidium inhibition (Table 2). Since the only simulation rate constant that differed between propidium and gallamine was  $k_{-1}$ , it is clear that  $\beta$  was sensitive to this rate constant. For propidium  $k_{-1}$  was much less than  $k_2$  and  $k_3$ , whereas for gallamine  $k_{-1}$  was comparable to  $k_2$  and  $k_3$ . Thus with propidium the apparent  $k_{cat}$  is partially limited by  $k_{-1}$ , meaning that with a saturating concentration of propidium and intermediate concentrations of substrate (i.e., roughly between  $K_{app}$  and  $K_{app}' \cong ak_2/k_{S2}$ ), most catalytic turnovers of  $EAI_P$  are followed by slow dissociation of the  $EI_P$  product before the next catalytic turnover. A similar effect of inhibitor dissociation rate constant on  $k_{cat}$  was noted previously for a simpler version of Scheme 2 in which  $EAI_P$  but not  $ESI_P$  can form (1, 20). In contrast, for gallamine  $k_2$  and  $k_3$  alone remain largely rate limiting as in the equilibrium model in eq 5. When  $k_{-1}$  was set to a value at least 10 times  $k_2$  or  $k_3$  in case 1 of Table 1,  $\beta$  became 1.0 and  $k_{-1}$  had no influence on the relative value of  $k_{cat}$  (data not shown).

The nonequilibrium simulations in Tables 1 and 2 generated slope replots that fit eq 6 with high precision, as indicated by the low standard errors for  $\alpha$  in Table 2. The intercept replots tended to be bell shaped rather than hyperbolic (see Figure 3d), and this led to greater uncertainty in the estimates of  $\beta$ . The bell-shaped curves arose from slight error that was introduced in the reciprocal plot intercepts by the curvature of the reciprocal plots that was noted in the Results in describing Figures 3c and 4c. Not all of the curvature was eliminated by restricting the simulation analyses to the low concentrations of substrate indicated. The curvature occurs because inhibition in our steric blockade model here arises exclusively from a decrease in the substrate association constant when inhibitor occupies the peripheral site ( $k_{S2}/k_S \ll 1$ ). At high substrate concentrations with this model (i.e., as  $[S]$  approaches and exceeds  $K_{app}' \cong ak_2/k_{S2}$ ), most catalytic turnovers of  $EAI_P$  are followed by substrate association with  $EI_P$  that is faster than the slow dissociation of  $EI_P$ . Hydrolysis rates approach those in the absence of inhibitor because  $ak_2$  and  $bk_3$  become rate limiting, and inhibitor does not affect these steps because the model sets  $a = b = 1$ . A logical extension of Scheme 2 consistent with the steric blockade model is to propose that bound peripheral site ligand not only reduces association and dissociation rate constants for substrate binding to the acylation site but also reduces the dissociation rate constant for product release from this site. If product affinity for the acylation site is sufficiently high, then product release may become partially rate-limiting when the peripheral site is occupied. We have found that this extension can eliminate the curvature in the reciprocal plots and give quantitative agreement between simulated and experimental data over the entire range of substrate concentrations. Furthermore, if substrate can form a low affinity complex at the peripheral site and block product dissociation from the acylation site, this extended model can account quantitatively for substrate inhibition.<sup>5</sup> The necessity for slight revision of the simplest version of the steric blockade hypothesis offered here also is indicated by consistent observations of small decreases in the affinity of ligands in ternary AChE complexes relative to the corresponding binary complex. In Table 3 this decrease, indicated by the ratio of  $K_{L2}/K_L$ , was a factor of  $4.7 \pm 1.4$  for huperzine A and of  $6.5 \pm 0.6$  for TMTFA in the AChE-propidium complex relative to the free enzyme. Other studies have shown an affinity decrease of about 5 for edrophonium (22) and 4 for methylacridinium (27) in the AChE-fasciculin 2 complex relative to free AChE. The consistent magnitude of these factors suggests that affinity decreases of cationic ligands in many AChE ternary complexes are governed by general properties such as electrostatic attraction rather than specific conformational interaction. Even though the steric blockade hypothesis here proposed no changes in equilibrium constants in AChE ternary complexes, a minor 5-fold decrease in ligand affinities in the ternary complexes can be incorporated into the hypothesis with virtually no effect on simulated values of  $\alpha$  and  $\beta$ . For example, a 5-fold increase in  $k_{-S2}$  and  $k_{-S1}$  from their values in case 1 of Table 1 changes the simulated values of  $\alpha$  and  $\beta$  by less than 8% (data not shown).

Despite the agreement of the simulated and experimental data for the two substrates and two inhibitors in Table 2, these data provide only a correlation and do not prove our



nonequilibrium steric blockade hypothesis. The predictive power of the hypothesis would be enhanced if *all* the rate constants in the simulations could be assigned independently, but independent estimates of  $k_{s2}$  and  $k_{-s2}$  for substrates are very difficult to obtain. Alternatively, the hypothesis predicts that not only substrates but also ligand inhibitors that bind to the acylation site should show decreased association and dissociation rate constants ( $k_{L2}$  and  $k_{-L2}$ ) when a peripheral site ligand like propidium is bound. Most acylation site ligands equilibrate too rapidly to test this prediction. For example, *N*-methylacridinium has a  $K_1$  in the micromolar range and equilibrates with AChE in about a msec or less (27, 40). However, huperzine A binds near the acylation site (28) and equilibrates slowly enough to allow measurement of association and dissociation rate constants (34). Furthermore, the AChE complex with the trifluoromethyl ketone TMTFA provides an excellent model of the transition state for acylation by acetylcholine. The crystal structure of the TMTFA-TcAChE complex shows a tetrahedral adduct that nearly superimposes on a calculated structure of acetylcholine in the active site (29). TMTFA has no leaving group, so it accumulates as the tetrahedral adduct. Molecular modeling of the ternary complexes of these ligands with TcAChE-propidium revealed that the bound propidium is separated by at least 1.6 Å from either bound huperzine A or bound TMTFA (Figure 8), indicating that no overlap occurs in the binding sites that could perturb equilibrium affinities in the ternary complexes. As noted above in support of this conclusion, the 4- to 7-fold decreases in ligand equilibrium affinities in these ternary complexes are comparable to those reported previously for ternary complexes involving fasciculin 2 in the peripheral site. Measured values of  $k_{L2}$  and  $k_{-L2}$  for huperzine A and TMTFA with the AChE-propidium complex provide compelling support for our steric blockade hypothesis. These rate constants are 49- and 10-fold lower for huperzine A and 380- and 60-fold lower for TMTFA than the respective rate constants  $k_L$  and  $k_{-L}$  for the interaction of these ligands with free AChE. It is particularly satisfying that the magnitude of these decreases for the acetylcholine analogue TMTFA agrees so well with the simulated  $k_s/k_{s2}$  ratio of about 70 that was found to provide the best correspondence to observed kinetic parameters for acetylthiocholine and propidium in Table 2.

Does the successful application of our steric blockade hypothesis in this report rule out any conformational interaction between the peripheral and acylation sites? We argue that it probably does when the peripheral site is occupied by small ligands such as propidium and gallamine. Proof of this conformational interaction now requires evidence beyond steady-state measurements of the extent of propidium inhibition. For example, with the larger ligand fasciculin 2 bound to the peripheral site, we previously reported not only steric blockade of ligand access to the acylation site (27) but also a conformational change in the acylation site that decreased the efficiency of the catalytic triad (22). This additional conformational effect of bound fasciculin is seen most clearly by comparing estimates of the dissociation rate constant  $k_{-L2}$  for TMTFA. In contrast to the 60-fold decrease in this rate constant observed here for the AChE-propidium-TMTFA complex relative to  $k_{-L}$  for AChE-TMTFA, a 20-fold increase in  $k_{-L2}$  relative to  $k_{-L}$  was reported for

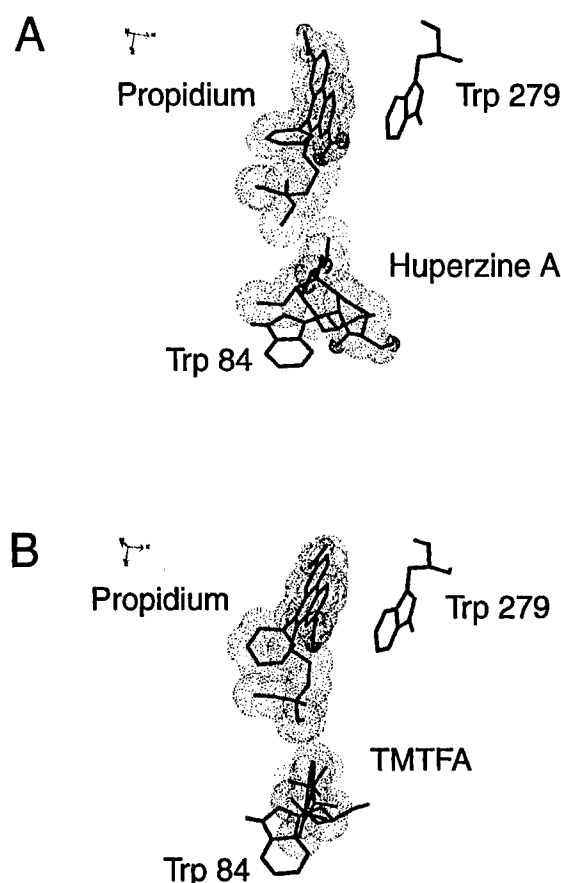


FIGURE 8: Molecular models of ternary complexes involving propidium and TcAChE. Residues are marked by a heavy line with propidium and acylation site ligand van der Waals spheres shown by a dotted surface. Nonpolar hydrogen atoms have been omitted for clarity. The conformation of propidium in the TcAChE-huperzine A complex (part A) was very similar to that in the TcAChE-TMTFA adduct (part B). The overall root mean square deviation between matched atoms in the two models was 0.25 Å. Atom to atom closest contacts between the propidium alkyl chain and the acylation site inhibitors are 1.6 Å (huperzine A) and 1.7 Å (TMTFA). Comparison of the propidium molecule between the two models revealed only minor changes in both the planarity of the aromatic ring and the position of the alkyl chain.

the AChE-fasciculin 2-TMTFA complex (37).<sup>6</sup> The increase results in conformational destabilization of the tetrahedral TMTFA adduct in this ternary complex ( $K_{L2}/K_L \approx 200$ ), and the conformational effect predominates over steric blockade of TMTFA egress in determining the net change in  $k_{-L2}$ . Crystal structure analyses of fasciculin-AChE complexes (8, 9) show that fasciculin 2 interacts not only with W279 in the peripheral site but also with residues on the outer surface of an  $\omega$ -loop within 4 Å of W84 in the acylation site, well beyond the region of the peripheral site occupied by propidium (see Figures 7 and 8). These more extensive surface interactions provide a structural basis for an inhibitory conformational effect on the acylation site when fasciculin rather than propidium is bound to the peripheral site.

#### ACKNOWLEDGMENT

We express our gratitude to Dr. Michel Roux at the Ecole Normale Supérieure in Paris, France, for bringing the SCOP

<sup>6</sup> J. Eastman, P. Thomas, G. Rogers, J. Yustein, and T. L. Rosenberry, unpublished observations.



program to our attention. We also acknowledge the technical assistance of Mr. Mark Frey in early measurements of propidium inhibition of substrate hydrolysis and thank Dr. Daniel Quinn in the Department of Chemistry at the University of Iowa for kindly supplying TMTFA.

## REFERENCES

- Rosenberry, T. L. (1975) Acetylcholinesterase, in *Advances in Enzymology* (Meister, A., Ed.) Vol. 43, pp 103–218, John Wiley & Sons, New York.
- Sussman, J. L., Harel, M., Frolow, F., Oefner, C., Goldman, A., Toker, L., and Silman, I. (1991) *Science* 253, 872–879.
- Taylor, P., and Lappi, S. (1975) *Biochemistry* 14, 1989–1997.
- Weise, C., Kreienkamp, H.-J., Raba, R., Pedak, A., Aaviksaar, A., and Hucho, F. (1990) *EMBO J.* 9, 3885–3888.
- Schalk, I., Ehret-Sabatier, L., Bouet, F., Goeldner, M., and Hirth, C. (1992) in *Multidisciplinary Approaches to Cholinesterase Functions* (Shafferman, A., and Velan, B., Eds.) pp 117–120, Plenum Press, New York.
- Radic, Z., Pickering, N. A., Vellom, D. C., Camp, S., and Taylor, P. (1993) *Biochemistry* 32, 12074–12084.
- Barak, D., Kronman, C., Ordentlich, A., Ariel, N., Bromberg, A., Marcus, D., Lazar, A., Velan, B., and Shafferman, A. (1994) *J. Biol. Chem.* 269, 6296–6305.
- Harel, M., Kleywegt, G. J., Ravelli, R. B. G., Silman, I., and Sussman, J. L. (1995) *Structure* 3, 1355–1366.
- Bourne, Y., Taylor, P., and Marchot, P. (1995) *Cell* 83, 503–512.
- Karlsson, E., Mbugua, P. M., and Rodriguez-Ithurralde, D. (1984) *J. Physiol. (Paris)* 79, 232–240.
- Marchot, P., Khelif, A., Ji, Y.-H., Masnuelle, P., and Bourgis, P. E. (1993) *J. Biol. Chem.* 268, 12458–12467.
- Nachmansohn, D., and Wilson, I. B. (1951) *Adv. Enzymol.* 12, 259–339.
- Briggs, G. E., and Haldane, J. B. S. (1925) *Biochem. J.* 19, 338–339.
- Quinn, D. M. (1987) *Chem. Rev.* 87, 955–979.
- Dixon, M., and Webb, E. C. (1958) *Enzymes*, pp 171–181, Academic Press, New York.
- Rosenberry, T. L., and Scoggin, D. M. (1984) *J. Biol. Chem.* 259, 5643–5652.
- Roberts, W. L., Kim, B. H., and Rosenberry, T. L. (1987) *Proc. Natl. Acad. Sci. U.S.A.* 84, 7817–7821.
- Riddles, P. W., Blakeley, R. L., and Zerner, B. (1979) *Anal. Biochem.* 94, 75–81.
- Ellman, G. L., Courtney, K. D., Andres, J. V., and Featherstone, R. M. (1961) *Biochem. Pharmacol.* 7, 88–95.
- Hodge, A. S., Humphrey, D. R., and Rosenberry, T. L. (1992) *Mol. Pharmacol.* 41, 937–942.
- Rosenberry, T. L. (1975) *Proc. Natl. Acad. Sci. U.S.A.* 72, 3834–3838.
- Eastman, J., Wilson, E. J., Cervenansky, C., and Rosenberry, T. L. (1995) *J. Biol. Chem.* 270, 19694–19701.
- Hindmarsh, A. C. (1983) in *Scientific Computing* (Stepleman, R. S., et al., Eds.) pp 55–64, North-Holland, Amsterdam.
- Petzhold, L. R. (1983) *SIAM J. Sci. Stat. Comput.* 4, 136–148.
- Froede, H. C., and Wilson, I. B. (1984) *J. Biol. Chem.* 259, 11010–11013.
- Gnagey, A. L., Forte, M., and Rosenberry, T. L. (1987) *J. Biol. Chem.* 262, 13290–13298.
- Rosenberry, T. L., Rabl, C. R., and Neumann, E. (1996) *Biochemistry* 35, 685–690.
- Raves, M. L., Harel, M., Pang, Y.-P., Silman, I., Kozikowski, A. P., and Sussman, J. L. (1997) *Nat. Struct. Biol.* 4, 57–63.
- Harel, M., Quinn, D. M., Nair, H. K., Silman, I., and Sussman, J. L. (1996) *J. Am. Chem. Soc.* 118, 2340–23346.
- Botts, J., and Morales, M. (1953) *Trans. Faraday Soc.* 49, 696–707.
- Bernhard, S. A. (1968) The Structure and Function of Enzymes, in *Biology Teaching Monograph Series* (Levinthal, C., Ed.) pp 80–85, W. A. Benjamin, Inc., New York.
- Krupka, R. M., and Laidler, K. J. (1961b) *J. Am. Chem. Soc.* 83, 1454–1458.
- Barnett, P., and Rosenberry, T. L. (1977) *J. Biol. Chem.* 252, 7200–7206.
- Ashani, Y., Grunwald, J., Kronman, C., Velan, B., and Shafferman, A. (1994) *Mol. Pharmacol.* 45, 555–560.
- Nair, H. K., Lee, K., and Quinn, D. M. (1993) *J. Am. Chem. Soc.* 115, 9939–9941.
- Wilson, I. B., and Bergmann, F. (1950) *J. Biol. Chem.* 185, 479–489.
- Radic, Z., Quinn, D. M., Vellom, D. C., Camp, S., and Taylor, P. (1995) *J. Biol. Chem.* 270, 20391–20399.
- Barak, D., Ordentlich, A., Bromberg, A., Kronman, C., Marcus, D., Lazar, A., Ariel, N., Velan, B., and Shafferman, A. (1995) *Biochemistry* 34, 15444–15452.
- Ordentlich, A., Barak, D., Kronman, C., Flashner, Y., Leitner, M., Segall, Y., Ariel, N., Cohen, S., Velan, B., and Shafferman, A. (1993) *J. Biol. Chem.* 268, 17083–17095.
- Rosenberry, T. L., and Neumann, E. (1977) *Biochemistry* 16, 3870–3878.

BI972158A

## Substrate Binding to the Peripheral Site of Acetylcholinesterase Initiates Enzymatic Catalysis. Substrate Inhibition Arises as a Secondary Effect<sup>†</sup>

Tivadar Szegletes,<sup>‡</sup> William D. Mallender,<sup>‡</sup> Patrick J. Thomas,<sup>§</sup> and Terrone L. Rosenberry<sup>\*,‡</sup>

Department of Pharmacology, Mayo Foundation for Medical Education and Research, Department of Research, Mayo Clinic Jacksonville, Jacksonville, Florida 32224, and Department of Pharmacology, Case Western Reserve University School of Medicine, Cleveland, Ohio 44120-4965

Received June 9, 1998; Revised Manuscript Received October 13, 1998

**ABSTRACT:** Two sites of ligand interaction in acetylcholinesterase (AChE) were first demonstrated in ligand binding studies and later confirmed by crystallography, site-specific mutagenesis, and molecular modeling: an acylation site at the base of the active site gorge and a peripheral site at its mouth. We recently introduced a steric blockade model which demonstrated how small peripheral site ligands such as propidium may inhibit substrate hydrolysis [Szegletes, T., Mallender, W. D., and Rosenberry, T. L. (1998) *Biochemistry* 37, 4206–4216]. In this model, the only effect of a bound peripheral site ligand is to decrease the association and dissociation rate constants for an acylation site ligand without altering the equilibrium constant for ligand binding to the acylation site. Here, we first provide evidence that not only rate constants for substrates but also dissociation rate constants for their hydrolysis products are decreased by bound peripheral site ligand. Previous reaction schemes for substrate hydrolysis by AChE were extended to include product dissociation steps, and acetylthiocholine hydrolysis rates in the presence of propidium under nonequilibrium conditions were simulated with assigned rate constants in the program SCoP. We next showed that cationic substrates such as acetylthiocholine and 7-acetoxy-*N*-methylquinolinium (M7A) bind to the peripheral site as well as to the acylation site. The neurotoxin fasciculin was used to report specifically on interactions at the peripheral site. Analysis of inhibition of fasciculin association rates by these substrates revealed  $K_S$  values of about 1 mM for the peripheral site binding of acetylthiocholine and 0.2 mM for the binding of M7A. The AChE reaction scheme was further extended to include substrate binding to the peripheral site as the initial step in the catalytic pathway. Simulations of the steric blockade model with this scheme were in reasonable agreement with observed substrate inhibition for acetylthiocholine and M7A and with mutual competitive inhibition in mixtures of acetylthiocholine and M7A. Substrate inhibition was explained by blockade of product dissociation when substrate is bound to the peripheral site. However, our analyses indicate that the primary physiologic role of the AChE peripheral site is to accelerate the hydrolysis of acetylcholine at low substrate concentrations.

The hydrolysis of the neurotransmitter acetylcholine by acetylcholinesterase (AChE)<sup>1</sup> is one of the most efficient enzyme catalytic reactions known (1). The basis of this high efficiency has been investigated with ligand binding studies interpreted in the context of the AChE three-dimensional structure determined by X-ray crystallography (2). The long and narrow active site gorge is about 20 Å deep and includes two sites of ligand interaction: an *acylation site* at the base of the gorge and a *peripheral site* at its mouth. In the acylation site, residue S200 (TcAChE sequence numbering) is acylated and deacylated during substrate turnover, H440 and

E327 participate with S200 in a catalytic triad, and W84 binds to the trimethylammonium group of acetylcholine as acyl transfer to S200 is initiated. The peripheral site involves other residues including W279 (3–8). Ligands can bind selectively to either the acylation or the peripheral sites, and ternary complexes with distinct ligands bound to each site can form (9). Ligands that bind specifically to the peripheral site include the phenanthridinium derivative propidium and the fasciculins, a family of very similar snake venom neurotoxins comprised of 61-amino acid polypeptides (7, 8, 10, 11).

Despite its prominence, the role of the peripheral site in the AChE catalytic pathway has remained obscure. From analysis of the effect of ionic strength on  $k_{cat}/K_{app}$ , we proposed several years ago that acetylthiocholine binding to the active site is controlled by a high net negative charge near the active site that can electrostatically attract cationic substrates and inhibitors (12). Molecular modeling calculations (13, 14) from the three-dimensional structure support this notion by suggesting that the AChE catalytic subunit has a dipole moment aligned with the active site gorge that can accelerate association rate constants for cationic ligands. The extent of this acceleration, measured as a ratio of the

<sup>†</sup> This work was supported by Grant NS-16577 from the National Institutes of Health and by grants from the Muscular Dystrophy Association of America. W.D.M. was supported by a Kendall-Mayo Postdoctoral Fellowship.

\* To whom correspondence should be addressed.

<sup>‡</sup> Mayo Clinic Jacksonville.

<sup>§</sup> Case Western Reserve University School of Medicine.

<sup>1</sup> Abbreviations: AChE, acetylcholinesterase; TcAChE, acetylcholinesterase from *Torpedo californica*; DTNB, 5,5'-dithiobis(2-nitrobenzoic acid); TMTFA, *m*-(*N,N,N*-trimethylammonio)trifluoroacetophenone; M7A, 7-acetoxy-*N*-methylquinolinium; M7H, 7-hydroxy-*N*-methylquinolinium.

association rate constant at low ionic strength to that at high ionic strength, depends on the cationic ligand and the species of AChE, but it appears to be about a factor of 7.5 for the cation TMTFA with mouse AChE at zero ionic strength (15). However, mutation of up to seven negatively charged residues at or near the peripheral site on the gorge rim reduced this factor by less than 60% (15, 16), indicating that the peripheral site makes only a modest contribution to the electrostatic field at the active site. A second possibility is that ligand binding to the peripheral site results in a conformational change that promotes catalysis. Many peripheral site ligands inhibit substrate hydrolysis, and AChE inhibition by propidium has been attributed entirely to a conformational change at the acylation site induced by the binding of propidium to the peripheral site (17). If substrate interacted with the peripheral site on entering the active site gorge, this interaction in principle could induce a conformational change that might promote substrate hydrolysis. However, we recently introduced a steric blockade model which demonstrated how small peripheral site ligands such as propidium may inhibit substrate hydrolysis without inducing a conformational change in the acylation site (18). This model includes the simple hypothesis that the only effect of a bound peripheral site ligand is to decrease the association and dissociation rate constants for an acylation site ligand without altering the equilibrium constant for ligand binding to the acylation site. This hypothesis was generally supported by our direct demonstration that bound propidium decreased the association and dissociation rate constants for the acylation site ligands huperzine A and TMTFA by factors of 10–400. Therefore, there is little evidence that the binding of substrates and other small ligands to the peripheral site induces a conformational change that is significant with respect to catalysis.

In this paper, we show that further examination of our steric blockade model leads directly to a proposed new role for the peripheral site, namely, the initial binding of substrate on the AChE catalytic pathway. A similar role has been suggested for a peripheral site in the closely related enzyme butyrylcholinesterase (19). The first step in clarifying this role in AChE was to analyze further the inhibition of substrate hydrolysis by peripheral site ligands. We conducted nonequilibrium simulations that accounted quantitatively for inhibition by peripheral site ligands at low substrate concentrations but diverged from experimental data at higher substrate concentrations (18). The discordance prompted us here to extend the model to include steric blockade of product dissociation as well as of substrate association and dissociation by a bound peripheral site ligand. The extended model not only brought the simulations into quantitative agreement with experimental data at all substrate concentrations but also suggested that substrate binding to the peripheral site could block product release and account for the well-known phenomenon of substrate inhibition with AChE. With a competition assay for fasciculin binding to quantify the affinity of substrates for the peripheral site, we then demonstrated a satisfactory correspondence of the simulated and observed substrate inhibition data. The complete model indicates that the peripheral site serves as an initial binding site for substrate entry to the acylation site and that this initial binding accelerates the rate constant ( $k_{\text{cat}}/K_{\text{app}}$ ) for substrate hydrolysis at low substrate concentrations.

## EXPERIMENTAL PROCEDURES

**Materials.** Human erythrocyte AChE was purified as outlined previously, and active site concentrations were determined by assuming 410 units/nmol (20, 21). Propidium iodide was purchased from Calbiochem. M7H iodide and some stocks of M7A iodide were obtained from Molecular Probes, while other stocks of M7A iodide were synthesized by the Mayo Clinic Jacksonville Organic Synthesis Core Facility. Fasciculin was the fasciculin 2 form obtained from C. Cervenansky at the Instituto de Investigaciones Biológicas (Clemente Estable, Montevideo, Uruguay) (22).

**Steady State Measurements of AChE-Catalyzed Substrate Hydrolysis.** Hydrolysis rates  $v$  were measured at various substrate (S) concentrations in 1 mL assay solutions with buffer (20 mM sodium phosphate and 0.02% Triton X-100 at pH 7.0) at 25 °C. To maintain a constant ionic strength with protocols in which the acetylthiocholine concentration exceeded 1 mM, NaCl was added such that the sum of the acetylthiocholine and NaCl concentrations was 60 mM. Acetylthiocholine assay solutions included 0.33 mM DTNB, and hydrolysis was monitored by formation of the thiolate dianion of DTNB at 412 nm [ $\Delta\epsilon_{412\text{nm}} = 14.15 \text{ mM}^{-1} \text{ cm}^{-1}$  (23)] for 1–5 min on a Varian Cary 3A spectrophotometer (24). Hydrolysis of M7A was followed by formation of M7H at 406 nm ( $\Delta\epsilon_{406\text{nm}} = 9.2 \text{ mM}^{-1} \text{ cm}^{-1}$  at pH 7.0), and nonenzymatic hydrolysis rates were deducted (25, 26).

At high concentrations of acetylthiocholine and M7A,  $v$  declined below the maximal hydrolysis rates observed at lower S concentrations. The dependence of  $v$  on [S] was fitted to the Haldane equation for substrate inhibition (27) as shown in eq 1.

$$v = \frac{V_{\text{max}} [S]}{[S] \left( 1 + \frac{[S]}{K_{\text{SS}}} \right) + K_{\text{app}}} \quad (1)$$

In eq 1,  $V_{\text{max}} = k_{\text{cat}}[E]_{\text{tot}}$  where  $[E]_{\text{tot}}$  is the total concentration of AChE active sites. Data were fitted with Fig.P (BioSoft, version 6.0) to eq 1 by nonlinear regression analyses; with experimental data, weighting assumed that  $v$  has a constant percent error.

At low concentrations of acetylthiocholine and M7A, reciprocal plots of  $v^{-1}$  vs  $[S]^{-1}$  were linear. Competitive inhibition constants ( $K_i$ ) for inhibitors I were obtained by either (1) analysis of replots of reciprocal plot slopes obtained over a range of fixed concentrations of I (18) or (2) direct measurements of the second-order hydrolysis rate constants  $z$  in the presence and absence of I at low S concentrations. When I was a competing substrate,  $z$  was measured as an initial velocity at low S concentrations (i.e.,  $[S] < 0.1K_{\text{app}}$ ). The extent of acetylthiocholine hydrolysis in the presence of M7A was measured with 20  $\mu\text{M}$  pyridine disulfide (2,2'-dithiobispyridine; Acros) in place of DTNB. Absorbance of pyridine thiol was monitored at 347 nm [ $\Delta\epsilon_{341\text{nm}} = 8.1 \text{ mM}^{-1} \text{ cm}^{-1}$  (28)] because 347 nm corresponded to the isosbestic point of M7H and M7A. The extent of M7A hydrolysis in the presence of acetylthiocholine was measured on a Perkin-Elmer LS 50B luminescence spectrometer [excitation at 400 nm, emission at 500 nm (25)]. When I was an inhibitor that

was not metabolized,  $z$  was determined as a pseudo-first-order rate constant from eq 2 (22).

$$[S] = [S]_0 e^{-zt} \quad (2)$$

Equation 2 is valid when the initial substrate concentration  $[S]_0$  is low (i.e.,  $[S]_0 \ll K_{SS}$  and  $[S]_0 < \text{about } 0.2K_{app}$ ). In the absence of I,  $z$  is denoted  $z_{I=0} = V_{max}/K_{app}$  and eq 2 corresponds to the integrated form of eq 1. Measured  $z$  values at various I concentrations were fitted to eq 3 to obtain  $K_I$  and the constant  $\alpha$  (18).

$$\frac{z}{z_{I=0}} = \frac{\left(1 + \frac{[I]}{K_I}\right)}{\left(1 + \frac{\alpha[I]}{K_I}\right)} \quad (3)$$

For inhibitors that bind to the peripheral site and form ternary complexes  $ESI_P$  (see Scheme 1 below),  $\alpha$  is a measure of the acylation rate constant through the ternary complex at low substrate concentrations relative to  $k_{cat}/K_{app}$  (18). In contrast, for inhibitors that bind preferentially to the acylation site,  $\alpha$  is essentially zero.

**Slow Equilibration of Fasciculin in the Presence of Peripheral Site Inhibitors.** The rates of fasciculin binding to the AChE peripheral site were analyzed by an extension of procedures used previously (22). Association reactions (2 mL) were initiated by adding small volumes of AChE and acetylthiocholine to final concentrations of 0.5–10 nM fasciculin and 0.1 mM DTNB in buffer (with  $[NaCl] = 60$  mM –  $[S]$  as above) at 25 °C. Some reaction mixtures also included 20  $\mu$ M propidium. The extent of fasciculin binding was measured under approximate first-order conditions in which the concentrations of all ligands were adjusted to at least 8 times the concentration of AChE and the acetylthiocholine level was not significantly depleted (<20%). Acetylthiocholine hydrolysis was monitored by continuous spectrophotometric assay as outlined above, and assay rates  $v$  over 2 s intervals were fitted by nonlinear regression analysis (Fig.P) to eq 4. In eq 4,  $v_{initial}$  and  $v_{final}$  are the calculated values of  $v$  at time zero and at the final steady state when fasciculin binding has reached equilibrium, and  $k$  is the observed first-order rate constant for the approach to equilibrium.

$$v = v_{final} + (v_{initial} - v_{final}) e^{-kt} \quad (4)$$

Each series of binding measurements included reactions at a fixed acetylthiocholine (S) concentration and at least four fasciculin concentrations  $[F]$ . The observed  $k$  for each reaction was given by eq 5, and  $k_{on}$ , the apparent association rate constant, was determined by weighted linear regression analysis in which  $k$  was assumed to have a constant percent error.

$$k = k_{on}[F] + k_{off} \quad (5)$$

If ligand binding to the peripheral site is unaffected by the presence of ligands or an acyl group at the acylation site, then only three sets of enzyme species need be considered:  $\Sigma E$ ,  $\Sigma ES_P$ , and  $\Sigma EI_P$ . These are the sums of the concentrations

of all enzyme species in which nothing, S, or propidium (I), respectively, is bound to the peripheral site. Assuming that fasciculin (F) reacts only with species in  $\Sigma E$  and  $\Sigma ES_P$ ,  $k_{on}$  is given by eq 6.

$$k_{on} = \frac{k_F + k_{FP} \frac{[S]}{K_S}}{1 + \frac{[S]}{K_S} + \frac{[I]}{K_I}} \quad (6)$$

In eq 6,  $k_F$  is the intrinsic association rate constant for E and F,  $k_{FP}$  is the intrinsic association rate constant for  $ES_P$  and F, and  $K_S$  and  $K_I$  are the equilibrium dissociation constants for S and I, respectively, at the peripheral site. When eq 6 was employed, mean values of  $k_{on}$  obtained at each S concentration were fitted with Fig.P by nonlinear regression analysis with the reciprocals of the variances as weighting factors to give apparent  $K_S$  estimates. If ligand binding to the peripheral site is altered by the presence of a ligand at the acylation site, then  $k_{on}$  in eq 6 in principle must be extended by additional terms (26, 29). We will assume that these additional terms can be grouped in  $\Sigma EX_A$  as shown in eq 7, where the specific terms in each sum are given in Scheme 5 in the Appendix and  $k_{FA}$  is the intrinsic association rate constant for species in  $\Sigma EX_A$  and F.

$$k_{on} = \frac{k_F([E] + [EA]) + k_{FP} \Sigma ES_P + k_{FA} \Sigma EX_A}{[E] + [EA] + \Sigma ES_P + \Sigma EX_A + \Sigma EI_P} \quad (7)$$

Equation 7 cannot be solved analytically, but it can be solved numerically with the SCoP simulation program as outlined in the text.

The value of  $K_S$  for M7A was obtained by a modification of the above procedure in which fasciculin association reactions were measured at 412 nm with 2 nM fasciculin, 0.25 mM acetylthiocholine, and 0–300  $\mu$ M M7A in 1.0 mL of buffer without added NaCl. Observed  $k$  values were assumed to approximate  $k_{on}$ , and  $K_S$  was calculated from eq 6 (with  $[I]$  and  $k_{FP}$  set to 0).

**Simulations of Kinetic Equations and Assignment of Simulation Rate Constants.** The calculation of substrate hydrolysis rates from AChE reaction pathways in which reversible reactions are not at equilibrium is difficult because solutions to the corresponding differential equations are too complex for useful comparison to experimental data. We previously described our application of the program denoted SCoP (version 3.51), developed through the NIH National Center for Research Resources and available from Simulation Resources, Inc. (Redlands, CA), to solve these equations numerically (18). To obtain the simulated solutions to reaction schemes with the SCoP program, values for all reaction rate constants must be assigned or fitted. For Scheme 1, the second-order rate constant for substrate hydrolysis in the absence of inhibitor is given by eq 8.

$$\frac{k_{cat}}{K_{app}} = \frac{k_S k_2}{k_S + k_2} \quad (8)$$

We previously showed (18) that values of  $k_S$  and  $k_{-S}$  in eq 8 could be assigned if (1) estimates of  $k_{cat}$ ,  $K_{app}$ , and  $k_2$  were

Table 1: Rate Constants for Simulated Substrate Hydrolysis and Substrate Inhibition with AChE<sup>a</sup>

substrate	$k_S$ ( $\mu\text{M}^{-1} \text{s}^{-1}$ )	$k_{-S}$ ( $\text{s}^{-1}$ )	$k_1^b$ ( $\text{s}^{-1}$ )	$k_{-1}^b$ ( $\text{s}^{-1}$ )	$k_2, k_3$ ( $\text{s}^{-1}$ )	$k_{-P}^c$ ( $\text{s}^{-1}$ )	$k_{-P2}/k_{-P}$ ( $\text{s}^{-1}$ )	$a-f, i$
acetylthiocholine	150 <sup>d</sup>	$2 \times 10^5$	$3 \times 10^6$	$4 \times 10^4$	$1.4 \times 10^4$	$1.3 \times 10^5$	0.01	1
M7A	200	$4 \times 10^4$	$8 \times 10^4$	$4 \times 10^3$	$1.4 \times 10^4$	$1.3 \times 10^3$	0.01	1

<sup>a</sup> Simulations for both substrates were generated as outlined in the text with the indicated values of rate constants defined in Scheme 5 in the Appendix. <sup>b</sup> Calculated from eq 9 or 10 with an  $R_S$  that was assumed to be 1.0 (see Experimental Procedures). <sup>c</sup> Assigned from measured values for  $K_P$  of  $0.66 \pm 0.03$  mM for thiocholine or  $6.4 \pm 0.6$   $\mu\text{M}$  for M7H as outlined in Experimental Procedures. <sup>d</sup> The extent of substrate inhibition with acetylthiocholine was measured at a constant ionic strength slightly higher than that in other experiments (see Experimental Procedures). Ionic strength affects primarily  $K_{app}$  but not  $k_{cat}$  (12);  $k_S$ , assumed to be the only rate constant sensitive to ionic strength, was recalculated from  $K_{app}$ .

available and (2) the solvent deuterium oxide isotope effects  $R$ ,  $R_S$ , and  $R_2$  were known, where  $R$ ,  $R_S$ , and  $R_2$  are the respective ratios of  $k_{cat}/K_{app}$ ,  $k_S$ , and  $k_2$  in  $\text{H}_2\text{O}$  to that in  $\text{D}_2\text{O}$ . When  $R_2$  was assigned a typical value of 2.5 and  $R_S$  was assumed to be 1.0, for example,  $k_S = 1.5(k_{cat}/K_{app})/(2.5 - R)$ .

The second-order substrate hydrolysis rate constant in Scheme 3 in the Results is given by eq 9.

$$\frac{k_{cat}}{K_{app}} = \frac{k_S k_1 k_2}{k_S k_{-1} + k_2 (k_S + k_1)} \quad (9)$$

Assuming again that  $k_2$  and  $k_S$  are the only intrinsic rate constants in this equation that are altered when  $\text{H}_2\text{O}$  is replaced by  $\text{D}_2\text{O}$  and that  $R_2 = 2.5$ , eq 10 may be derived.

$$1 + \frac{k_S}{k_1} = \frac{1.5 k_{cat}}{K_{app} \left( 2.5 - \frac{R}{R_S} \right)} \quad (10)$$

To assign the intrinsic rate constants in eq 9, we inserted independent estimates of  $k_{cat}$  and  $K_{app}$  into eq 10. For example, for acetylthiocholine and human AChE, we previously estimated that  $k_{cat} = 7000 \text{ s}^{-1}$  and  $k_2 = k_3 = 1.4 \times 10^4 \text{ s}^{-1}$  (18). With a measured value for  $K_{app}$  of  $58 \mu\text{M}$  (Table 2 below), eq 10 requires that  $k_S > k_{cat}/K_{app} = 120 \mu\text{M}^{-1} \text{ s}^{-1}$ . For M7A, we obtained  $k_{cat}/K_{app}$  from parallel measurements of  $V_{max}/K_{app}$  (as the constant  $z_{1=0}$  in eq 2) for M7A and acetylthiocholine. The  $k_{cat}/K_{app}$  for M7A was  $82 \pm 2\%$  of the  $k_{cat}/K_{app}$  for acetylthiocholine (data not shown). From our measured values of  $K_S$  [1.5 mM for acetylthiocholine (Figure 2B below) and  $0.18 \pm 0.01$  mM for M7A (data not shown)],  $k_{-S}$  values were calculated from  $k_{-S} = K_S k_S$ . Assignments of  $k_1$  and  $k_{-1}$  become problematic when  $R$  approaches 1.0 because of uncertainty in  $R_S$ .  $R_S$  has been considered to be as high as 1.25, the ratio of the viscosities of  $\text{D}_2\text{O}$  to  $\text{H}_2\text{O}$  at  $25^\circ\text{C}$  (see, e.g., refs 30 and 31). For acetylthiocholine,  $R = 1.21 \pm 0.02$  (22), and for M7A,  $R = 1.09 \pm 0.05$  (data not shown);  $k_1$  calculated from eq 10 was very sensitive to the values of both  $k_S$  and  $R_S$ . In practical terms, the simulations were not sensitive to the absolute values of  $k_S$ ,  $k_1$ , and  $k_{-1}$  as long as  $k_1$  was calculated from eq 10 and  $k_{-1}$  from eq 9. For example, simulated substrate inhibition curves for acetylthiocholine (Figure 3A below) were fitted to the Haldane equation (eq 1) by varying  $k_S$  from 120 to  $500 \mu\text{M}^{-1} \text{ s}^{-1}$  and calculating the corresponding values of  $k_{-S}$ ,  $k_1$ , and  $k_{-1}$  (with all other rate constants fixed). The resulting fitted  $K_{app}$  and  $K_{SS}$  values varied by less than 5% (data not shown). We assigned  $k_S$  values of  $200 \mu\text{M}^{-1} \text{ s}^{-1}$  (at the ionic strength of buffer alone) to correspond to the general ligand association rate constant used in our previous simulations (18). The

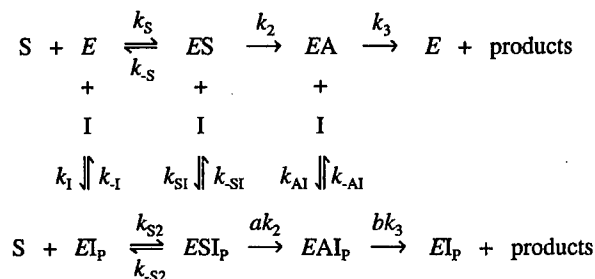
assigned values of  $k_2$  and  $k_3$  for M7A were the same as those for acetylthiocholine because (1) the  $k_3$  reaction is identical with both substrates and (2) the simulations were quite insensitive to  $k_2$  when  $k_2$  exceeded  $k_{-P}$ ; 8-fold increases or decreases in  $k_2$  resulted in less than a factor of 2 change in fitted parameters when simulated  $v$  versus  $[S]$  curves were analyzed with the Haldane equation.

For all substrates, we obtained estimates of  $k_{-P}$  (Schemes 2 and 3) from  $k_{-P} = K_I k_P$ , where  $K_I = K_P$  was the competitive inhibition constant for reaction product P measured with a different substrate. Since estimates of  $k_P$  are unavailable for any of the substrates used in this study,  $k_P$  was assumed to have the same value as  $k_S$ . The steric blockade parameter  $k_{-P2}/k_{-P}$  was assumed to be 0.01–0.04, consistent with our previous observations that ligand binding to the peripheral site decreases ligand dissociation rate constants from the acylation site by 10–100-fold (18). Assigned intrinsic rate constants for acetylthiocholine and M7A are summarized in Table 1.

## RESULTS

*Expansion of Our Steric Blockade Model To Include Inhibition of Product Dissociation.* When a ligand binds to the peripheral site of AChE, the ensuing inhibition of substrate hydrolysis is often interpreted according to Scheme 1.

Scheme 1



Inhibitor (I) can bind to each of the three enzyme species E, ES, and EA. For example,  $\text{ESI}_P$  represents a ternary complex with substrate (S) at the acylation site and I at the peripheral site (denoted by the subscript P). The acylation rate constant  $k_2$  is altered by a factor  $a$  in this ternary complex, and the deacylation rate constant  $k_3$  is altered by a factor  $b$  in the  $\text{EAI}_P$  complex. To obtain a tractable solution to the steady state substrate hydrolysis rate  $v$  that corresponds to Scheme 1, it has often been assumed that the reversible reactions are at equilibrium (with  $k_{-X}/k_X = K_X$ ). Although this assumption cannot be justified for AChE (1), the mixed, partial inhibition patterns that are often observed with peripheral site inhibitors of AChE can be fitted to the equilibrium solution (18). These fits require that  $a$  (or  $b$  and

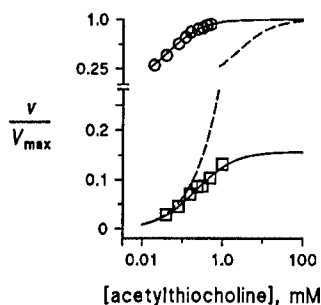


FIGURE 1: Propidium inhibition of the AChE-catalyzed hydrolysis of acetylthiocholine. Points represent initial velocities measured as outlined in Experimental Procedures at 25 pM AChE and the indicated acetylthiocholine concentrations with (□) or without (○) 50  $\mu$ M propidium. Lines were generated by the SCoP simulation program for rate constants in Scheme 1 (O—O and - - -) or Scheme 4 (□—□). Rate constant values assigned previously (18) were as follows:  $k_S = k_1 = k_{S1} = k_{A1} = 200 \mu\text{M}^{-1} \text{s}^{-1}$ ;  $k_{S2} = 3 \mu\text{M}^{-1} \text{s}^{-1}$ ;  $k_{-S} = 3 \times 10^3 \text{s}^{-1}$ ;  $k_{-S2} = 45 \text{s}^{-1}$ ;  $k_{-1} = k_{-S1} = k_{-A1} = 200 \text{s}^{-1}$ ;  $k_2 = k_3 = 1.4 \times 10^4 \text{s}^{-1}$ ; and  $a = b = 1$ . New rate constants required to extend Scheme 1 to Scheme 4 were assigned as follows:  $k_{-P} = 6 \times 10^4 \text{s}^{-1}$ ;  $k_{-P2} = 9 \times 10^2 \text{s}^{-1}$ ; and  $c = d = e = f = i = 1$ .

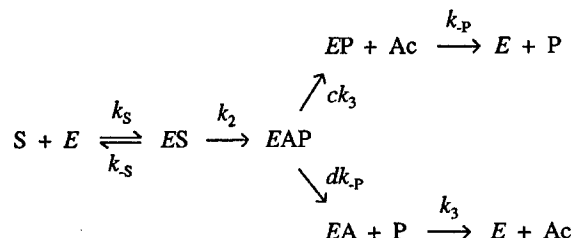
$K_S/K_{S2}$  be much less than 1, and interpretation of such low values would appear to indicate a conformational interaction between the two sites.

To avoid assumptions of equilibrium in Scheme 1, we introduced a nonequilibrium analysis that involved numerical solution of the rate equations that arise from Scheme 1 with the SCoP program (18). The analysis required assignment of all the rate constants in Scheme 1 and generated simulated values of  $v$ . We simplified these assignments by proposing our steric blockade model in which the only effect of bound peripheral site ligand is to decrease  $k_{S2}$  relative to  $k_S$  and  $k_{-S2}$  relative to  $k_{-S}$  while maintaining  $K_S = K_{S2}$  and  $a = b = 1$ . Since  $k_S$  is rate-limiting at low substrate concentrations without inhibitor and  $k_{S2}$  becomes rate-limiting at low substrate concentrations and saturating concentrations of inhibitor, the model with Scheme 1 correctly predicts that increasing concentrations of inhibitor should progressively decrease the second-order hydrolysis rate measured at low substrate concentrations (18). However, at high substrate concentrations, neither  $k_S$  nor  $k_{S2}$  remains rate-limiting, and the model with Scheme 1 predicts that inhibitor should have no effect on the  $V_{\text{max}}$  obtained at high substrate concentrations. This prediction is not supported experimentally, as illustrated in Figure 1. This figure shows  $v$  as a function of acetylthiocholine concentration. In the absence of propidium, the observed  $v$  (○) were fitted well by the line simulated with the steric blockade model. With the peripheral site occupied by a saturating concentration of propidium (50  $\mu$ M), the simulated  $v$  (dashed line) corresponded well with the observed  $v$  (□) at low substrate concentrations but increased much more than the observed  $v$  at higher substrate concentrations. Near 100 mM acetylthiocholine, the simulated lines for  $v$  with and without propidium converged. Therefore, the steric blockade model with Scheme 1 fails to incorporate an inhibition component that becomes apparent at high substrate concentrations. This inhibition component might involve substrate inhibition, a phenomenon observed with some cationic substrates such as acetylthiocholine that is addressed below. However, the experimental acetylthiocholine concentrations in Figure 1 are below the range where substrate inhibition is observed. Furthermore, the divergence in Figure

1 between simulated and observed  $v$  values in the presence of propidium is also seen with other substrates such as phenyl acetate that do not exhibit substrate inhibition (18).

Schemes 2 and 4 incorporate a logical extension of Scheme 1 which, as we now show, can eliminate disagreement between the steric blockade model and observed  $v$  at the higher substrate concentrations investigated experimentally in Figure 1. Scheme 2 makes explicit the dissociation rate constant  $k_{-P}$  for the first product P, the alcohol leaving group (e.g., thiocholine) generated by acylation of the active site serine. For simplicity, inclusion of a peripheral site inhibitor is deferred to Scheme 4 in the Appendix.

#### Scheme 2



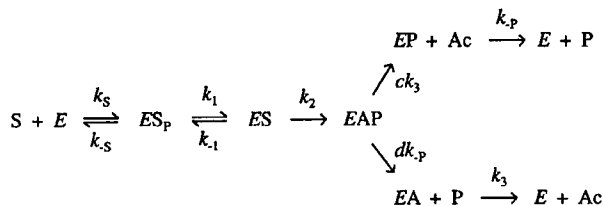
The first intermediate following enzyme acylation in Scheme 2 is EAP. To maintain generality, P may dissociate before ( $dk_{-P}$ ) or after ( $k_{-P}$ ) the deacylation step. EAP has not been included explicitly in most catalytic pathways previously considered for AChE because  $dk_{-P}$  has been assumed to be sufficiently fast to render any accumulation of EAP negligible. This appears to be a good assumption for most AChE substrates. For example, we estimated  $k_{-P}$  for acetylthiocholine to be  $1.3 \times 10^5 \text{s}^{-1}$  from the relationship  $k_{-P} = k_P K_P$ , where a  $K_P$  of 0.66 mM was measured as the competitive inhibition constant for thiocholine inhibition of M7A hydrolysis (data not shown) and the association rate constant  $k_P$  for thiocholine was assigned the same value assumed for acetylthiocholine ( $200 \mu\text{M}^{-1} \text{s}^{-1}$ ). Since this  $k_{-P}$  is nearly 1 order of magnitude larger than  $k_2$  or  $k_3$ , its inclusion in the model has little effect on the experimental kinetic parameters; calculations based on Schemes 1 and 2 (with  $d = 1$ ) show that  $k_{\text{cat}}$  is decreased by less than 1% and  $k_{\text{cat}}/K_{\text{app}}$  is unaltered.

We extend our steric blockade hypothesis with Scheme 4 (Appendix) by proposing that a bound peripheral site inhibitor not only reduces association and dissociation rate constants for substrate binding to the acylation site but also reduces the dissociation rate constant for release of P. In this case, a simulated nonequilibrium analysis demonstrates that product dissociation rate constants can become important. A key rate constant in this analysis was  $k_{-P2}$ , the rate constant for dissociation of P from the  $\text{EPI}_P$  ternary complex, since our steric blockade model proposes that the only consequences of ligand binding to the peripheral site are low ratios of  $k_{S2}/k_S$ ,  $k_{-S2}/k_{-S}$ , and  $k_{-P2}/k_{-P}$ . For example, if bound propidium at the peripheral site reduced  $k_{-P2}$  in Scheme 4 to 1.5% of  $k_{-P}$ , the same reduction previously deduced for  $k_{-S2}$  relative to  $k_{-S}$  for acetylthiocholine (18), then thiocholine dissociation does contribute to a reduction in  $v$ . With a  $k_{-P}$  of  $1.3 \times 10^5 \text{s}^{-1}$  as calculated above, most of the divergence between the experimental points with 50  $\mu$ M propidium and the corresponding simulated line in Figure 1 was eliminated. Assigning just a 2-fold lower value of  $k_{-P}$  ( $6 \times 10^4 \text{s}^{-1}$ ) completely eliminated this divergence and gave the simulated

lower line shown in Figure 1. Therefore, if product affinity for the acylation site is sufficiently high, product release may become partially rate-limiting when the peripheral site is occupied. Specifically,  $v$  will be affected when the product dissociation rate constant  $k_{-p2}$  falls within the range of the acylation ( $k_2$ ) and deacylation ( $k_3$ ) rate constants. Thiocholine, a cationic leaving group P, illustrates this point in Figure 1. In contrast, the acetate product (Ac) of acetylthiocholine hydrolysis has an affinity for the acylation site that is too low ( $K_1 > 100$  mM) to contribute any rate limitation even with propidium bound to the peripheral site. The analysis in Figure 1 completes our demonstration that the steric blockade can explain AChE inhibition by peripheral site ligands. Specifically, direct measurement of association and dissociation rate constants for the acylation site ligands huperzine A and TMTFA revealed decreases of 10–380-fold when propidium was bound to the peripheral site (18), and decreases in these rate constants alone for substrates and their hydrolysis products are sufficient to account for inhibition by bound peripheral site ligands at both low (18) and high (Figure 1) substrate concentrations.

**Acetylcholine Can Bind to the Peripheral Site.** We turn next to the questions of whether acetylthiocholine, a close analogue of the physiological substrate acetylcholine, can bind to the peripheral site and whether this binding is of significance on the catalytic pathway. Scheme 3 defines an initial complex  $ES_P$  of substrate with the peripheral site and incorporates this species into the previous catalytic pathway from Scheme 2.

Scheme 3



$ES_P$  can reversibly proceed to  $ES$ , the complex of substrate with the acylation site, where acylation occurs. For simplicity, we have not included the additional complexes  $ESS_P$ ,  $EAPS_P$ ,  $EAS_P$ , and  $EPS_P$  in Scheme 3, but they are made explicit in Scheme 5 in the Appendix. These complexes are important in the phenomenon of substrate inhibition considered below, and they also must be considered in any measurement of substrate affinity for the peripheral site.

A direct way of measuring substrate affinity for the peripheral site is to measure the effect of substrate on the association rate constant  $k_{\text{on}}$  for a slowly equilibrating ligand that binds exclusively to the peripheral site. Fasciculin is such a ligand, and we previously confirmed the affinity of propidium for the peripheral site by measuring its inhibition constant  $K_I$  during fasciculin binding (22). The analysis was straightforward with an inhibitor like propidium (I) that competes with fasciculin, because only a single complex  $EL_P$  is formed to alter the observed  $k_{\text{on}}$ . If our steric blockade model is correct and ligand binding to the peripheral site is unaffected by the presence of ligands or an acyl group at the acylation site, then this analysis can be extended directly to include substrate. Only species with S bound to the peripheral site are relevant, and the resulting analysis should

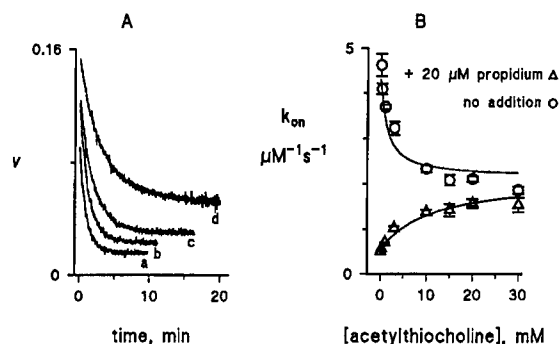


FIGURE 2: Acetylthiocholine binding to the AChE peripheral site. (A) The hydrolysis rate  $\nu$  ( $\Delta A_{412\text{nm}}$  per minute) for the approach to equilibrium fasciculin (F) binding was measured with 10 mM acetylthiocholine, 50 pM AChE, F (a, 5 nM; b, 3 nM; c, 2 nM and d, 1 nM), and buffered 50 mM NaCl by continuous spectrophotometric assay as outlined in Experimental Procedures. Rate constants ( $k$ ) obtained from eq 4 were then plotted against the fasciculin concentration (eq 5) to obtain  $k_{\text{on}}$  (plot not shown). (B) The dependence of  $k_{\text{on}}$  on the acetylthiocholine concentration was analyzed with eqs 6 and 7. Indicated points representing the average of three or four  $k_{\text{on}}$  measurements (except at 15 mM) were fitted with eq 6 to give apparent  $K_S$  estimates of  $3.6 \pm 1.0$  mM in the absence of propidium ( $\circ$ ) and  $0.6 \pm 0.1$  mM with 20  $\mu\text{M}$  propidium ( $\Delta$ ). (This fitting is not shown here but is given in Figure 2B of ref 45.) A mean  $K_S$  of 1.5 mM was used to assign  $k_{-5}$  in Table 1 and to generate *both* lines representing the simulated dependence of  $k_{\text{on}}$  on  $[S]$  from eq 7. The simulations were based on Scheme 5 as outlined in the text with the rate constant assignments in Table 1 except that  $k_{-p} = 6 \times 10^4 \text{ s}^{-1}$ ; in addition,  $k_{-1}$  and  $k_{-p2}$  for propidium were the same as in Figure 1 but  $k_1 = 70 \mu\text{M}^{-1} \text{ s}^{-1}$  (due to the change in ionic strength from Figure 1). The simulated lines also were fitted well by eq 6 with a  $K_S$  value of  $1.36 \pm 0.01$  mM both in the absence of propidium and with 20  $\mu\text{M}$  propidium.

be compatible with eq 6. However, in the presence of both S and I, Scheme 5 includes 14 liganded enzyme species as noted in the Appendix. It is certainly possible that our model is oversimplified and that ligands bound to the acylation site will alter ligand binding to the peripheral site. We can address this possibility by simulation analysis of the more general eq 7. We began our experimental analysis by measuring the observed rate constants  $k$  for fasciculin binding during continuous substrate hydrolysis as shown in Figure 2A. Apparent association rate constants  $k_{\text{on}}$  were then calculated from a series of  $k$  values obtained at fixed acetylthiocholine concentrations [S] according to eq 5. Plots of  $k_{\text{on}}$  versus [S] in the absence of propidium revealed that  $k_{\text{on}}$  did decrease at higher S concentrations and reasonably conformed to eq 6 (O in Figure 2B). This decrease suggested that acetylthiocholine competes with fasciculin at the peripheral site, but to our surprise, the competition was only partial. Values of  $k_{\text{on}}$  at high S concentrations leveled off at about one-half of the  $k_{\text{on}}$  extrapolated to zero S concentration. According to eq 6, this observation indicates that  $k_{\text{FP}}$  for fasciculin binding to  $ES_{\text{P}}$  is about one-half of  $k_{\text{F}}$ , the intrinsic association rate constant for fasciculin binding to the peripheral site in free AChE. In contrast,  $k_{\text{on}}$  for fasciculin was observed previously to decrease to near zero at high propidium concentrations, and the absence of any detectable  $k_{\text{FP}}$  for fasciculin with the propidium-AChE complex was taken as evidence that fasciculin and propidium were completely competitive (22). Our immediate concern was that the partial acetylthiocholine inhibition of fasciculin binding did not reflect an interaction



of acetylthiocholine at the peripheral site but instead was an indirect effect of acetylthiocholine bound at the acylation site. Three points argued against this interpretation. First, the apparent  $K_S$  for the acetylthiocholine that competes with fasciculin according to eq 6 was in the low millimolar range (Figure 2B). This value was nearly 2 orders of magnitude higher than  $K_{app}$  for acetylthiocholine, which roughly indicates the affinity of substrate complexes at the acylation site. Second, inclusion of edrophonium, an inhibitor specific for the acylation site, at high concentrations (90 times its  $K_I$ ) with acetylthiocholine and fasciculin only slightly altered the upper plot in Figure 2B (data not shown). Third, when in contrast a high concentration of propidium (nearly 10 times its  $K_I$ ) was included, progressively higher S concentrations actually increased the observed  $k_{on}$  substantially ( $\Delta$  in Figure 2B). Since propidium affinity for the peripheral site is at most slightly affected by the binding of ligands to the acylation site (9, 18), this observation appears to require that acetylthiocholine and propidium compete at the peripheral site and that displacement of propidium by acetylthiocholine result in an increased rate of fasciculin association.

To confirm this indication of acetylthiocholine binding to the peripheral site, we conducted nonequilibrium simulations in which  $k_{on}$  was calculated from eq 7. Differential equations corresponding to the rate expressions from Scheme 5 were solved numerically by the SCoP program with rate constants (Table 1 and Figure 2B) assigned as outlined in Experimental Procedures. The geometric mean of the apparent  $K_S$  estimates from eq 6 with and without propidium was about 1.5 mM (Figure 2B), and from this value and the previously estimated  $k_S$ , a  $k_{-S}$  of  $2 \times 10^5 \text{ s}^{-1}$  was assigned. Two other key assignments involved the relative values of  $k_{FP}/k_F$  and  $k_{FA}/k_F$  in eq 7. The decision to limit the 14 possible fasciculin association rate constants to only these three in the numerator in eq 7 was largely based on the close conformity of the data in Figure 2B to eq 6. This conformity indicated that fasciculin associated with several enzyme species with identical rate constants. We sorted these enzyme species into four groups. The first consisted of those with no bound cationic ligands (i.e.,  $[E] + [EA]$ ) with a fasciculin association rate constant of  $k_F$ . The second contained those in which substrate was bound to the peripheral site ( $\Sigma ES_P$ ) and was characterized by a relative rate constant of  $k_{FP}/k_F$ . The third included those in which the peripheral site was free but substrate or its thiocholine product was bound to the acylation site ( $\Sigma EX_A$ ), and these were given a relative rate constant of  $k_{FA}/k_F$ . The fourth involved those with propidium bound to the peripheral site ( $\Sigma EI_P$ ) and with a relative rate constant of zero. We first simulated our steric blockade model, in which ligand binding to the peripheral site is unaffected by the presence of ligands or an acyl group at the acylation site. Fasciculin association was assumed to be partially blocked by substrate bound at the peripheral site ( $k_{FP}/k_F = 0.5$ ) but unaffected by substrate or product bound at the acylation site ( $k_{FA}/k_F = 1$ ). In support of the latter assignment, previous data (22) and our results above indicated that fasciculin association rate constants are not affected by edrophonium bound to the acylation site. With these assignments, the simulation program calculated the concentrations of all the enzyme intermediates in Scheme 5, with and without propidium, and solved eq 7 for  $k_{on}$  as a function of S concentration. The simulated values of  $k_{on}$  are shown as the

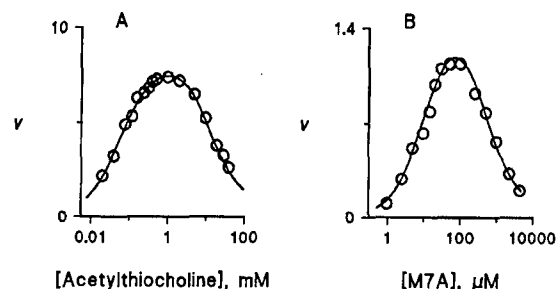


FIGURE 3: Substrate inhibition with acetylthiocholine and M7A. Points represent initial velocities ( $\mu\text{M min}^{-1}$ ) measured at the indicated substrate concentrations as outlined in Experimental Procedures. (A) Reaction mixtures with acetylthiocholine and 20 pM AChE were supplemented with NaCl such that  $[S] + [\text{NaCl}] = 60 \text{ mM}$  to maintain a constant ionic strength. The line was generated by the SCoP simulation program with assigned rate constants in Table 1 except that  $k_{-P} = 6 \times 10^4 \text{ s}^{-1}$ . When fitted to the Haldane equation (eq 1), the simulated line corresponded to a  $K_{app}$  of  $57.9 \pm 0.4 \mu\text{M}$  and a  $K_{SS}$  of  $17.9 \pm 0.1 \text{ mM}$ . (B) Initial velocities for M7A in 20 mM sodium phosphate buffer with the experimental AChE concentrations (20–2000 pM) were normalized to 20 pM AChE for comparison to Figure 3A. The line was generated by the SCoP simulation program with assigned rate constants in Table 1 except that  $k_{-P}$  was slightly increased to  $1.5 \times 10^3 \text{ s}^{-1}$  and thermodynamic interaction between sites was allowed, with  $i = 4$ ,  $k_{-S} = 2 \times 10^4 \text{ s}^{-1}$ ,  $k_I = 4 \times 10^4 \text{ s}^{-1}$ , and  $k_{-P}/k_{-P} = 0.04$ . When fitted to the Haldane equation, the simulated line corresponded to a  $K_{app}$  of  $9.3 \pm 0.1 \mu\text{M}$  and a  $K_{SS}$  of  $640 \pm 3 \mu\text{M}$ .

lines in Figure 2B. They superimposed well with the original fits of the experimental data to eq 6, and they confirmed that eq 6 provides an excellent approximation when fasciculin association is affected only by substrate bound to the peripheral site. The  $K_S$  of 1.4 mM calculated from the simulations agreed with the assigned  $K_S$ . In contrast, when both  $k_{FP}/k_F$  and  $k_{FA}/k_F$  were assigned a value of 0.5, the simulated  $K_S$  with 20  $\mu\text{M}$  propidium was unchanged but the simulated  $K_S$  without propidium decreased 5-fold. This trend was the opposite of that observed experimentally in Figure 2B. We also examined whether a small decrease in the relative fasciculin association rate with substrate or product bound to the acylation site ( $k_{FA}/k_F = 0.5$ ) could be superimposed on complete competition between substrate and fasciculin at the peripheral site ( $k_{FP}/k_F = 0$ ). In this case, the simulations showed that  $k_{on}$  with 20  $\mu\text{M}$  propidium did not change significantly with increased S concentrations, again in contrast to the observations in Figure 2B. These simulations confirmed the indication in the previous paragraph that acetylthiocholine and propidium must compete at the peripheral site for acetylthiocholine to accelerate fasciculin association in the presence of propidium.

Since the individual rate constants on the catalytic pathway in Scheme 3 in general are too high to measure by rapid kinetic techniques, there are relatively few phenomena involving substrate hydrolysis by AChE that allow us to obtain experimental evidence to support Schemes 3 and 5 and the rate constant assignments in Figure 2B. Two pertinent phenomena are substrate inhibition and mixed substrate hydrolysis, and these are examined in the following sections.

**Substrate Inhibition.** When rates of acetylthiocholine hydrolysis with AChE are measured as a function of acetylthiocholine concentration  $[S]$ , the profile in Figure 3A is observed. This profile does not correspond to a simple



Table 2: Simulated and Observed Kinetic Parameters for Substrate Hydrolysis and Substrate Inhibition with AChE<sup>a</sup>

substrate	$k_{\text{cat}}$ (s <sup>-1</sup> )	$K_{\text{app}}$ ( $\mu\text{M}$ )	$K_{\text{SS}}$ (mM)
Observed Values			
acetylthiocholine	7000 <sup>b</sup>	58 $\pm$ 2	18.6 $\pm$ 0.7
M7A	1300 $\pm$ 160 <sup>c</sup>	10 $\pm$ 1	0.7 $\pm$ 0.1
Simulated Values			
acetylthiocholine	$d$	$d$	44.4 $\pm$ 0.1
M7A	1120 $\pm$ 30 <sup>c</sup>	8.8 $\pm$ 0.04	0.25 $\pm$ 0.001

<sup>a</sup> Kinetic parameters were determined by fitting the dependence of  $v$  on the substrate concentration to the Haldane equation (eq 1). Simulated values were obtained with Scheme 5 (Appendix) and the rate constants in Table 1. <sup>b</sup> From previous literature values (see ref 18). <sup>c</sup> Calculated from the product of  $k_{\text{cat}}/K_{\text{app}} \times K_{\text{app}}$ . <sup>d</sup> Matched to observed parameters by rate constant assignments.

Michealis–Menten kinetic pattern, and the bell-shaped curve with the decline at high  $S$  concentrations has long been referred to as substrate inhibition (32). This curve can be fitted to the Haldane equation (eq 1), which contains three experimental parameters:  $V_{\text{max}}$  ( $= k_{\text{cat}}[E]_{\text{tot}}$ ),  $K_{\text{app}}$ , and the substrate inhibition constant  $K_{\text{SS}}$ . Since the Haldane equation is not restricted to any mechanistic scheme, it provides a useful quantitative standard for assessing data simulated from our nonequilibrium analysis of Scheme 5 with the rate constant assignments in Table 1. It is important to note that these rate constants were assigned from data unrelated to the substrate inhibition phenomenon itself.

For acetylthiocholine  $K_{\text{SS}}$  was the only parameter independently obtained from this fitting procedure, as known values of  $k_{\text{cat}}$  and  $K_{\text{app}}$  were incorporated into the rate constant assignments. The simulation in fact generated a curve exhibiting substrate inhibition with a  $K_{\text{SS}}$  value of 44.4 mM, about twice the observed  $K_{\text{SS}}$  of 18.6 mM (Table 2). We assessed changes in assigned rate constants that could reconcile this difference. Although substrate inhibition results from a low value of  $k_{-p2}/k_{-p}$ , the value of  $K_{\text{SS}}$  obtained from the simulation was only moderately sensitive to the  $k_{-p2}/k_{-p}$  assignment (e.g., changing  $k_{-p2}/k_{-p}$  from 0.01 to 0 only decreased the simulated  $K_{\text{SS}}$  to 28 mM). In contrast, the simulated  $K_{\text{SS}}$  value was more sensitive to the assigned value of  $k_{-p}$ , with the two values appearing virtually proportional. For example, decreasing the assigned  $k_{-p}$  from  $1.3 \times 10^5$  to  $6 \times 10^4$  s<sup>-1</sup> decreased the  $K_{\text{SS}}$  obtained from the simulation to 17.9 mM and gave an excellent fit of the simulated curve to the experimental data, as shown in Figure 3A. Since the original assignment of  $k_{-p}$  assumed that  $k_p = k_s$ , an assumption that cannot be tested experimentally with available techniques, the agreement between the observed and simulated substrate inhibition data appears to be quite reasonable.

We next turned to M7A, a substrate that previously exhibited substrate inhibition with eel AChE (26, 33) and also showed this inhibition pattern with human AChE (Figure 3B). This substrate is of particular interest in testing our steric blockade model because it binds to the peripheral site ( $K_S = 0.18 \pm 0.01$  mM from competition with fasciculin, data not shown), and its hydrolysis product M7H has a high affinity for AChE and a consequent low calculated  $k_{-p}$  of  $1.3 \times 10^3$  s<sup>-1</sup> (Table 1). Analysis of the simulated  $v$  versus  $[S]$  curve with the Haldane equation and the constants for M7A in Table 1 gave independent estimates of  $K_{\text{SS}}$  and  $k_{\text{cat}}$ , since only the ratio  $k_{\text{cat}}/K_{\text{app}}$  was incorporated into the rate

constant assignments. The simulated  $K_{\text{SS}}$  of 0.25 mM was nearly 3 times smaller than the observed  $K_{\text{SS}}$  of 0.7 mM, but the simulated  $k_{\text{cat}}$  was within 20% of that observed (Table 2). The reasonably close agreement supported our steric blockade model. In particular, the observed  $k_{\text{cat}}$  for M7A was only 19% of the  $k_{\text{cat}}$  for acetylthiocholine (Table 2), and this low relative  $k_{\text{cat}}$  was explained in the steric blockade model by the low  $k_{-p}$  for the M7H product. In contrast to the interaction of acetylthiocholine with AChE, the most abundant simulated intermediate with M7A at concentrations below  $K_{\text{SS}}$  was  $EP$ , the AChE complex with the M7H product, and dissociation of this complex was the step that limited the value of  $k_{\text{cat}}$ . As a consequence, a slight increase in  $k_{-p}$  resulted in an almost proportionate increase in  $k_{\text{cat}}$  but in almost no effect on  $K_{\text{SS}}$ . The most straightforward way to achieve agreement between the simulated and observed  $K_{\text{SS}}$  values<sup>2</sup> was to relax the stringent assumption in our steric blockade model that the affinity of ligands for the peripheral and acylation sites was unchanged when both sites were occupied simultaneously in a ternary complex (see Discussion). Good agreement was then observed in Figure 3B, where the affinities of M7A and M7H in ternary complexes were assigned to be 25% of their affinities in binary complexes (e.g.,  $i = 4$ ). The simulation in Figure 3B also assumed that the apparent  $K_S$  of 0.18 mM for M7A was an average of the actual  $K_S$  and of  $iK_S$ , where  $iK_S$  is the dissociation constant for M7A binding to the peripheral site when the acylation site is occupied by M7A or M7H.

**Mixed Substrate Hydrolysis.** When two substrates are mixed with AChE, each substrate inhibits the hydrolysis of the other. We measured the extent of competitive inhibition of acetylthiocholine hydrolysis by M7A and, conversely, the extent of competitive inhibition of M7A hydrolysis by acetylthiocholine by monitoring the hydrolysis of each substrate independently. Competitive inhibition was assessed from relative second-order hydrolysis rate constants  $z$  by plotting the data according to eq 3. If none of the enzyme intermediates generated by the competing substrate can react with the monitored substrate, then the  $K_I$  for the competing substrate should equal its  $K_{\text{app}}$ . This is typically the case for simple models of substrate competition, and it is also the case when M7A is the competing substrate during acetylthiocholine hydrolysis. In Figure 4A, the solid line represents the inhibition calculated from eq 3 when  $K_I$  for M7A equals its  $K_{\text{app}}$  from Figure 3B. The observed points were within experimental error of this line. Furthermore, simulation of this competition with the steric blockade model applied to Scheme 5 and the assigned rate constants in panels A and B of Figure 3 generated the dashed line that also closely followed the solid line. The data indicate that acetylthiocholine does not initiate its catalytic pathway with any

<sup>2</sup> Assigned rate constants could also be adjusted in the following way to obtain agreement of the simulated and observed  $K_{\text{SS}}$  for M7A in Figure 3B. A 7-fold decrease in  $k_2$  combined with a 3-fold increase in  $k_{-p}$ , relative to the assignments in Table 1, shifted the rate-limiting step in  $k_{\text{cat}}$  from product dissociation to acetylation and gave a simulated curve virtually identical to the one in Figure 3B. These adjustments were not a very attractive option because they seem to run counter to observations that the M7H leaving group promotes excellent acylation of AChE. For example, dimethylcarbamoylated M7H shows a higher acylation rate constant than dimethylcarbamoylated choline (25, 34). Furthermore, these adjustments gave a less than satisfactory fit of the simulated curve to the experimental points in Figure 4B.

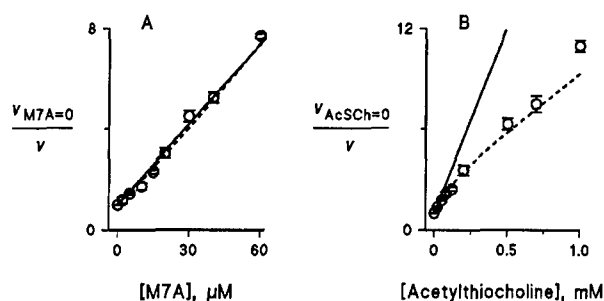


FIGURE 4: Inhibition of hydrolysis of one substrate by a second substrate. (A) Points denote second-order rate constants  $z$  for acetylthiocholine (AcSch) measured in the presence of competing M7A as the inhibitor (see Experimental Procedures). The points were normalized to  $z_{M7A=0}$  for acetylthiocholine in the absence of M7A and plotted according to eq 3. (B) Points denote second-order rate constants  $z$  for M7A in the presence of competing acetylthiocholine (AcSch) normalized to  $z_{AcSch=0}$  for M7A in the absence of acetylthiocholine. M7A hydrolysis was monitored by spectrofluorometry. In each panel, indicated points represent averages of two to four measurements. The solid line is the extent of calculated inhibition if the  $K_i$  for the competing substrate were equal to its  $K_{app}$ . The dashed line is the extent of inhibition simulated for the steric blockade model with Scheme 5 and the assigned rate constants in panels A and B of Figure 3. New rate constants resulting from mixed ternary complexes (e.g.,  $i_{ST} = i_{TS} = 1$ , see Appendix) were assigned assuming no thermodynamic interaction between the bound ligands in these complexes.

enzyme intermediate produced by M7A. However, when acetylthiocholine is the competing substrate during M7A hydrolysis, the observed inhibition points fell below the solid line expected if  $K_i$  for acetylthiocholine were equal to its  $K_{app}$  (Figure 4B). A similar pattern of inhibition of M7A hydrolysis by acetylthiocholine was observed previously with eel AChE (26). The level of inhibition in Figure 4B corresponded well to the level of inhibition simulated with Scheme 5 (dashed line in Figure 4B), thereby supporting our steric blockade model. The simulation was particularly sensitive to two parameters,  $k_{-S}$  for M7A and  $k_{-P2}/k_{-P}$  for thiocholine product dissociation when M7A was bound to the peripheral site. A decrease in  $k_{-S}$  or an increase in this  $k_{-P2}/k_{-P}$  resulted in less inhibition by acetylthiocholine. This pattern indicates that an M7A molecule can initiate its catalytic pathway by binding to the peripheral site when acetylthiocholine is bound to the acylation site. The dissociation of this M7A is sufficiently slow that it will wait at the peripheral site while acetylation by the acetylthiocholine and deacetylation occur and the thiocholine product dissociates from the enzyme. This M7A then will proceed to the acylation site. A corresponding phenomenon is not seen during M7A inhibition of acetylthiocholine hydrolysis because acetylthiocholine dissociates too rapidly from the peripheral site and product M7H dissociates too slowly from the acylation site. These data provide the most direct evidence in support of our proposal in Schemes 3 and 5 that initial substrate binding to the peripheral site occurs on the catalytic pathway. This pathway does not require release of substrate from the peripheral site to the solution and its direct reassociation with the acylation site for catalysis to occur.

## DISCUSSION

A key observation in this report is that acetylthiocholine can bind to the AChE peripheral site with an equilibrium dissociation constant  $K_S$  of about 1 mM. This value was

determined from the effect of the acetylthiocholine concentration on the rate at which fasciculin associates with the peripheral site. The approach to equilibrium fasciculin binding was monitored by continuous spectrophotometric assay of acetylthiocholine hydrolysis. We employed this method previously with the high-affinity bisquaternary inhibitor ambenonium and found that acetylthiocholine inhibited ambenonium association by binding to a site on AChE with a  $K_S$  of about 1 mM (29), in good agreement with our current estimate. However, since ambenonium binds to both the acylation and peripheral sites simultaneously, it was difficult to assign this acetylthiocholine binding to the peripheral site. Our current assay has the advantages that fasciculin binds only to the peripheral site and that its slower rate of binding allows greater precision. Noise levels with the Cary 3A spectrophotometer are low enough to allow velocity estimates over 2 s intervals, and rate constants ( $k$ ) for the approach to equilibrium fasciculin binding (Figure 3A) were fitted with typical standard errors of 1–5%.

When acetylthiocholine binding to the peripheral site is incorporated into our steric blockade model, a wide range of kinetic data, including substrate inhibition, can be explained. To keep the model conceptually simple, we have examined the very limited hypothesis that the only effect of substrates or inhibitors bound to the peripheral site is to decrease association and dissociation rate constants for acylation site ligands without changing their ratio, the equilibrium dissociation constant. Thus, we hypothesize that a bound peripheral site ligand has no effect on the thermodynamics of binding of acylation site ligands or on their reactivity at the acylation site. Even with this assumption, some of the rate constants in Schemes 3 and 5 cannot be assigned uniquely. The simulations revealed that an important assignment is the rate constant for product dissociation  $k_{-P}$ . This rate constant has not been measured directly for either thiocholine or M7H, the hydrolysis products of the substrates examined here. It is therefore reassuring that a single assignment for  $k_{-P}$  of  $6 \times 10^4 \text{ s}^{-1}$  for thiocholine results in excellent agreement of the simulations with the observed data for propidium inhibition of acetylthiocholine hydrolysis (Figure 1), acetylthiocholine competition with fasciculin and propidium (Figure 2B), and substrate inhibition with acetylthiocholine (Figure 3A). While we are convinced that the steric blockade model offers the best understanding to date of ligand interactions with AChE, further refinements can be made. For example, we noted previously that association rate constants were decreased more than dissociation rate constants for both huperzine A and TMTFA when propidium was bound to the peripheral site (18). The difference corresponded to about a 5-fold decrease in affinity for the ligands in the ternary complex relative to the affinities of either ligand in the binary complexes with the free enzyme. We suggested that this difference might reflect an electrostatic interaction between these cationic ligands in the ternary complexes, and we do not view it as a serious challenge to the general steric blockade model. In terms of Scheme 4 or 5, this refinement would dictate a larger value of  $k_{-S2}/k_{-S}$  than of  $k_{S2}/k_S$  and in turn require thermodynamically that  $i$  be greater than 1. Increasing  $i$  to 4 gave the best agreement of the simulated and the observed data for M7A in Figures 3B and 4. Furthermore, when similar changes were incorporated into the simulations for acetylthiocholine with eq 7

in Figure 2B and the simulated data were then fitted with eq 6, a higher  $K_S$  was obtained without propidium than with propidium. This appears to be an improvement, because a similar divergence in  $K_S$  values was seen in our experimental fits in Figure 2B. However, these simulations for acetylthiocholine also require small adjustments in other assigned rate constants, and we have not attempted to find a self-consistent set of adjustments that would retain the agreement of the simulations to the observed data for acetylthiocholine in Figures 1, 2B, 3A, and 4 noted above.

The steric blockade model in Schemes 3 and 5 resolves a long controversy over the mechanistic interpretation of substrate inhibition with AChE. The controversy involved two alternative mechanisms. One proposal was that substrate inhibition arises from S binding to the anionic site of acetylated AChE to give an EAS complex in which deacylation is blocked (26, 35–37). This proposal predicted that the substrate inhibition constant  $K_{SS}$  fitted by the Haldane equation (eq 1) will depend not only on the substrate affinity in EAS but also on the relative amount of EA. It was supported by observations that uncompetitive inhibition constants as well as  $K_{SS}$  increased for substrates with a lower  $k_{cat}$  (since these formed less EA). Alternatively, it was proposed that substrate inhibition arises from binding of two molecules of S in an ESS complex in which enzyme acetylation is blocked. Either the two S molecules could bind in the acylation site (38), or one S could bind in the acylation site and one in the peripheral site (39, 40). This proposal predicted that  $K_{SS}$  from the Haldane equation should equal the dissociation constant for the lower-affinity S site in the ESS complex. It was supported when values for  $K_S$  of 15–25 mM for acetylcholine or acetylthiocholine binding to the peripheral site, determined by competition in a fluorescence titration of propidium with DFP-inactivated AChE, were the same as the corresponding  $K_{SS}$  estimates (40). It is unclear why these  $K_S$  estimates are so much higher than those we have determined from acetylthiocholine inhibition of the association reactions of ambenonium (29) or fasciculin (Figure 2B) with the peripheral site.<sup>3</sup> Our steric blockade model combines features from both of these proposals and extends them in a nonequilibrium context. The complex responsible for inhibition is neither EAS nor ESS but instead is  $EPS_P$ . This intermediate accumulates because S binding to the peripheral site blocks the dissociation of P, a feature that agrees with the contention in the second proposal that substrate bound to the peripheral site is responsible for substrate inhibition. Furthermore, for a series of substrates with similar  $K_S$  and  $k_{-P}$  values but varying  $k_2$  values,  $K_{SS}$  will increase as  $k_{cat}$  decreases. Thus, our steric blockade model can account for the variations in  $K_{SS}$  which originally led to the first proposal.

Some previous reports (5) have noted that measured  $v$  values at high S concentrations fall above the overall substrate inhibition curve fitted to the Haldane equation (eq 1). Such deviations have been attributed to a low acetylation

activity in the ESS complex. While no significant deviations of this type were observed over the range of S concentrations investigated in our experiments, it is worth noting that such deviations can be accounted for within our steric blockade model. As  $k_{-P_2}/k_{-P}$  increases from the low value of 0.01 assumed in Table 1, simulated values of  $v$  at high S concentrations fall above the curve predicted by the Haldane equation because the rate of product dissociation even with S bound to the peripheral site makes a significant contribution to  $v$ .

Our observation in Figure 2B that acetylthiocholine and fasciculin were only partially competitive in binding to the peripheral site was unexpected. From our analyses with eqs 6 and 7,  $k_{FP}$  for fasciculin binding to the  $ES_P$  complex was nearly 50% of the  $k_F$  for fasciculin binding to the free enzyme. However, these equations do not address the stability of the  $ES_P F_P$  complex in which both acetylthiocholine and fasciculin are bound to the peripheral site. To explore the stability of this complex, we considered an extension of Schemes 4 and 5 in which a set of 20 complete time courses for fasciculin binding in the presence of acetylthiocholine (e.g., like those in Figure 2A) were fitted with the SCoP program (see examples involving TMTFA binding in ref 18). Only rough approximations were attempted because fasciculin exerts a conformational effect on the acylation site in addition to its steric blockade (i.e.,  $a < 1$ ; 18, 22). However, the fitting procedure indicated a 2–3 order of magnitude decrease in the affinities of acetylthiocholine and fasciculin in this  $ES_P F_P$  ternary complex relative to the affinities of either ligand in the binary complexes with the free enzyme. To rationalize the formation of this ternary complex, we reviewed the kinetic properties of previously reported AChE mutants and examined the crystal structures of the fasciculin–AChE complexes (7, 8) to identify a potential acetylthiocholine binding site that largely overlaps with that of propidium but only slightly overlaps with that of fasciculin. D72 is a residue midway along the active site gorge that some reports have included in the peripheral site, and its mutation decreases  $k_{cat}/K_m$  for acetylthiocholine about 50-fold (5). D72 appears to be important in the initial binding of TMTFA, because mutation to D72N reduced the overall TMTFA association rate constant at high ionic strengths more than 20-fold without an effect on the corresponding rate constant for the neutral analogue of TMTFA (15). D72 also was shown to be responsible for the enhanced reactivity of cationic organophosphates relative to their uncharged counterparts (41). Since D72 does not make contact with fasciculin in the crystal structures, it appears to be possible that acetylthiocholine could interact with D72 and still allow a nearly normal association rate constant for the binding of fasciculin to the remainder of the peripheral site to form the ternary complex. Studies with D72 mutants are currently underway to examine this possibility.

Our discussion of the steric blockade model has focused entirely on the point that ligand binding to the peripheral site can have an inhibitory effect on substrate turnover at the acylation site. However, inhibitor binding to the peripheral site is not apparent *in vivo* and thus is not suspected to play any regulatory role under physiological conditions of acetylcholine hydrolysis by AChE. Furthermore, the concentrations of acetylcholine itself are not high enough to give rise to any significant substrate inhibition during synaptic

<sup>3</sup> Preliminary measurement of  $K_S$  for *Torpedo* AChE gave a value of about 0.5 mM with techniques identical to those in Figure 2 (T. Szegletes, W. D. Mallender, and T. L. Rosenberry, manuscript in preparation), indicating that the higher affinity of acetylthiocholine for the peripheral site reported here is not unique to human AChE. We suspect that the lower affinities in the previous reports were subject to technical limitations.

transmission at the neuromuscular junction (42). Therefore, it is important to note that our model indicates a key role for the peripheral site under physiological conditions in which AChE is not saturated with acetylcholine. The hydrolysis rate  $v$  under these conditions is proportional to the second-order rate constant  $k_{cat}/K_{app}$  as given by eq 9, and initial binding of the substrate to the peripheral site increases this rate constant in several ways. It increases  $k_S$  because the peripheral site enlarges the enzyme surface and increases the frequency of productive substrate encounters; it decreases  $k_{-S}$  and thus allows a greater proportion of substrate molecules initially associated with the peripheral site to proceed to the acylation site, and it may well accelerate  $k_1$  by optimally positioning substrate to diffuse rapidly into the acylation site.

Most previous kinetic analyses of AChE have employed equilibrium interpretations of reaction schemes similar to that in Scheme 1. Under what conditions do the conclusions from these analyses remain valid? We offer three guidelines. (1) If the intent is only to obtain an estimate of an inhibition constant  $K_I$ , an equilibrium analysis of Scheme 1 will provide an accurate estimate of the thermodynamic affinity of an inhibitor for either the acylation site or the peripheral site in free AChE (18). (2) If a substrate under investigation essentially equilibrates with AChE during reaction, an equilibrium analysis of Scheme 1 can be applied. Many slowly reacting substrates such as organophosphates (43) fall into this category. (3) If, however, one is investigating ligand binding to the peripheral site with substrates that do not equilibrate with AChE, kinetic parameters can be misinter-

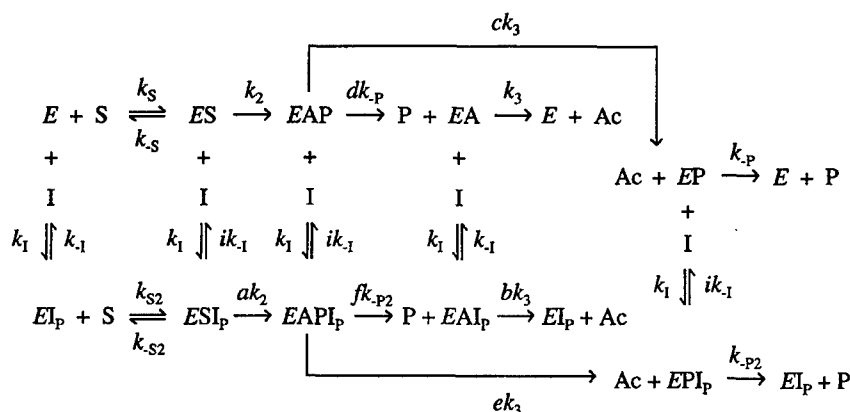
preted with an equilibrium analysis. In particular,  $K_{app}$  and  $K_{SS}$  (eq 1) will not reflect equilibrium values, and  $a$  and  $b$  (Scheme 1) will not be relative acylation and deacylation rate constants.

## APPENDIX

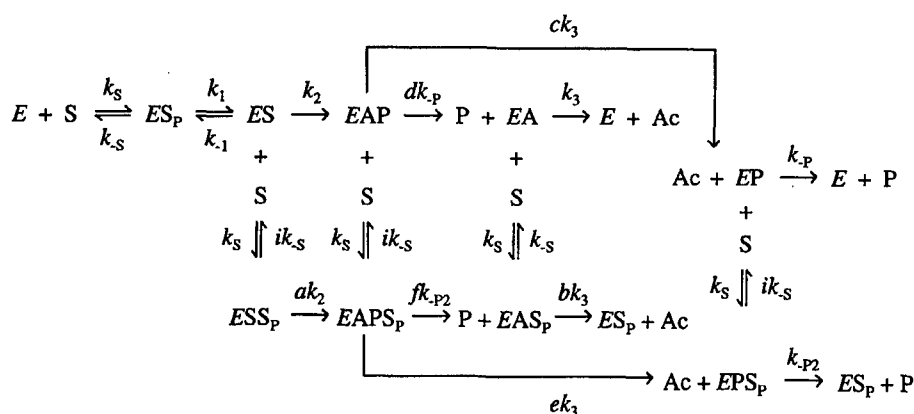
Scheme 4 is an extension of Scheme 2 in which all complexes involving bound peripheral site inhibitor (I) are included. Our steric blockade model postulates that peripheral site binding is unaffected by acylation site ligands (i.e.,  $i = 1$  and the same association rate constant  $k_1$  and the same dissociation rate constant  $k_{-1}$  characterize I binding in the  $EI_P$ ,  $ESI_P$ ,  $EAPI_P$ ,  $EAI_P$ , and  $EPI_P$  complexes) and that bound peripheral site ligand has no effect on acylation and deacylation rate constants (i.e.,  $a = b = 1$ ). Our current treatment of Scheme 5 also assumes for simplicity that product P bound to the acylation site does not alter the rate constant for deacetylation ( $c = e = 1$ ) and that P dissociation rate constants for dissociation from the acetylated enzyme are identical to those from free enzyme ( $d = f = 1$ ). These assumptions may require future refinement in view of reported interactions between ligands and acyl groups at the acylation site (25, 44). The important feature of the steric blockade model here is that  $k_{S2}/k_S = k_{-S2}/k_{-S} < 1$  and that  $k_{-P2}/k_{-P} < 1$ .

In Scheme 3, we proposed a more detailed model of AChE catalysis in which the first step involved the formation of an  $ES_P$  complex at the peripheral site. Scheme 5 is an extension of Scheme 3 in which all other complexes

Scheme 4



Scheme 5



involving bound peripheral site substrate are included. As in Scheme 4, our steric blockade model postulates that  $a = b = i = 1$  and that  $k_{S2}/k_S = k_{-S2}/k_{-S} < 1$  and  $k_{-P2}/k_{-P} < 1$ , and again for simplicity, we assume that  $c = d = e = f = 1$ . When both S and I are present and compete for binding to the peripheral site (i.e., no enzyme species involving  $S_P I_P$  can form, such as  $ES_P I_P$ ), then the five enzyme species involving  $I_P$  in Scheme 4 ( $EI_P$ ,  $ESI_P$ ,  $EAPI_P$ ,  $EAI_P$ , and  $EPI_P$ ) must be added to Scheme 5 to describe the complete system. While we do not show the scheme corresponding to this system, in eqs 6 and 7 we define the following combinations of enzyme species:  $\sum ES_P = [ES_P] + [ESS_P] + [EAPS_P] + [EAS_P] + [EPS_P]$ ,  $\sum EI_P = [EI_P] + [ESI_P] + [EAPI_P] + [EAI_P] + [EPI_P]$ , and  $\sum EX_A = [ES] + [EAP] + [EP]$ . Furthermore, in the text description of eq 6,  $\sum E = [E] + [EA] + \sum EX_A$ . When acetylthiocholine (S) and M7A (T) are substrates simultaneously, 17 liganded species from Scheme 5 for the substrates must be considered (EA is common to both substrates) as well as six additional species representing mixed complexes (e.g.,  $EST_P$ ). New rate constants also are introduced by these mixed complexes (e.g.,  $i_{STk-T}$  is the rate constant for dissociation of T from  $EST_P$ ).

#### ACKNOWLEDGMENT

We express our gratitude to Dr. Michel Roux at the Ecole Normale Supérieure in Paris, France, for bringing the SCOP program to our attention. We also thank Dr. Abdul Fauq (Director of the Organic Synthesis Core Facility at Mayo Clinic Jacksonville) for synthesis of M7A iodide.

#### REFERENCES

- Rosenberry, T. L. (1975) Acetylcholinesterase, in *Advances in Enzymology* (Meister, A., Ed.) Vol. 43, pp 103–218, John Wiley & Sons, New York.
- Sussman, J. L., Harel, M., Frolow, F., Oefner, C., Goldman, A., Tokar, L., and Silman, I. (1991) *Science* 253, 872–879.
- Weise, C., Kreienkamp, H.-J., Raba, R., Pedak, A., Aaviksaar, A., and Hucho, F. (1990) *EMBO J.* 9, 3885–3888.
- Schalk, I., Ehret-Sabatier, L., Bouet, F., Goeldner, M., and Hirth, C. (1992) in *Multidisciplinary Approaches to Cholinesterase Functions* (Shafferman, A., and Velan, B., Eds.) pp 117–120, Plenum Press, New York.
- Radic, Z., Pickering, N. A., Vellom, D. C., Camp, S., and Taylor, P. (1993) *Biochemistry* 32, 12074–12084.
- Barak, D., Kronman, C., Ordentlich, A., Ariel, N., Bromberg, A., Marcus, D., Lazar, A., Velan, B., and Shafferman, A. (1994) *J. Biol. Chem.* 269, 6296–6305.
- Harel, M., Kleywegt, G. J., Ravelli, R. B. G., Silman, I., and Sussman, J. L. (1995) *Structure* 3, 1355–1366.
- Bourne, Y., Taylor, P., and Marchot, P. (1995) *Cell* 83, 503–512.
- Taylor, P., and Lappi, S. (1975) *Biochemistry* 14, 1989–1997.
- Karlsson, E., Mbugua, P. M., and Rodriguez-Ithurralde, D. (1984) *J. Physiol. (Paris)* 79, 232–240.
- Marchot, P., Khelif, A., Ji, Y.-H., Masnuelle, P., and Bourgis, P. E. (1993) *J. Biol. Chem.* 268, 12458–12467.
- Nolte, H. J., Rosenberry, T. L., and Neumann, E. (1980) *Biochemistry* 19, 3705–3711.
- Ripoll, D. R., Faerman, C. H., Axelsen, P. H., Silman, I., and Sussman, J. L. (1993) *Proc. Natl. Acad. Sci. U.S.A.* 90, 5128–5132.
- Antosiewicz, J., McCammon, J. A., Wlodek, S. T., and Gilson, M. K. (1995) *Biochemistry* 34, 4211–4219.
- Radic, Z., Kirchhoff, P. D., Quinn, D. M., McCammon, J. A., and Taylor, P. (1997) *J. Biol. Chem.* 272, 23265–23277.
- Shafferman, A., Ordentlich, A., Barak, D., Kronman, C., Ber, R., Bino, T., Ariel, N., Osman, R., and Velan, B. (1994) *EMBO J.* 13, 3448–3455.
- Barak, D., Ordentlich, A., Bromberg, A., Kronman, C., Marcus, D., Lazar, A., Ariel, N., Velan, B., and Shafferman, A. (1995) *Biochemistry* 34, 15444–15452.
- Szegletes, T., Mallender, W. D., and Rosenberry, T. L. (1998) *Biochemistry* 37, 4206–4216.
- Masson, P., Legrand, P., Bartels, C. F., Froment, M.-T., Schopfer, L. M., and Lockridge, O. (1997) *Biochemistry* 36, 2266–2277.
- Rosenberry, T. L., and Scoggin, D. M. (1984) *J. Biol. Chem.* 259, 5643–5652.
- Roberts, W. L., Kim, B. H., and Rosenberry, T. L. (1987) *Proc. Natl. Acad. Sci. U.S.A.* 84, 7817–7821.
- Eastman, J., Wilson, E. J., Cervenansky, C., and Rosenberry, T. L. (1995) *J. Biol. Chem.* 270, 19694–19701.
- Riddles, P. W., Blakeley, R. L., and Zerner, B. (1979) *Anal. Biochem.* 94, 75–81.
- Ellman, G. L., Courtney, K. D., Andres, J. V., and Featherstone, R. M. (1961) *Biochem. Pharmacol.* 7, 88–95.
- Rosenberry, T. L., and Bernhard, S. A. (1971) *Biochemistry* 10, 4114–4120.
- Rosenberry, T. L., and Bernhard, S. A. (1972) *Biochemistry* 11, 4308–4321.
- Haldane, J. B. S. (1930) *Enzymes*, p 84, Longmans, Green, New York.
- Stuchbury, T., Shipton, M., Norris, R., Malthouse, J. P. G., and Brocklehurst, K. (1975) *Biochem. J.* 151, 417–432.
- Hodge, A. S., Humphrey, D. R., and Rosenberry, T. L. (1992) *Mol. Pharmacol.* 41, 937–942.
- Bazelyansky, M., Robey, E., and Kirsch, J. F. (1986) *Biochemistry* 25, 125–130.
- Kasianowicz, J. J., and Bezrukov, S. M. (1995) *Biophys. J.* 69, 94–105.
- Nachmansohn, D., and Wilson, I. B. (1951) *Adv. Enzymol.* 12, 259–339.
- Prince, A. K. (1966) *Arch. Biochem. Biophys.* 113, 195–204.
- Kitz, R. J., Ginsburg, S., and Wilson, I. B. (1967) *Biochem. Pharmacol.* 16, 2201–2209.
- Krupka, R. M., and Laidler, K. J. (1961) *J. Am. Chem. Soc.* 83, 1445–1447.
- Krupka, R. M., and Laidler, K. J. (1961) *J. Am. Chem. Soc.* 83, 1448–1454.
- Froede, H. C., and Wilson, I. B. (1971) in *The Enzymes* (Boyer, P. D., Ed.) 3rd ed., Vol. V, pp 87–114, Academic Press, New York.
- Zeller, E. A., and Bissegger, A. (1943) *Helv. Chim. Acta* 26, 1619–1630.
- Aldridge, W. N., and Reiner, E. (1969) *Biochem. J.* 115, 147–162.
- Radic, Z., Reiner, E., and Taylor, P. (1991) *Mol. Pharmacol.* 39, 98–104.
- Hosea, N. A., Radic, Z., Tsigelny, I., Berman, H. A., Quinn, D. M., and Taylor, P. (1996) *Biochemistry* 35, 10995–11004.
- Rosenberry, T. L. (1979) *Biophys. J.* 26, 263–290.
- Mallender, W. D., Szegletes, T., and Rosenberry, T. L. (1999) *J. Biol. Chem.* (in press).
- Barnett, P., and Rosenberry, T. L. (1977) *J. Biol. Chem.* 252, 7200–7206.
- Rosenberry, T. L., Mallender, W. D., Thomas, P. J., and Szegletes, T. (1999) *Chem.-Biol. Interact.* (in press).

BI9813577

# Organophosphorylation of Acetylcholinesterase in the Presence of Peripheral Site Ligands

DISTINCT EFFECTS OF PROPIDIUM AND FASCICULIN\*

(Received for publication, October 6, 1998, and in revised form, December 17, 1998)

William D. Mallender‡, Tivadar Szegeletes, and Terrone L. Rosenberry§

From the Department of Pharmacology, Mayo Foundation for Medical Education and Research,  
and the Department of Research, Mayo Clinic Jacksonville, Jacksonville, Florida 32224

Structural analysis of acetylcholinesterase (AChE) has revealed two sites of ligand interaction in the active site gorge: an acylation site at the base of the gorge and a peripheral site at its mouth. A goal of our studies is to understand how ligand binding to the peripheral site alters the reactivity of substrates and organophosphates at the acylation site. Kinetic rate constants were determined for the phosphorylation of AChE by two fluorogenic organophosphates, 7-[(diethoxyphosphoryl)oxy]-1-methylquinolinium iodide (DEPQ) and 7-[(methylethoxyphosphonyl)oxy]-4-methylcoumarin (EMPC), by monitoring release of the fluorescent leaving group. Rate constants obtained with human erythrocyte AChE were in good agreement with those obtained for recombinant human AChE produced from a high level *Drosophila* S2 cell expression system. First-order rate constants  $k_{OP}$  were  $1,600 \pm 300 \text{ min}^{-1}$  for DEPQ and  $150 \pm 11 \text{ min}^{-1}$  for EMPC, and second-order rate constants  $k_{OP}/K_{OP}$  were  $193 \pm 13 \mu\text{M}^{-1} \text{ min}^{-1}$  for DEPQ and  $0.7 \pm 0.1 \mu\text{M}^{-1} \text{ min}^{-1}$  for EMPC. Binding of the small ligand propidium to the AChE peripheral site decreased  $k_{OP}/K_{OP}$  by factors of 2–20 for these organophosphates. Such modest inhibitory effects are consistent with our recently proposed steric blockade model (Szegeletes, T., Mallender, W. D., and Rosenberry, T. L. (1998) *Biochemistry* 37, 4206–4216). Moreover, the binding of propidium resulted in a clear increase in  $k_{OP}$  for EMPC, suggesting that molecular or electronic strain caused by the proximity of propidium to EMPC in the ternary complex may promote phosphorylation. In contrast, the binding of the polypeptide neurotoxin fasciculin to the peripheral site of AChE dramatically decreased phosphorylation rate constants. Values of  $k_{OP}/K_{OP}$  were decreased by factors of  $10^3$  to  $10^5$ , and  $k_{OP}$  was decreased by factors of 300–4,000. Such pronounced inhibition suggested a conformational change in the acylation site induced by fasciculin binding. As a note of caution to other investigators, measurements of phosphorylation of the fasciculin-AChE complex by AChE inactivation gave misleading rate constants because a small fraction of the AChE was resistant to inhibition by fasciculin.

Acetylcholinesterase (AChE)<sup>1</sup> terminates neurotransmission by catalyzing hydrolysis of the neurotransmitter acetylcholine at rates near that of a diffusion-controlled process (1). The x-ray crystal structure of AChE reveals that despite the impressive turnover rate of the enzyme, substrate molecules must penetrate 20 Å into a deep active site gorge to be hydrolyzed (2–4). This gorge contains two sites of ligand interaction: a peripheral site at the surface of the enzyme and an acylation site at the base of the gorge where the substrate acyl group is first transferred to residue Ser<sup>200</sup> (*Torpedo californica* AChE sequence numbering) and then hydrolyzed. In the acylation site, a catalytic triad consisting of residues Ser<sup>200</sup>, His<sup>440</sup>, and Glu<sup>327</sup> promotes the acyl transfers, and Trp<sup>84</sup> binds the acetylcholine trimethylammonium group, positioning the substrate for hydrolysis. Certain ligands can bind selectively to either the acylation site or the peripheral site, and ternary complexes can be formed in which ligands are bound to both sites simultaneously (5, 6). Ligands specific for the peripheral site include the small aromatic compound propidium and the snake venom neurotoxin fasciculin, both of which are potent inhibitors of the hydrolysis of the chromogenic acetylcholine analog, acetylthiocholine.

The AChE peripheral site is an attractive target for the design of new classes of therapeutic agents, so it is important to understand how ligand binding to the peripheral site affects substrate hydrolysis. We recently provided evidence for a steric blockade model which proposes that small peripheral site ligands like propidium inhibit substrate hydrolysis by decreasing the association and dissociation rate constants for an acylation site ligand without significantly altering their ratio, the ligand equilibrium constant (7, 8). Cationic substrates like acetylthiocholine also were shown to bind to the peripheral site as the first step in their catalytic pathway, and steric blockade arising from this substrate binding accounted for the well known phenomenon of substrate inhibition for AChE at very high concentrations of substrate (8). A key feature of the steric blockade model is that ligand binding to the peripheral site results in significant inhibition only if substrate fails to reach equilibrium binding prior to reaction at the acylation site. Substrates that are thought to form equilibrium complexes at the acylation site can be examined to test this prediction. Among these substrates are the organophosphates (OPs), a class of compounds that inactivate cholinesterases because they are poor substrates (9–11). OPs readily phosphorylate the active site serine of AChE, but very slow hydrolysis of this

\* This work was supported in part by National Institutes of Health Grant NS-16577, United States Army Medical Research Acquisition Activity Grant DAMD 17-98-2-8019, and by grants from the Muscular Dystrophy Association of America. The costs of publication of this article were defrayed in part by the payment of page charges. This article must therefore be hereby marked "advertisement" in accordance with 18 U.S.C. Section 1734 solely to indicate this fact.

‡ Supported by a Kendall-Mayo postdoctoral fellowship.

§ To whom correspondence should be addressed. Tel.: 904-953-7375; Fax: 904-953-7370; E-mail: rosenberry@mayo.edu.

<sup>1</sup> The abbreviations used are: AChE, acetylcholinesterase; DTNB, 5,5'-dithiobis-(2-nitrobenzoic acid); OP, organophosphate; EMPC, 7-[(methylethoxyphosphonyl)oxy]-4-methylcoumarin; 7HMC, 7-hydroxy-4-methylcoumarin; DEPQ, 7-[(diethoxyphosphoryl)oxy]-1-methylquinolinium iodide; 7HMQ, 7-hydroxy-1-methylquinolinium iodide; TMTFA, *m*-(*N,N,N*-trimethylammonio)trifluoroacetophenone.

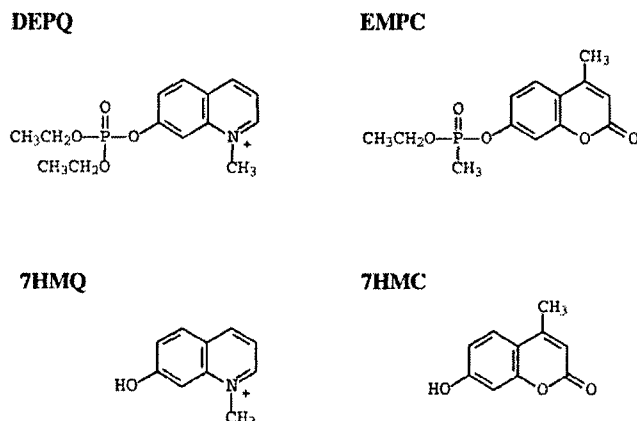


Fig. 1. Chemical structures of OPs and their fluorescent hydrolysis products in these studies.

phosphoryl enzyme results in essentially irreversible inactivation of the enzyme (12). In this paper we examine the effects of ligand binding to the peripheral site on OP phosphorylation of AChE in the context of the steric blockade model. Rate constants of phosphorylation are measured in two ways. The classical method involves periodic measurements of AChE activity toward substrates as the enzyme becomes inactivated. The second method involves continuous assay of the phosphorylation reactions either with mixtures of acetic acid ester substrates and OPs (13, 14) or by monitoring loss of a fluorogenic OP leaving group (15, 16). This method can be adapted to stopped-flow kinetic techniques to allow determination of both first- and second-order phosphorylation rate constants (13, 14). Here we monitor the reactions of two fluorogenic OPs, EMPC and DEPQ (Fig. 1), with erythrocyte and recombinant human AChE. Phosphorylation rate constants obtained directly by fluorescence measurement of their AChE-mediated hydrolysis products 7HMC and 7HMQ, respectively (Fig. 1), are compared with those obtained by enzyme inactivation.

#### EXPERIMENTAL PROCEDURES

**Materials**—Human erythrocyte AChE was purified as outlined previously, and active site concentrations were determined by assuming 410 units/nmol (17, 18).<sup>2</sup> DEPQ (15, 19) and EMPC were synthesized by established procedures (see Ref. 16). [(Methylethoxyphosphonyl)oxy]chloride was reacted with 7HMC (Molecular Probes, Inc.) to give EMPC, and [(diethoxyphosphoryl)oxy]chloride was linked to 7-hydroxyquinoline (Acros Organics) and quaternized by methylation to form DEPQ. Structures were confirmed by <sup>1</sup>H NMR and <sup>31</sup>P NMR, and stock concentrations were determined by absorbance ( $\epsilon_{310 \text{ nm}} = 11.0 \text{ mM}^{-1} \text{ cm}^{-1}$  for EMPC, and  $\epsilon_{317 \text{ nm}} = 8.3 \text{ mM}^{-1} \text{ cm}^{-1}$  for DEPQ). Fasciculin was the fasciculin 2 form obtained from Dr. Carlos Cervenansky at the Instituto de Investigaciones Biológicas, Clemente Estable, Montevideo, Uruguay (6). Propidium iodide was purchased from Calbiochem.

**Recombinant Human AChE**—The full-length cDNA for human G<sub>4</sub> AChE was obtained from Dr. Avigdor Shafferman in the vector pACHE10 (20). To obtain a secreted dimeric form of human AChE, a 96-base pair truncation sequence including a stop codon was synthesized and inserted just downstream from the exon 4/5 boundary (see Ref. 21). Insertion of the modified exon 4/5 sequence (corresponding to <sup>644</sup>ASEAPSTC-DGDSS-stop, human AChE sequence numbering) resulted in a partial duplication of the 3'-end of the exon 4 region of the gene. To remove this duplicated segment, the *NotI*-*NheI* 3'-segment of the gene was cloned into *NotI*-*NheI*-digested pCIneo (Promega Corp.). This construct, pCIneo3'-AChE, contained an *EspI* site in both the original and modified sections of exon 4. The unwanted duplicated gene segment was removed by digestion with *EspI* followed by cloning of the resolved *NotI*-*NheI* fragment back into the AChE gene cassette. The final gene construct was confirmed by DNA sequencing carried out at

the Mayo Clinic Rochester Molecular Biology Core Facility. The modified human AChE cDNA was moved into the pPac vector for transfection into and expression from *Drosophila* S2 cells in tissue culture (21). S2 cells were maintained in Schneider's *Drosophila* medium (Life Technologies, Inc.) with 10% fetal bovine serum and appropriate antibiotics at 28 °C. S2 cells were cotransfected with pPac carrying the hygromycin phosphotransferase gene for selection of cells with hygromycin B. After selection with 0.2 mg/ml hygromycin B, monoclonal cell lines were isolated from colonies formed using a modified soft agar cloning protocol (21). Briefly, 10<sup>4</sup> to 10<sup>5</sup> selected cells were suspended in complete medium with 0.3% low melting temperature agarose. This mixture was plated onto a base layer of solidified 1.5% low melting temperature agarose (in complete medium with 0.15 M NaCl) in 12-well tissue culture plates. After cell/medium layer solidification, a layer of complete medium was placed on top of the agarose. Colonies (>2 mm) were picked and grown in 24-well plates until confluence. At this point clones were assayed for AChE activity, and lines with high activity were kept for large scale culturing and long term propagation. AChE was purified from culture medium by two cycles of affinity chromatography on acridinium resin (17). Purified recombinant AChE samples analyzed by SDS-polyacrylamide gel electrophoresis (22) showed no contaminants. In the absence of disulfide reducing agents, a prominent band of 140-kDa dimer and a minor band of 70-kDa monomer were apparent, whereas in the presence of reducing agents a single 70-kDa band was observed. Comparison of the recombinant AChE with purified human erythrocyte AChE showed no differences in  $k_{\text{cat}}$ ,  $K_{\text{app}}$ , or  $K_{\text{SS}}$  for acetylthiocholine hydrolysis (8), in  $K_i$  for propidium inhibition, in  $k_{\text{on}}$ , the fasciculin association rate constant (8), or in phosphorylation rate constants (see Table I below).

**AChE Phosphorylation Determined with Fluorogenic OPs**—Direct reaction of AChE with EMPC or DEPQ was followed by formation of their respective fluorescent leaving groups 7HMC or 7HMQ on a Perkin-Elmer LS-50B luminescence spectrometer in 20 mM sodium phosphate buffer and 0.02% Triton X-100 at 23 °C. Because these groups are fluorescent only when their 7-OH substituents are deprotonated (7HMC,  $\text{p}K_{\text{a}} = 7.8$  (catalog from Molecular Probes, Inc.); 7HMQ,  $\text{p}K_{\text{a}} = 5.9$  (23)), measurements were conducted at pH 8.0 for EMPC and pH 7.0 for DEPQ. Ratios of OP to AChE concentrations were adjusted to at least 20 for EMPC and 9 for DEPQ in all cases to prevent significant depletion of OP during the course of the reaction. Formation of 7HMC ( $\epsilon_{360 \text{ nm}} = 19.0 \text{ mM}^{-1} \text{ cm}^{-1}$  at pH 9.0; catalog of Molecular Probes, Inc.) was monitored with excitation at 360 nm and emission at 450 nm, and 7HMQ formation was monitored with excitation at 400 nm and emission at 500 nm (for 7HMQ,  $\epsilon_{406 \text{ nm}} = 10.0 \text{ mM}^{-1} \text{ cm}^{-1}$  at pH 9.0). For reactions that were completed in less than 1 min, a Hi-Tech SFA 20 stopped-flow apparatus was used to mix equal volumes (300  $\mu\text{l}$ ) of AChE (or AChE with inhibitor) and OP solutions rapidly, and fluorescence was recorded at fixed intervals as short as 20 ms. Formation of 7HMC or 7HMQ did not follow a simple exponential time course. Nonenzymatic hydrolysis of EMPC under all conditions and of DEPQ in the presence of propidium or fasciculin as inhibitors was significant, and under these conditions data were fitted by nonlinear regression analysis (Fig. P version 6.0, BioSoft, Inc.) to Equation 1.

$$f = f_{\text{initial}} + \Delta f(1 - e^{-kt}) + Ct \quad (\text{Eq. 1})$$

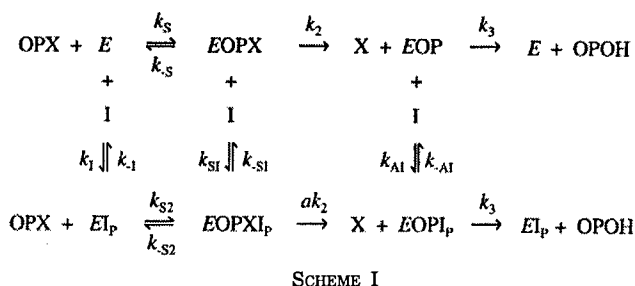
In Equation 1,  $f_{\text{initial}}$  is the fluorescence at time zero,  $\Delta f$  is the fluorescence change corresponding to an amount of fluorescent product equal to the AChE concentration (23),  $C$  is the nonenzymatic hydrolysis rate, and  $k$  is the rate constant for the approach to the steady-state level of phosphorylation. With DEPQ in the absence of inhibitors the release of 7HMQ occurred in two phases, a large rapid phase and a small slower phase (see "Results") for both erythrocyte and recombinant AChE. These data were fitted to Equation 2, where  $\Delta f_2$  and  $k_2$  were the respective amplitude and the rate constant for the slower phase, and the other parameters were as defined in Equation 1.

$$f = f_{\text{initial}} + \Delta f(1 - e^{-kt}) + \Delta f_2(1 - e^{-k_2t}) \quad (\text{Eq. 2})$$

The rate constants  $k$  were analyzed according to the catalytic pathway in Scheme 1. In this Scheme, OPX is the intact OP with leaving group X; EOPX is the initial complex of the OP with AChE, characterized by the equilibrium dissociation constant  $K_{\text{S}} = k_{-5}/k_5$ ; and EOP is the phosphorylated enzyme. The inhibitor I can bind to the peripheral site in each of the enzyme species (as denoted by the subscript P). This scheme is identical to a general pathway for substrate hydrolysis by AChE considered elsewhere (7). Kinetic analysis of this scheme was simplified here in two ways. First, dephosphorylation rate constants ( $k_3$  in Scheme 1), which appeared consistent with a value of  $2-4 \times 10^{-4}$

<sup>2</sup> One unit corresponds to 1  $\mu\text{mol}$  of acetylthiocholine hydrolyzed/min under standard pH-stat assay conditions (3.67  $\Delta A_{412 \text{ nm}}$ /min in our standard spectrophotometric assay (17)).





min<sup>-1</sup> reported previously for diethoxyphosphorylated eel AChE (24, 15; data not shown), were assumed to be negligible in all our experiments. Second, OPs were assumed to equilibrate with the AChE acylation site even when inhibitors were bound to the peripheral site. This assumption was supported by nonequilibrium kinetic simulations with the program SCoP, as noted under "Results,"<sup>3</sup> and it obviated the need for more complex mechanistic schemes that apply to substrates that do not equilibrate with AChE (8). With these assumptions, the dependence of  $k$  evaluated from either Equation 1 or Equation 2 on the OP concentration was analyzed by weighted nonlinear regression analysis (assuming constant percent error in  $k$ ) according to Equation 3 to give  $k_{OP}$  and  $k_{OP}/K_{OP}$ , the respective first- and second-order rate constants of phosphorylation.

$$k = \frac{k_{OP}[\text{OP}]}{K_{OP} + [\text{OP}]} \quad (\text{Eq. 3})$$

These rate constants are related to the intrinsic rate constants in Scheme 1 as shown Equations 4 and 5.

$$k_{OP} = \frac{k_2 \left( 1 + \frac{a[\text{I}]}{K_{SI}} \right)}{\left( 1 + \frac{[\text{I}]}{K_{SI}} \right)} \quad (\text{Eq. 4})$$

$$\frac{k_{OP}}{K_{OP}} = \frac{k_2 \left( 1 + \frac{a[\text{I}]}{K_{SI}} \right)}{K_S \left( 1 + \frac{[\text{I}]}{K_I} \right)} \quad (\text{Eq. 5})$$

In the absence of I,  $k_{OP} = k_2$  and  $K_{OP} = K_S$ . In the presence of I,  $K_{OP}$  is given by Equation 6.

$$K_{OP} = \frac{K_S \left( 1 + \frac{[\text{I}]}{K_I} \right)}{\left( 1 + \frac{[\text{I}]}{K_{SI}} \right)} \quad (\text{Eq. 6})$$

Assays with the peripheral site inhibitors propidium (30  $\mu\text{M}$ ) or fasciculin (0.5–10  $\mu\text{M}$ ) were conducted at inhibitor concentrations at least 30 times their respective  $K_I$  values to ensure that most of the AChE was complexed with inhibitor. Values of  $K_I$  were taken as  $1.0 \pm 0.1 \mu\text{M}$  for propidium (7),  $11 \pm 0.2 \text{ pM}$  for fasciculin (6), and 100 pM for fasciculin in the presence of DTNB and acetylthiocholine in the standard assay (6, 8). Measurements that included fasciculin were modified in several ways. First, the enzyme was incubated with fasciculin for 5–10 min to generate equilibrated complex before the addition of OP. Second, the reaction buffer with EMPC was adjusted to pH 7.0 to reduce nonenzymatic

hydrolysis of the OP. Finally, a four-cell cuvette changer was employed (except where noted) for reaction times as long as 4 h. This device minimized fluorophore photobleaching because the sample was cycled in and out of the light path. Each reaction was measured in parallel with cuvettes corresponding to an air blank and a nonenzymatic hydrolysis control devoid of AChE.

**AChE Phosphorylation Determined by OP Inactivation of AChE-catalyzed Substrate Hydrolysis**—AChE activity was monitored by a modified acetylthiocholine assay (25). Standard assays were conducted in 3.0 ml of 20 mM sodium phosphate, 0.02% Triton X-100, 0.33 mM DTNB, and 0.5 mM acetylthiocholine (pH 7.0) at 25 °C. Enzyme hydrolysis was monitored by formation of the thiolate dianion of DTNB at 412 nm ( $\Delta\epsilon_{412 \text{ nm}} = 14.15 \text{ mM}^{-1} \text{ cm}^{-1}$  (26)) for 1–5 min on a Varian Cary 3A spectrophotometer.<sup>4</sup> The inactivation of AChE by an OP was initiated by mixing AChE and OP at 23 °C in 20 mM phosphate buffer and 0.02% Triton X-100 (pH = 7.0). At various times a 1.0-ml aliquot was removed to a cuvette, 40  $\mu\text{l}$  of acetylthiocholine and DTNB were added to final concentrations of 0.5 mM and 0.33 mM, respectively, and a continuous assay trace was recorded immediately at 412 nm. Background hydrolysis rates in the absence of AChE were subtracted. To assess the effects of peripheral site inhibitors on OP inactivation rates, propidium (30  $\mu\text{M}$ ) or fasciculin (50–250 nM) was incubated with AChE for at least 10–30 min prior to the addition of the OP. In some cases, DEPQ was also added (to 10–60 nM) for 60–120 min after incubation of fasciculin with AChE to eliminate a minor population of AChE which was refractory to normal fasciculin inhibition (see "Results"). Titrations of AChE activity with substoichiometric amounts of DEPQ were conducted by procedures similar to those in other inactivation measurements except that initial incubation mixtures contained higher concentrations of AChE (28–260 nM) and fasciculin (0–2  $\mu\text{M}$ ) and that after 90–120 min small aliquots of the mixtures (15–20  $\mu\text{l}$ ) were diluted into the standard acetylthiocholine assay solution.

OP inactivation reactions were measured under pseudo first-order conditions in which the ratio of OP to AChE concentrations was adjusted to at least 5. Assay rates  $v$  during inactivation were divided by the control assay rate in the absence of OP to give a normalized value  $v_{(N)}$ , and these values were fitted by nonlinear regression analysis (Fig. P) to Equation 7, where  $v_{(N)\text{initial}}$  and  $v_{(N)\text{final}}$  are the calculated values of  $v_{(N)}$  at time zero and in the final steady state, respectively.

$$v_{(N)} = v_{(N)\text{final}} + (v_{(N)\text{initial}} - v_{(N)\text{final}})e^{-kt} \quad (\text{Eq. 7})$$

OP concentrations also were sufficiently low that the observed inactivation rate constant  $k$  was proportional to  $[\text{OP}]$ . The second-order rate constant for inactivation  $k_{OP}/K_{OP}$  was fitted by weighted linear regression analysis of the relationship  $k = (k_{OP}/K_{OP})[\text{OP}]$  (see Equation 3), assuming a constant percent error in  $k$ .

## RESULTS

**Direct Fluorometric Measurement of AChE Phosphorylation by OPs in the Presence and Absence of Peripheral Site Ligands**—The rapid reactions of EMPC and DEPQ with AChE require the use of stopped-flow methods if both first- and second-order phosphorylation rate constants are to be measured. Fig. 2A illustrates the measurement of an individual  $k$  value for the reaction of DEPQ with AChE. The release of the fluorescent product 7HMQ occurred largely with a single rapid exponential time course, but a slower phase corresponding to about 10% of the overall reaction also was apparent. The amplitude, or amount of product released, in the predominant faster reaction phase equaled the AChE concentration (Equations 1 and 2) and thus corresponded to a fluorescence titration of the enzyme normality which reacted rapidly with DEPQ (15, 23). Fitted  $k$  values for the rapid phase were analyzed according to Equation 3 (Fig. 2B) to obtain the first-order phosphorylation rate constant  $k_{OP}$  and the second-order rate constant  $k_{OP}/K_{OP}$ . A second, slower phase was not apparent in reactions of EMPC with AChE or in reactions of either OP in the presence of the pe-

<sup>3</sup> To ensure that EMPC and DEPQ were close enough to equilibrium with AChE in the presence of 30  $\mu\text{M}$  propidium or 0.5–10  $\mu\text{M}$  fasciculin to justify application of Equations 4–6, we applied the SCoP simulation program (7) to Scheme 1 with the following rate constant assignments:  $k_S = 1 \times 10^7 \text{ M}^{-1} \text{ s}^{-1}$  for EMPC and  $2 \times 10^8 \text{ M}^{-1} \text{ s}^{-1}$  for DEPQ, values similar to those assigned previously for neutral and cationic acetic acid ester substrates (7);  $k_1 = k_{SI} = 2 \times 10^8 \text{ M}^{-1} \text{ s}^{-1}$  for propidium (7);  $k_1 = k_{SI} = 3 \times 10^7 \text{ M}^{-1} \text{ s}^{-1}$  for fasciculin with free AChE, and  $k_1 = k_{SI} = 1 \times 10^7 \text{ M}^{-1} \text{ s}^{-1}$  for fasciculin with AChE in the presence of DTNB and acetylthiocholine (6);  $k_3 = 5 \times 10^{-6} \text{ s}^{-1}$ ;  $k_{-S}$ ,  $k_{-1}$ ,  $k_2$ , and  $a$  from Table I and "Experimental Procedures" (with  $k_{-X} = K_X k_X$ );  $k_{-SI}$  from  $K_{SI}$  from Equation 6; and  $k_{-S2} = k_{S2} K_S K_{SI}/K_I$ . Simulated values of  $k_{OP}$  and  $k_{OP}/K_{OP}$  were then compared for complete equilibrium ( $k_{S2}/k_S = 1$ ) and pronounced steric blockade ( $k_{S2}/k_S = 0.00001$ ) and found to differ by less than 10%, justifying the equilibrium assumption.

<sup>4</sup> Enzyme activities were standardized to 0.1  $\Delta A_{412 \text{ nm}}/\text{min}$  by applying the observed relationship  $v_{\text{std}} = 0.1(v/0.1)^{1/r}$ , where  $v$  was the measured activity,  $v_{\text{std}}$  was the standardized activity, and  $r = 0.95$ .  $R$  was the slope of a plot of log measured activity versus log enzyme concentration over a 200-fold range of enzyme dilution.



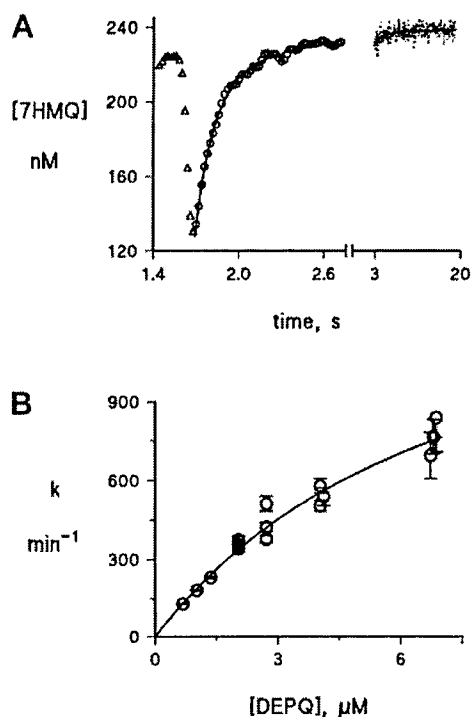


FIG. 2. Reaction of DEPQ with recombinant AChE. Panel A, equal volumes of DEPQ and AChE were mixed rapidly with the stopped-flow accessory to final concentrations of 2  $\mu\text{M}$  and 100 nM, respectively, and generation of 7HMQ was monitored by spectrofluorometry as outlined under "Experimental Procedures." Prior to the reaction, the stopped-flow cuvette was washed extensively with the DEPQ stock solution alone; fluorescence in this wash solution results from about 5% contamination of the stock DEPQ with 7HMQ. In this recording, data collection on the spectrometer was triggered manually at time zero, and mixing was initiated at 1.6 s. Points observed for the reaction from 1.7 to 19 s ( $\circ$  and dotted line) were fitted to Equation 2 (solid line), with approximately 90% of the reaction amplitude corresponding to a reaction rate constant of  $356 \pm 13 \text{ min}^{-1}$  and 10% to a rate constant of  $24 \pm 2 \text{ min}^{-1}$ . Fluorescence units were converted to 7HMQ product formed (nM) by comparison with a 7HMQ standard solution. Panel B, rate constants for the faster phase of the reaction of DEPQ with AChE obtained as in panel A were plotted against the DEPQ concentration according to Equation 3 to obtain first- and second-order rate constants of  $1,600 \pm 200 \text{ min}^{-1}$  and  $205 \pm 11 \mu\text{M}^{-1} \text{ min}^{-1}$ , respectively (Table I).

ripheral site inhibitors propidium or fasciculin. These reaction time courses, however, were superimposed upon significant nonenzymatic OP hydrolysis rates that were incorporated into the curve fitting of the  $k$  values. Estimates of  $k_{\text{OP}}$  and  $k_{\text{OP}}/K_{\text{OP}}$  were obtained from these  $k$  values by analyses similar to that in Fig. 2B (Table I). Purified recombinant human AChE expressed in *Drosophila* S2 cells gave rate constants for both OPs and relative amplitudes for DEPQ which were in good agreement with those for purified human erythrocyte AChE. Furthermore, our  $k_{\text{OP}}/K_{\text{OP}}$  value for DEPQ ( $1.9\text{--}2.1 \times 10^5 \text{ M}^{-1} \text{ min}^{-1}$ ) agreed with previous estimates of this second-order phosphorylation rate constant determined by inactivation of eel AChE (15, 27; see below and Table I). No previous estimates of  $k_{\text{OP}}$  for either DEPQ or EMPC or of  $k_{\text{OP}}/K_{\text{OP}}$  for EMPC have been reported. We observe that  $k_{\text{OP}}/K_{\text{OP}}$  is about 200–300 times larger for DEPQ than for EMPC and that  $k_{\text{OP}}$  is about 10 times larger for DEPQ than for EMPC. These differences are consistent with previous expectations that the cationic nature of DEPQ and the lower  $\text{pK}_a$  of its leaving group relative to neutral EMPC should result in higher rates of AChE phosphorylation (14, 27, 28).

The effects of the small peripheral site ligand propidium on phosphorylation of AChE by OPs have not been widely studied.

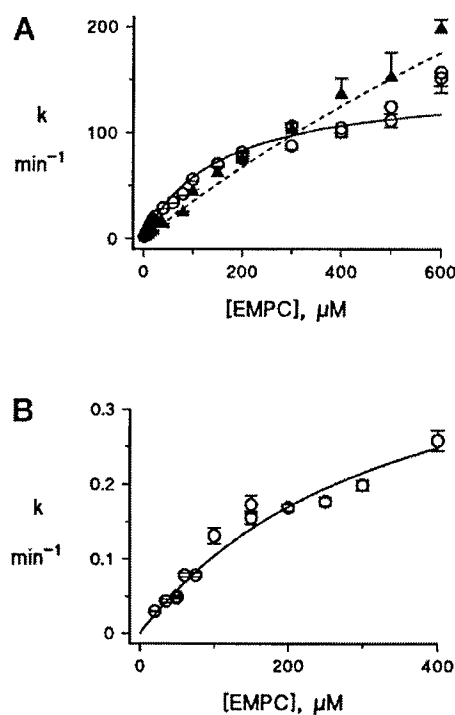


FIG. 3. Phosphorylation of erythrocyte AChE by EMPC in the presence and absence of peripheral site ligands. Rate constants  $k$ , measured by spectrofluorometric detection of 7HMC as outlined under "Experimental Procedures" (see also Fig. 2A), were plotted against the EMPC concentration and fitted to Equation 3 (lines) to obtain  $k_{\text{OP}}$  and  $k_{\text{OP}}/K_{\text{OP}}$  (Table I). Panel A,  $\circ$  indicates no inhibitor;  $k_{\text{OP}} = k_2 = 149 \pm 9 \text{ min}^{-1}$  and  $k_{\text{OP}}/K_{\text{OP}} = k_2/K_S = 0.95 \pm 0.04 \mu\text{M}^{-1} \text{ min}^{-1}$ .  $\blacktriangle$  indicates plus 30  $\mu\text{M}$  propidium;  $k_{\text{OP}} = 900 \pm 500 \text{ min}^{-1}$  and  $k_{\text{OP}}/K_{\text{OP}} = 0.37 \pm 0.02 \mu\text{M}^{-1} \text{ min}^{-1}$ . Points for  $[\text{EMPC}] \geq 200 \mu\text{M}$  are shown as means of two to nine  $k$  measurements. Panel B,  $\circ$  indicates plus 1.3  $\mu\text{M}$  fasciculin;  $k_{\text{OP}} = 0.46 \pm 0.09 \text{ min}^{-1}$  and  $k_{\text{OP}}/K_{\text{OP}} = 0.0013 \pm 0.0001 \mu\text{M}^{-1} \text{ min}^{-1}$ .

In Fig. 3A we show that propidium decreased  $k_{\text{OP}}/K_{\text{OP}}$  but increased  $k_{\text{OP}}$  for the phosphorylation of AChE by EMPC. The decrease in  $k_{\text{OP}}/K_{\text{OP}}$  was small (2.6- and 1.5-fold, for the erythrocyte and recombinant enzymes, respectively (Table I)) and consistent with those reported previously for neutral OPs with *T. californica* AChE (29). This small decrease appears consistent with the prediction of our steric blockade model that small peripheral site inhibitors like propidium will have little effect on the reaction of substrates that equilibrate with AChE (7; see Footnote 3 and Discussion). The extent of the increase in  $k_{\text{OP}}$  made extrapolation to  $k_{\text{OP}}$  problematic. Inclusion of 30  $\mu\text{M}$  propidium increased the  $K_{\text{OP}}$  for EMPC by factors of  $15 \pm 9$  and  $6 \pm 2$  for the two AChEs to a value greater than 1 mM, and increased signal to noise prevented us from extending the EMPC concentration into the mM range to improve the precision of these factors. Insertion of these factors into Equation 6 and calculation from Equation 5 indicated that both  $K_{\text{S}}/K_{\text{I}}$  and  $\alpha$  in Scheme 1 were on the order of 10 (Table I), indicating both lower affinity and higher reactivity of EMPC in the ternary complex with AChE and propidium. Propidium (30  $\mu\text{M}$ ) had a more pronounced effect on  $k_{\text{OP}}/K_{\text{OP}}$  for DEPQ, producing 18- and 14-fold decreases for the two AChEs (Table I). These factors again are consistent with those reported previously for cationic OPs with *T. californica* AChE (29). As observed for EMPC, bound propidium also increased  $K_{\text{OP}}$  for DEPQ to the point where it became technically difficult to measure the corresponding  $k_{\text{OP}}$ . It appeared that  $k_{\text{OP}}$  for DEPQ with propidium was at least as large as  $k_{\text{OP}}$  for DEPQ alone (Table I), but more

TABLE I  
 Rate constants for the phosphorylation of AChE by OPs

 Rate constants were calculated from the dependence of  $k$  on [OP] as outlined under "Experimental Procedures."

Enzyme, OP, and inhibitor	Fluorescent product release				Enzyme inactivation	
	$k_{OP}$		$k_{OP}/K_{OP}$		$k_{OP}/K_{OP}$	
	min <sup>-1</sup>	$\alpha$	$\mu\text{M}^{-1} \text{min}^{-1}$	Relative decrease (fold)	$\mu\text{M}^{-1} \text{min}^{-1}$	Relative decrease (fold)
Erythrocyte						
EMPC						
None	149 ± 9		0.95 ± 0.04		0.82 ± 0.03	
Propidium	900 ± 500 <sup>a</sup>	11 ± 12	0.37 ± 0.02	2.6	0.30 ± 0.01	2.7
Fasciculin	0.46 ± 0.09	0.003	0.0013 ± 0.0001	730	0.18 ± 0.01	4.6
Fasciculin + DEPQ <sup>b</sup>					0.0013 ± 0.0001	630
DEPQ						
None	1,600 ± 300		193 ± 13		151 ± 8	
Propidium	1,100 ± 500	≥1	11 ± 1	18	6.0 ± 0.2	25
Fasciculin	0.45 ± 0.09 <sup>a</sup>	0.0003	0.0016 ± 0.0001	120,000	63 ± 10	2.4
Recombinant						
EMPC						
None	150 ± 11		0.67 ± 0.03		0.83 ± 0.02	
Propidium	570 ± 140 <sup>a</sup>	4.4 ± 1.5	0.45 ± 0.02	1.5	0.31 ± 0.02	2.7
Fasciculin	0.23 ± 0.08	0.002	0.0011 ± 0.0002	600	0.24 ± 0.02	3.5
Fasciculin + DEPQ <sup>b</sup>					0.0019 ± 0.0002	440
DEPQ						
None	1,600 ± 200		205 ± 11		99 ± 3	
Propidium	1,200 ± 400	≥1	15 ± 1	14	5.2 ± 0.4	19
Fasciculin	0.66 ± 0.10 <sup>a</sup>	0.0003	0.0010 ± 0.0001	220,000	32 ± 17	3.0

<sup>a</sup> The maximum [OP] employed did not exceed 80% of the estimated  $K_{OP}$ , and therefore estimates of  $k_{OP}$  are approximate.

<sup>b</sup> AChE was first preincubated with fasciculin then with DEPQ to eliminate the fasciculin-resistant AChE population (see "Results").

precise estimates were not possible.

Unlike propidium, the binding of fasciculin to the AChE peripheral site had a drastic effect on the phosphorylation of AChE by OPs (Fig. 3B). At saturating fasciculin concentrations ( $10^4$  to  $10^6$  times greater than its  $K_1$ ),  $k_{OP}/K_{OP}$  was decreased about 700-fold for EMPC and by about  $10^5$  for DEPQ. Bound fasciculin also decreased  $k_{OP}$  for both OPs by factors of 300–4,000 (Table I). The amplitudes of the OP reactions with the fasciculin-AChE complex again were consistent with the AChE normality, indicating that most of the enzyme was involved in the slowly reacting complex. A previous report of the effects of bound fasciculin on the reaction of AChE with the OPs echothiophate and paraoxon found only modest decreases of less than an order of magnitude for either  $k_{OP}/K_{OP}$  or  $k_{OP}$  (30). These relative changes in rate constants, however, were determined from rates of enzyme inactivation monitored by progressive reductions in the residual activity of the fasciculin-AChE complex, not from the release of the OP leaving group. To assess whether there were discrepancies between these methods, we repeated measurements of EMPC and DEPQ reaction rate constants by following enzyme inactivation.

**Measurement of AChE Phosphorylation by OPs by Enzyme Inactivation.**—We measured AChE inactivation by EMPC and DEPQ without the use of stopped-flow kinetic methods, and our determinations were limited to the second-order phosphorylation rate constants  $k_{OP}/K_{OP}$ . With either OP alone or in the presence of propidium, values of  $k_{OP}/K_{OP}$  determined by inactivation were in agreement with those from spectrofluorometric assays within about a factor of 2 (Table I). However, when the reaction of either OP was measured in the presence of fasciculin, a striking discrepancy between the two methods became apparent. Bound fasciculin decreased  $k_{OP}/K_{OP}$  determined by inactivation only 2–5-fold (Table I), in agreement with the above report by Radic *et al.* (30) but in contrast to the decreases of up to  $10^5$ -fold determined by spectrofluorometry (Table I). The discrepancy raised a concern that the enzyme activity observed during inactivation by OPs did not arise from the fasciculin-AChE complex. Because fasciculin binding reduces the activity of human AChE preparations to a residual 0.1–1%

of the activity of the free enzyme (6), a tiny fraction of the AChE preparation resistant to fasciculin inhibition for any reason could become the dominant activity during the OP inactivation measurements. To examine this possibility, we altered the ratio of the OP to the AChE concentrations for the inactivation reaction in the presence of saturating fasciculin. When the DEPQ/AChE ratio was a typical value of 8, about 80% of the residual fasciculin-AChE activity was inactivated with a rate constant  $k$  consistent with the  $k_{OP}/K_{OP}$  of  $6.2 \times 10^7 \text{ M}^{-1} \text{min}^{-1}$  in Table I (*lower trace*, Fig. 4). The inactivation reaction was then repeated at the same concentration of DEPQ but with 50 times as much AChE (*i.e.* [AChE]/[DEPQ] = 6). If all of the fasciculin-AChE complex could react with DEPQ at the previous rate, only about 17% of the residual activity should have been inactivated before DEPQ was completely depleted; in fact we continued to observe 80% inactivation with about the same  $k$  value (data not shown). Repeating the inactivation reaction again with a ratio [AChE]/[DEPQ] = 60 finally did result in depletion of the DEPQ but not before more than 40% of the residual fasciculin-AChE activity was inactivated (*upper trace*, Fig. 4). These data indicated that only a few percent of the total AChE concentration was involved in the observed inactivation reaction.

To quantify this point, we titrated several AChE stocks with DEPQ in the presence and absence of fasciculin by measuring inactivation. Examples of these titrations are shown in Fig. 5. As expected in the absence of fasciculin, the stoichiometric amount of DEPQ required for complete inactivation was within about 15% of the AChE active site concentration calculated from the initial activity (Fig. 5A). In the presence of saturating fasciculin, however, less than 100% of the residual activity was rapidly inactivated (Fig. 5, B and C). We fitted these titration data to a model with two enzyme populations, one that was relatively rapidly inactivated by DEPQ and the other that reacted with DEPQ at the very low rate constants measured by the fluorescence assays in Table I. The rapidly inactivated population corresponded to 5% of the total AChE concentration in Fig. 5B and 40% in Fig. 5C. These percentages varied among AChE stocks, with erythrocyte AChE typically giving about 5%

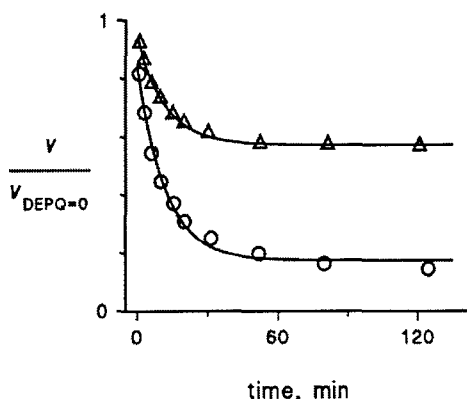


FIG. 4. Inactivation of the residual activity of the fasciculin-AChE complex by DEPQ at two ratios of the DEPQ to AChE concentrations. Erythrocyte AChE at 0.16 nM (○) and 80 nM (△) was incubated for 10 min with fasciculin at 50 nM (○) and 500 nM (△), and inactivation was initiated by the addition of DEPQ to a final concentration of 1.4 nM. Aliquots were assayed at the indicated times as outlined under "Experimental Procedures." Assay points  $v$  were normalized to corresponding control residual activities with fasciculin but without DEPQ ( $v_{\text{DEPQ}=0}$ ) and fitted to Equation 7 (lines) to obtain a value of  $k$  for each curve.

and two preparations of recombinant AChE exhibiting 2 and 40%, respectively. These data thus are consistent with the assignment of a small but variable fraction of the AChE as a population that is largely resistant to fasciculin inhibition.

We next confirmed that the residual activity remaining after the rapid inactivation by DEPQ in Fig. 5, B and C, in fact did correspond to the fasciculin-AChE complex. This involved demonstrating that this residual activity was slowly inactivated by OPs at the same low rate constants determined with the fluorescence assays in Table I. AChE was incubated with fasciculin, and activity from the fasciculin-resistant population was removed by rapid inactivation with 10–60 nM DEPQ (see "Experimental Procedures"). The activity remaining after this treatment (e.g. the activity remaining after 60 min in the lower trace of Fig. 4) was then progressively inactivated by further incubation with EMPC, and  $k_{\text{OP}}/K_{\text{OP}}$  was determined as above. These values of  $k_{\text{OP}}/K_{\text{OP}}$  from inactivation were now in good agreement with the values of  $k_{\text{OP}}/K_{\text{OP}}$  obtained for the reaction of EMPC with the fasciculin-AChE complexes by fluorescence assay (e.g.  $1.3 \times 10^3 \text{ M}^{-1} \text{ min}^{-1}$  for erythrocyte AChE in Table I).

**Detection of More Than One Population of AChE in the Presence of Fasciculin by Fluorometry**—As our last demonstration of the consistency between the fluorescence- and inactivation-based assays, we reexamined the release of fluorescent 7HMQ from the reaction of DEPQ with AChE when fasciculin was present. Because this method does not depend on residual enzyme activity, the fasciculin-resistant population can be monitored separately from the fasciculin-AChE complex simply by altering the time of measurement and the concentration of DEPQ (Fig. 6). In Fig. 6A, DEPQ was 7–14-fold in excess of the expected fasciculin-resistant population of AChE. A burst of 7HMQ was released in the initial minute of reaction, and the amplitude of this burst indicated that approximately 2–3% of the recombinant AChE concentration had reacted. This percentage agreed with the percentage of rapidly inactivated AChE obtained by an inactivation titration like those in Fig. 5 for this recombinant AChE sample (data not shown). When the DEPQ concentration was increased by a factor of 25 (Fig. 6B), the initial burst in Fig. 6A became too fast to measure, but the slower reaction of DEPQ with the fasciculin-AChE complex became apparent. As expected, the amplitude of this reaction corresponded to the total AChE concentration, and the  $k$  value

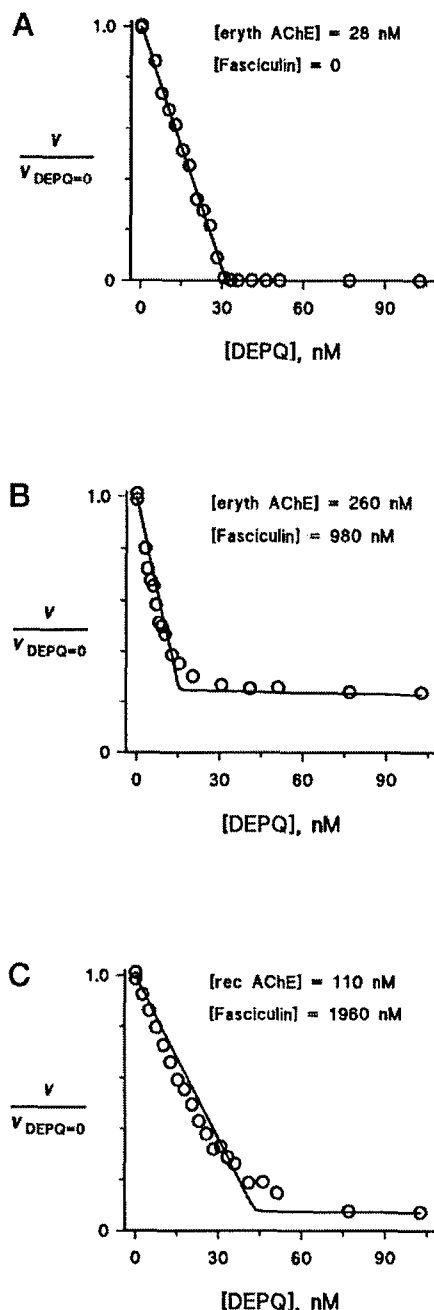


FIG. 5. Titration of AChE with DEPQ in the presence and absence of fasciculin. Erythrocyte (eryth) or recombinant (rec) AChE was incubated with or without fasciculin for 10–30 min and mixed with an equal volume of DEPQ for 90–120 min as outlined under "Experimental Procedures." Each point represents one mixture with the indicated final concentrations of DEPQ, AChE, and fasciculin. Aliquots (15–20  $\mu\text{l}$ ) were then diluted 50-fold (panels B and C) or 200-fold (panel A) into the standard acetylthiocholine solution for assay. Observed  $v$  were normalized to  $v_{\text{DEPQ}=0}$  obtained in the absence of DEPQ, and titration lines fitting the stoichiometric amount of DEPQ required to give complete rapid inactivation were calculated with the SCoP program. The calculated concentrations of rapidly inactivated AChE were 32 nM (panel A), 13 nM (panel B), and 43 nM (panel C) and correspond closely to the intersections of the lines in the plots. [The SCoP simulation program (7) was applied to two populations of AChE which reacted with DEPQ according to Scheme 1 to fit the data in Fig. 5, B and C. Rate constant assignments for the fasciculin-inhibited population were taken from Footnote 3;  $k_{\text{OP}}/K_{\text{OP}}$  for DEPQ with the fasciculin-resistant population was assigned as  $1 \times 10^8 \text{ M}^{-1} \text{ min}^{-1}$ , and the measured nonenzymatic DEPQ hydrolysis rate was  $1.4 \times 10^{-4} \text{ min}^{-1}$  (data not shown). The fitted variables were the ratio of the concentrations of the two populations and the ratio of their acetylthiocholine hydrolysis rates.]

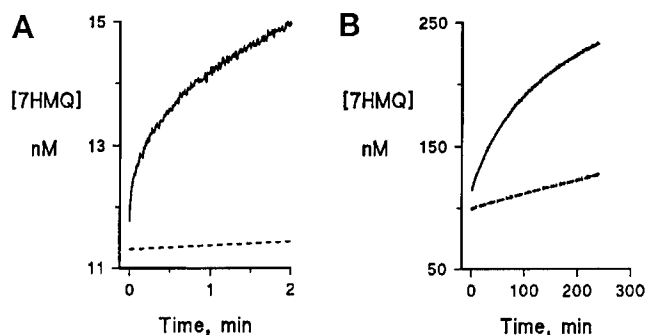


FIG. 6. Resolution of more than one population of AChE in the presence of fasciculin by fluorometric assay with DEPQ. Panel A, recombinant AChE (200 nM) was preincubated with fasciculin (1.0  $\mu$ M) before mixing with an equal volume of 380 nM DEPQ in the stopped-flow accessory, and generation of 7HMQ was monitored by spectrofluorometry as in Fig. 2. Panel B, recombinant AChE (200 nM) was preincubated with fasciculin (1.0  $\mu$ M) before conventional mixing with an equal volume of 10  $\mu$ M DEPQ, and generation of 7HMQ was monitored as in panel A. A value of  $k = 0.01 \text{ min}^{-1}$  was estimated by fitting the data in panel B with Equation 1. Dashed lines indicate blank DEPQ hydrolysis rates measured in the absence of AChE.

was consistent with the  $k_{OP}/K_{OP}$  determined by fluorometry for the reaction of DEPQ with AChE in the presence of fasciculin (Table I).

#### DISCUSSION

In this paper, we report kinetic parameters for the phosphorylation of AChE by two fluorogenic OPs, EMPC and DEPQ (Fig. 1). Both human erythrocyte AChE and recombinant human AChE produced from a high level *Drosophila* S2 cell expression system were examined. Because this expression system yields more than 20 mg of purified AChE from 2 liters of medium after 10 days of continuous culture, it is attractive for the preparation of wild type and site-specific mutants of AChE for comparative kinetic analyses and x-ray crystallography. The agreement of the phosphorylation kinetic parameters in Table I for the two AChEs provides important confirmation that the recombinant enzyme retains the catalytic properties of endogenous AChEs. EMPC and DEPQ were particularly useful organophosphorylation reagents because their reactions with AChE were observed both directly by fluorometry and indirectly by enzyme inactivation, their high phosphorylation rate constants approximated those for OPs used in chemical warfare applications, and their charges differed, allowing comparison of neutral EMPC with cationic DEPQ. We focused specifically on the effects of bound peripheral site ligands on AChE phosphorylation by OPs. Characterization of these effects is of great interest because it may be possible to design a peripheral site ligand that will block OP inactivation of AChE specifically while allowing sufficient acetylcholine hydrolysis activity to maintain synaptic transmission.

To pursue this goal we first compared the effects on AChE phosphorylation of two ligands that bind specifically to the peripheral site, the small phenanthridinium derivative propidium and the 61-residue polypeptide fasciculin. Propidium is a potent inhibitor of substrate hydrolysis by AChE, decreasing the second-order rate constant  $k_{cat}/K_{app}$  for acetylthiocholine and phenyl acetate by factors of 15–50 and the first-order rate constant  $k_{cat}$  by factors of 2–10 (7). To account for this inhibition, we proposed a steric blockade model in which the primary effect of a small peripheral site ligand like propidium is to slow the association and dissociation rate constants for ligand binding to the acylation site without significantly altering their ratio, the equilibrium constant (7, 8). One objective in proposing this model was to demonstrate that inhibition by peripheral site ligands could be explained without invoking a confor-

tional change in the acylation site induced by the binding of ligand to the peripheral site. Our steric blockade model was supported by direct measurements with the acylation site ligands huperzine A and TMTFA: bound propidium decreased the association rate constants 49- and 380-fold and the dissociation rate constants 10- and 60-fold, respectively, relative to the rate constants for these acylation site ligands with free AChE (7). The model also was supported by computer simulations of substrate hydrolysis based on Scheme 1. When the binding of substrate to the acylation site failed to reach equilibrium, the observed level of propidium inhibition could be reproduced (7). On the other hand, the model predicts that propidium should have little effect on the reaction of a substrate that essentially equilibrates with the acylation site. Few reports in the literature include data that allow this prediction to be examined, but it is supported by a recent investigation of aryl acylamidase activity in AChE (31). The peripheral site ligands propidium and gallamine failed to inhibit AChE-catalyzed hydrolysis of aryl acylamides, which are hydrolyzed slowly by AChE and thus should equilibrate with the acylation site (32), but gave typical inhibition of acetylthiocholine hydrolysis.

The reaction of OPs, including EMPC and DEPQ, with AChE appears to involve equilibration of the OP with the acylation site (see Footnote 3). Table I indicates that propidium did have modest effects on  $k_{OP}$  and  $k_{OP}/K_{OP}$  for both EMPC and DEPQ. Do these observations invalidate our steric blockade model and require that the binding of propidium induce a conformational change in the acylation site? We argue that they do not, if the model is extended to allow an unfavorable electrostatic interaction or a steric overlap between propidium at the peripheral site and an OP at the acylation site in the AChE ternary complex. The need for such an extension in fact has been recognized in our previous studies because small decreases in the affinity of ligands in ternary AChE complexes relative to the corresponding binary complex are observed consistently (7). For example, from the rate constants noted above one can calculate that the affinities of huperzine A and TMTFA for the acylation site decreased by factors of 5–6 when propidium was bound to the peripheral site. Computer modeling revealed no steric overlap between the ligands in these ternary complexes (7), so the decreased affinity must result from unfavorable electrostatic interaction between these cationic ligands. Extending these observations to the OPs, a decrease in affinity for EMPC and DEPQ also was apparent when propidium was bound to the peripheral site. Insertion of data from Table I into Equation 6 indicated that this decrease (given by  $K_{S1}/K_1 = K_{S2}/K_S$ ) was about an order of magnitude for both OPs. There was also a clear increase in the  $k_{OP}$  for EMPC ( $\alpha > 1$  in Table I) and a possible increase in  $k_{OP}$  for DEPQ when propidium was bound, consistent with an acceleration of first-order phosphorylation rate constants by bound peripheral site ligands reported recently by Radic (33, 34). It has long been known that  $k_{OP}/K_{OP}$  for the reaction of neutral OPs with AChE varies smoothly and monotonically with the  $pK_a$  of the leaving group (27). This suggests that cleavage of the leaving group ester bond of the OP is prominent in the rate-limiting step for phosphorylation of AChE. Computer modeling revealed a clear unfavorable steric overlap between propidium in the peripheral site and the leaving group of either EMPC or DEPQ in the acylation site (data not shown; 35). This steric overlap could contribute to the decrease in affinity for both neutral EMPC and cationic DEPQ, and it could induce molecular or electronic strain caused by the proximity of propidium to the OP in the ternary complex to increase  $k_{OP}$ . This increase would not require an induced conformational change in the acylation site

when propidium alone is bound but would result from a change in ligand configuration or overall conformation in the ternary complex.

The consequences of fasciculin binding to the peripheral site of AChE on phosphorylation kinetic parameters for EMPC and DEPQ were qualitatively different from those of propidium. Values of  $k_{OP}/K_{OP}$  were decreased by factors of  $10^3$  to  $10^5$ , and  $k_{OP}$  was decreased by factors of 300–4,000 (Table I). Fasciculin has been shown to present a substantial steric blockade to the entrance and exit of ligands that bind to the acylation site: association and dissociation rate constants for the binding of *N*-methylacridinium were decreased 8,000- and 2,000-fold, respectively, when fasciculin was bound (36). However, steric blockade of OP association and dissociation rate constants cannot account for the effects of fasciculin on the phosphorylation rate constants. Because OPs essentially equilibrate with the acylation site, a steric blockade of OPs by fasciculin that resulted in even a 100,000-fold decrease in association rate constant ( $k_{S2}/k_S = 10^{-5}$ ) would result in less than a 10% decrease in  $k_{OP}/K_{OP}$  and no change in  $k_{OP}$  (see Footnote 3). The pronounced fasciculin inhibition of AChE phosphorylation requires an additional interaction between fasciculin and the acylation site. One possibility might be an unfavorable steric overlap between fasciculin at the peripheral site and an OP at the acylation site in the AChE ternary complex, but the three-dimensional structure of the fasciculin-AChE complex shows no penetration of the acylation site by fasciculin which would lead to such an interaction. Therefore, the additional interaction must involve a conformational change in the acylation site induced by bound fasciculin. Crystal structure analyses of fasciculin-AChE complexes (3, 4) show that fasciculin 2 interacts not only with Trp<sup>279</sup> in the peripheral site but also with residues on the outer surface of an  $\omega$ -loop within 4 Å of Trp<sup>84</sup> in the acylation site, well beyond the region of the peripheral site occupied by propidium (7, 37). These more extensive surface interactions provide a structural basis for an inhibitory conformational effect on the acylation site when fasciculin but not when propidium is bound to the peripheral site.

Second-order phosphorylation rate constants  $k_{OP}/K_{OP}$  obtained for EMPC or DEPQ alone or in the presence of propidium were in good agreement when measured either by release of the fluorescent leaving group or by enzyme inactivation (Table I). In the presence of fasciculin, however,  $k_{OP}/K_{OP}$  values determined by enzyme inactivation were 100-fold greater for EMPC and  $10^4$ -fold greater for DEPQ than the corresponding values measured fluorometrically. Through a series of titrations like those in Fig. 5, this discrepancy was shown to arise from misleading inactivation measurements caused by a small fraction of the total AChE (less than 5%, except for one preparation) which remained largely resistant to inhibition by fasciculin. This fraction thus accounted for most of the enzyme activity in the presence of fasciculin and was inactivated by both OPs much more rapidly than the fasciculin-AChE complex was phosphorylated. In support of this explanation, reexamination of the release of fluorescent 7HMQ from DEPQ in the presence of fasciculin revealed a small initial burst that was in stoichiometric agreement with the fraction of AChE that was rapidly inactivated (Fig. 6A). The population of AChE resistant to fasciculin inhibition may itself be heterogeneous. The titration curves in Fig. 5, B and C, were not fit precisely by a model with two forms of AChE, and the deviation suggested a third form with somewhat less resistance to fasciculin inhibition. In addition, the initial burst of 7HMQ release in Fig. 6A could not be fit to a single exponential release of 7HMQ but instead corresponded to two release reactions, the faster of which corresponded to the  $k_{OP}/K_{OP}$  initially observed for fasciculin inhi-

bition of inactivation by DEPQ (Table I). Other uncertainties involve the source of the population of fasciculin-resistant AChE or the process whereby it was produced. Each AChE preparation we examined, whether erythrocyte or recombinant, showed this resistant population, but its extent varied among different affinity chromatography preparations. This population may represent a portion of the AChE which has undergone an undefined chemical modification that alters the affinity of fasciculin for the peripheral site and/or the catalytic efficiency of the fasciculin-AChE complex. Estimates of  $k_{OP}/K_{OP}$  for this population in the presence of fasciculin from the inactivation data in Table I were only 2–5-fold lower than  $k_{OP}/K_{OP}$  for AChE alone, and these estimates were relatively insensitive to the saturating fasciculin concentration (data not shown). Furthermore, calculations from the titration data in Fig. 5 indicated an acetylthiocholine turnover rate for this population which was about 30% of that for free AChE (data not shown). These comparisons suggest that catalysis at the acylation site is only slightly less efficient in the fasciculin-resistant population than in the predominant conventional AChE. Fasciculin does appear to interact weakly with this resistant population, resulting in 3–5-fold decreases in  $k_{OP}/K_{OP}$  for EMPC and DEPQ (Table I). A fasciculin-resistant population also may dominate the activity of recombinant mouse AChE in the presence of fasciculin: the addition of fasciculin induced biphasic phosphorylation rates and only modest decreases in phosphorylation rate constants and TMTFA association and dissociation rate constants (less than 20-fold; 30). It is possible that the population of AChE resistant to fasciculin can be distinguished even in the absence of fasciculin as the fraction of AChE that underwent a slower reaction with DEPQ in Fig. 2. The amount of this fraction (about 10% of the total AChE) and its phosphorylation rate constant (about 10% of the  $k$  for the faster phase) are roughly consistent with the data for the fasciculin-resistant population.

Regardless of the origin of the fasciculin-resistant population, it is significant because it obscures the kinetic properties of the actual fasciculin-AChE complex measured by enzyme inactivation, both in our measurements (Table I) and apparently in those of Radic *et al.* (30). We overcame this problem by exploiting the relatively high sensitivity of the fasciculin-resistant population to DEPQ. Incubation of small amounts of AChE (3–20 nM) in the presence of fasciculin with 10–60 nM DEPQ was sufficient to inactivate this population in 60 min, and the kinetic parameters of the fasciculin-AChE complex then could be measured by inactivation. For example, measurement of  $k_{OP}/K_{OP}$  for EMPC after this treatment gave good agreement with the  $k_{OP}/K_{OP}$  values determined for EMPC with the fasciculin-AChE complex by fluorometry (Table I). In addition to phosphorylation kinetic parameters, it may be necessary to employ DEPQ inactivation to reevaluate kinetic parameters for the reaction of substrates (6) and TMTFA (30) with fasciculin-AChE complexes.

**Acknowledgments**—We express our gratitude to Dr. Abdul Fauq of the Mayo Clinic Jacksonville Organic Synthesis Core Facility for preparation of EMPC and DEPQ used in these studies. We thank Dr. Harvey Berman of the State University of New York at Buffalo and Dr. Yacov Ashani of the Israel Institute for Biological Research at Ness-Ziona for initial samples of EMPC and DEPQ, respectively. We also thank Dr. Avigdor Shafferman of the Israel Institute for Biological Research at Ness-Ziona for the cDNA for AChE in pACHE10 and Dr. Carlos Cervenansky for fasciculin 2. We acknowledge the technical assistance of Dr. John Incardona, Jean Eastman, Dr. Robert Haas, and Pat Thomas in the initial phases of construction and cloning the recombinant human AChE gene cassette.

#### REFERENCES

1. Rosenberry, T. L. (1975) *Adv. Enzymol.* **43**, 103–218
2. Sussman, J. L., Harel, M., Frolow, F., Oefner, C., Goldman, A., Tokar, L., and

- Silman, I. (1991) *Science* **253**, 872-879
3. Bourne, Y., Taylor, P., and Marchot, P. (1995) *Cell* **83**, 503-512
4. Harel, M., Kleywegt, G. J., Ravelli, R. B. G., Silman, I., and Sussman, J. L. (1995) *Structure* **3**, 1355-1366
5. Taylor, P., and Lappi, S. (1975) *Biochemistry* **14**, 1989-1997
6. Eastman, J., Wilson, E. J., Cervenansky, C., and Rosenberry, T. L. (1995) *J. Biol. Chem.* **270**, 19694-19701
7. Szegetes, T., Mallender, W. D., and Rosenberry, T. L. (1998) *Biochemistry* **37**, 4206-4216
8. Szegetes, T., Mallender, W. D., Thomas, P. J., and Rosenberry, T. L. (1999) *Biochemistry* **38**, 122-133
9. Burgen, A. S. V. (1949) *Br. J. Pharmacol.* **4**, 219-228
10. Wilson, I. B. (1951) *J. Biol. Chem.* **190**, 111-117
11. Aldridge, W. N., and Reiner, E. (1972) in *Frontiers of Biology*, 26th Ed., p. 328, Elsevier, North Holland, Amsterdam
12. Froede, H. C., and Wilson, I. B. (1971) in *The Enzymes* (Boyer, P. D., ed.) 3rd Ed., Vol. 5, pp. 87-114, Academic Press, New York
13. Hart, G. D., and O'Brien, R. D. (1973) *Biochemistry* **12**, 2940-2945
14. Berman, H. A., and Leonard, K. (1989) *J. Biol. Chem.* **264**, 3942-3950
15. Gordon, M. A., Carpenter, D. E., Barrett, H. W., and Wilson, I. B. (1978) *Anal. Biochem.* **85**, 519-527
16. Levy, D., and Ashani, Y. (1986) *Biochem. Pharmacol.* **35**, 1079-1085
17. Rosenberry, T. L., and Scoggin, D. M. (1984) *J. Biol. Chem.* **259**, 5643-5652
18. Roberts, W. L., Kim, B. H., and Rosenberry, T. L. (1987) *Proc. Natl. Acad. Sci. U. S. A.* **84**, 7817-7821
19. Ginsburg, S., Kitz, R. J., and Wilson, I. B. (1966) *J. Med. Chem.* **9**, 632-633
20. Kronman, C., Velan, B., Gozes, Y., Leitner, M., Flashner, Y., Lazar, A., Marcus, D., Sery, T., Papier, Y., Grosfeld, H., Cohen, S., and Shafferman, A. (1992) *Gene (Amst.)* **121**, 295-304
21. Incardona, J. P., and Rosenberry, T. L. (1996) *Mol. Biol. Cell* **7**, 595-611
22. Laemmli, U. K. (1970) *Nature* **227**, 680-685
23. Rosenberry, T. L., and Bernhard, S. A. (1971) *Biochemistry* **10**, 4114-4120
24. Magloth, J. A., Wins, P., and Wilson, I. B. (1975) *Biochim. Biophys. Acta* **403**, 370-387
25. Ellman, G. L., Courtney, K. D., Andres, J. V., and Featherstone, R. M. (1961) *Biochem. Pharmacol.* **7**, 88-95
26. Riddles, P. W., Blakeley, R. L., and Zerner, B. (1979) *Anal. Biochem.* **94**, 75-81
27. Kitz, R. J., Ginsburg, S., and Wilson, I. B. (1967) *Mol. Pharmacol.* **3**, 225-232
28. Hosea, N. A., Radic, Z., Tsigelny, I., Berman, H. A., Quinn, D. M., and Taylor, P. (1996) *Biochemistry* **35**, 10995-11004
29. Berman, H., and Leonard, K. (1990) *Biochemistry* **29**, 10640-10649
30. Radic, Z., Quinn, D. M., Vellom, D. C., Camp, S., and Taylor, P. (1995) *J. Biol. Chem.* **270**, 20391-20399
31. Costagli, C., and Galli, A. (1998) *Biochem. Pharmacol.* **55**, 1733-1737
32. Barlow, P. N., Acheson, S. A., Swanson, M. L., and Quinn, D. M. (1987) *J. Am. Chem. Soc.* **109**, 253-257
33. Radic, Z., and Taylor, P. (1999) *Chem.-Biol. Interact.*, in press
34. Radic, Z., and Taylor, P. (1998) in *Structure and Function of Cholinesterases and Related Proteins* (Doctor, B. P., Taylor, P., Quinn, D. M., Rotundo, R. L., and Gentry, M. K., eds) pp. 211-214, Plenum Press, New York
35. Albaret, C., Lacoutiere, S., Ashman, W. P., Foment, D., and Fortier, P.-L. (1997) *Proteins* **28**, 543-555
36. Rosenberry, T. L., Rabl, C. R., and Neumann, E. (1996) *Biochemistry* **35**, 685-690
37. Barak, D., Kronman, C., Ordentlich, A., Ariel, N., Bromberg, A., Marcus, D., Lazar, A., Velan, B., and Shafferman, A. (1994) *J. Biol. Chem.* **269**, 6296-6305



DEPARTMENT OF THE ARMY  
US ARMY MEDICAL RESEARCH AND MATERIEL COMMAND  
504 SCOTT STREET  
FORT DETRICK, MARYLAND 21702-5012

REPLY TO  
ATTENTION OF:

MCMR-RMI-S (70-1y)

18 Jun 02

MEMORANDUM FOR Administrator, Defense Technical Information  
Center (DTIC-OCA), 8725 John J. Kingman Road, Fort Belvoir,  
VA 22060-6218

SUBJECT: Request for Change in Distribution Statements

1. The U.S. Army Medical Research and Materiel Command has reexamined the need for the limitation assigned to technical reports written for Grants DAMD17-96-1-6096 and DAMD17-98-2-8019. Request the limited distribution statements for the Accession Documents listed at enclosure be changed to "Approved for public release; distribution unlimited." These reports should be released to the National Technical Information Service.

2. Point of contact for this request is Ms. Judy Pawlus at DSN 343-7322 or by e-mail at judy.pawlus@det.amedd.army.mil.

FOR THE COMMANDER:

Encl

*Phyllis M. Rinehart*  
PHYLLIS M. RINEHART  
Deputy Chief of Staff for  
Information Management

ACCESSION DOCUMENT NUMBERS

ADB238947

ADB252024

ADB259791

ADB251342